2013

Inflorescence branching in maize: A quantitative genetics approach to identifying key players in the inflorescence development pathway

Rebecca Lynne Weeks
Iowa State University

Inflorescence branching in maize: A quantitative genetics approach to identifying key players in the inflorescence development pathway

by

Rebecca Lynne Weeks

A dissertation submitted to the graduate faculty
in partial fulfillment of the requirements for the degree of
DOCTOR OF PHILOSOPHY

Major: Genetics

Program of Study Committee:
Erik Vollbrecht, Major Professor
Philip Becraft
Nick Lauter
Thomas Lübberstedt
Bing Yang

Iowa State University
Ames, Iowa
2013

TABLE OF CONTENTS

ABSTRACT

Inflorescence branch number in maize and other cereal crops has long been recognized as an important factor impacting grain yield. In maize, inflorescence architecture is determined by the collective actions of many genes. Among these, the *ramosa* mutants play an important role in regulating branch number by imposing short-branch identity on lateral meristems of the inflorescence. In addition, a number of QTL have been identified which alter the branching of male inflorescences, however few of these QTL co-localize with known inflorescence branching genes, indicating that some components of this pathway have yet to be discovered. We conducted a suppressor/enhancer screen to identify modifiers of the *ramosa* phenotype and discovered twenty two putative mutants that enhance or suppress the phenotypes of *ramosa* mutants. Mapping of a portion of these mutants revealed that a subset map to regions of the genome not known to harbor inflorescence genes. As an extension of this method, we performed a screen for natural suppressors and enhancers of the *ra1-63.3359* and *ra2-R* ear branching phenotypes using the intermated B73 × Mo17 (IBM) population of maize. Through this approach we discovered eight QTL that significantly alter the inflorescence branching phenotype of *ra1-63.3359* or *ra2-R* mutants. One of these QTL was present in both the *ramosa1* and *ramosa2* experiments indicating that it might function directly or in close association with the *ramosa* pathway. We fine-mapped this region using recombinants derived from a near-isogenic line and narrowed the interval to a region containing nine candidate genes. Ongoing efforts to map the induced mutations or natural variation underlying these *ramosa* modifiers will help elucidate the processes governing inflorescence architecture.

CHAPTER 1. GENERAL INTRODUCTION

DISSERTATION ORGANIZATION

This dissertation includes a general introduction (Chapter 1), three journal papers (Chapters 2-4), and general conclusions (Chapter 5). The general introduction contains a literature review including a discussion of the relationship between inflorescence branching and yield, a summary of maize inflorescence development, an overview of genetic diversity in maize, and a review of methods for mapping quantitative trait loci. Chapter 2 details a study to identify and map inflorescence development genes using a screen for suppressors and enhancers of *ramosa* mutants. My contributions to this project include the identification of a portion of the new mutants, generation and subsequent scoring of mapping populations, preparation of DNA assisted by Dr. Unger-Wallace and Stacey Barnes, development of methods to automate and streamline the processing of high throughput mapping data, analysis of the bulked segregant mapping results, and drafting of the manuscript in conjunction with Dr. Vollbrecht. Chapter 3 contains a paper on the identification and fine-mapping of QTL for ear branch number in *ra1-63.3359* mutants. My contributions include experimental design, generation of mapping populations, statistical analysis and QTL mapping, and writing of the manuscript in conjunction with Dr. Vollbrecht. Chapter 4 comprises a QTL mapping study for modifiers of the *ra2-R* ear branching phenotype. My contributions to this project include experimental design, statistical analysis and QTL mapping, identification of candidate genes, and drafting of the manuscript, again with the help of Dr. Vollbrecht. The final chapter is a summary of the results and a discussion of the general conclusions inferred from the three previous chapters.

LITERATURE REVIEW

Inflorescence Branching and Yield

In cereal crops, inflorescence architecture is a key determinant of yield and has consequently been a major target of selection during domestication and improvement. Many studies have attempted to investigate the molecular basis for the morphological features

accompanying increased yield and in rice, much progress has been made through the cloning of quantitative trait loci (QTL) that control grain yield or one of its basic components: number of tillers, number of grains per tiller, and grain weight. While many of these QTL show pleiotropic effects on two or more yield components, at least half alter inflorescence branch number, and molecular characterization of the underlying genes indicates that several function directly in the inflorescence development pathway (Table 1). The identification of genes in rice which, through regulating inflorescence branching, are able to impact yield implicates inflorescence branching as a potential target of selection using modern molecular breeding techniques. For example, the concept of QTL pyramiding, whereby favorable alleles for multiple QTL are mined from a wide sampling of wild and cultivated varieties and subsequently stacked in order to produce the greatest phenotypic effect, has been proven in rice, wheat, and barley (Ashikari et al., 2005; Riedel et al., 2011; Zhang et al., 2013). Similar approaches to identify and select for naturally occurring alleles that condition increased inflorescence branching could be of potential benefit to breeding efforts.

Maize bears its male and female flowers on separate, morphologically distinct inflorescences (commonly called the tassel and ear, respectively) and therefore the relationship between inflorescence branching and yield in maize is more complex. In fact, numerous studies have documented an *inverse* correlation between inflorescence branching and yield (Geraldi, 1978; Geraldi, 1985; Hunter, 1969; Sharma, 1968). Furthermore, *ramosa1*, a gene that functions to suppress inflorescence branching, is evidenced to have undergone positive selection during the domestication of maize from its wild relative, teosinte (Sigmon and Vollbrecht, 2010). In the United States, continued selection for yield over many years has resulted in modern inbreds with small, few-branched tassels. This trend was well-documented by Don Duvick, a forty year veteran corn breeder at Pioneer Hi-bred, in a study aimed at characterizing several morphological and yield component traits in 36 commercial hybrids spanning 58 years of the Pioneer corn breeding program (Duvick, 1997). Duvick found that over the 1932-1991 period, the tassels of Pioneer hybrids had diminished, losing an average of 2.5 branches per decade. A reduction of 0.5 grams in total tassel weight per decade was also observed. Similar trends were observed in a survey of public breeding materials spanning 40 years of development (Meghji et al., 1984). Although the reduction in

tassel size over time has been thoroughly characterized, little is known about the physiological benefit of a reduced tassel. A few of the hypotheses that have been put forth include reduced shading by smaller tassels, decreased apical dominance, and increased partitioning of resources into the ear (Hunter, 1969). While no one hypothesis has emerged as the predominant mechanism for increased yield, it is possible that some combination of these factors can account for the inverse relationship observed between tassel size and grain yield.

Despite being of benefit to yield, small tassels are often a hindrance to maize breeding efforts and hybrid seed production. Modern maize breeding proceeds through the development of separate male and female inbreds, which are then hybridized to produce seed for commercial sale. Lines with small, few-branched tassels are poor pollen producers (Fonseca et al., 2003) and are difficult to maintain and increase for hybrid production. Furthermore, male plants are present in limited quantities in hybrid production fields, which typically contain male and female rows in a 1:4 ratio. Poor pollen production by the male pollinator rows in these fields leads to reduced rates of fertilization for female rows and therefore less seed output per plot. This can be mitigated by increasing the ratio of male to female rows, however, output of the plot will still be somewhat reduced due to the loss of field space now occupied by the additional pollinator rows.

Because inflorescence branching has a strong relationship with yield, and because inflorescence architecture plays an important role in pollen production, it is of interest to study the inheritance of inflorescence traits and investigate the molecular mechanisms underlying inflorescence development. The cloning of mutants that perturb inflorescence development has been helpful in elucidating the inner workings of this process, however further progress depends on our ability to identify novel genes in the developmental pathway, which through induced or natural variation are able to confer phenotypic changes to maize inflorescences.

Review of Inflorescence Development Pathway

The structure of maize inflorescences is defined by the activity of meristems, small groups of stem cells present at the apices of growth in plants (Tanaka et al., 2003). Several

types of meristems function during inflorescence development and these meristems differ in the number and types of organs that they produce. Determinate meristems, for example, will be consumed after making a defined number of derivatives, while indeterminate meristems will go on to produce an indefinite number of primordia. For cereal crops, including maize, meristem determinacy is especially important as it influences inflorescence length and degree of branching, and therefore determines how many flowers (and hence seed) can potentially be produced by a single inflorescence (Kellogg et al., 2013).

Maize possesses two inflorescence types, the male tassel and the female ear. A typical mature tassel consists of a single rachis (main axis), several primary branches, and roughly two to three hundred pairs of spikelets, the flower-containing structures of grasses (Upadyayula et al., 2006). Early in tassel development, after the last leaf has emerged, a transition from vegetative to reproductive development occurs and the shoot apical meristem (SAM) is converted to an inflorescence meristem (IM). Following this transition, lateral meristems are initiated from the IM in a polystichous (multi-rowed) pattern. Near the base, a few of these meristems are indeterminate and will go on to produce long branches. These indeterminate meristems are called branch meristems (BM). The remainders, called spikelet pair meristems (SPM), are determinate and will terminate following the production of a pair of spikelet meristems (SM). Each of these spikelet meristems will produce a pair of floral meristems (FM) from which floral organs arise. Development of the tassel is complete when each floral meristem, which is subtended by a specialized bract called a lemma, has produced a palea, three lodicules, and three stamens (pistil development is aborted in the florets of the tassel).

A mature maize ear consists of a single rachis bearing a couple hundred pairs of spikelets, each of which contains a single mature seed. Development of the ear proceeds in a manner similar to the tassel, except that long branches are not produced and the lower floret of each spikelet is aborted (Vollbrecht and Schmidt, 2009). Additionally, stamens are not formed in the flowers of the ear. Instead, three carpels are produced, two of which subsequently fuse and elongate to produce a silk.

Besides sex-specific differences in the flowers, the morphological differences between tassels and ears can be mostly attributed to the determinacy of lateral meristems at

the base of the inflorescence. In fact, incipient tassel primordia are indistinguishable from ear primordia, but for the elongation of a few meristems at the base of the tassel, signaling the initiation of branches (Figure 1). Of the inflorescence mutants that alter early inflorescence development (i.e., non-floral mutants) most show phenotypic effects in both the tassel and ear. Among these, the *ramosa* mutants (*ra1, ra2, ra3*) are unique in their ability to produce tassel-like branching in the female inflorescence. This phenotype results from a derepression of lateral meristems, which are then free to develop into branches. *ramosa* mutants also display an increased number of long branches in the tassel, as well as a novel type of branch called a mixed branch. Mixed branches differ from long branches in that they produce spikelets both singly and in pairs. In this sense, a meristem producing a mixed branch behaves more like a less-determinate SPM than a BM, which consistently initiates SPMs in a distichous manner.

The various degrees of increased branching observed in *ramosa* mutants indicate a molecular role for the *ramosa* genes in regulating meristem determinacy. All three *ramosa* genes have been cloned; *ra1* encodes a cys2-his2 zinc finger transcription factor (Vollbrecht et al., 2005), *ra2* encodes a LATERAL ORGAN BOUNDARY (LOB) domain transcription factor (Bortiri et al., 2006), and *ra3* encodes a trehalose-6-phosphate phosphatase metabolic enzyme (Satoh-Nagasawa et al., 2006). An additional factor called *ramosa1 enhancer locus2* (*rel2*) encodes a *TOPLESS*-like co-repressor and has been shown to physically interact with the *ramosa1* protein (Gallavotti et al., 2010). The *ramosa* genes are co-expressed in overlapping domains near the base of developing SPMs and mutation of *ra2* or *ra3* leads to reduced *ra1* expression indicating that they function upstream of *ramosa1* and promote its expression (Bortiri et al., 2006; Satoh-Nagasawa et al., 2006; Vollbrecht et al., 2005). Mutagenesis has produced a number of additional mutants that alter branching of tassels—*barren stalk1*, *liguleless1/2*, and *tasselsheath1/4*, to name a few—however many of these phenotypes are due to the pleiotropy that often exists between tassel branching and flowering and leaf traits (Brown et al., 2011). Thus far, a connection to determinacy through the *ramosa* pathway has been established for only one of these genes, *tasselsheath4* (*tsh4*). However, the increased determinacy observed in *tsh4* meristems appears to be the

consequence of competition with the subtending bract for resources, rather than a *ramosa*-mediated reprogramming of meristems (Chuck and Bortiri, 2010).

The generation and cloning of new mutants through traditional mutagenesis techniques will be helpful in elucidating the network of genes required for meristem determinacy, however future progress also depends on our ability to detect mutants with subtle phenotypes. One way this can be achieved is through the use of suppressor/enhancer screens, which are able to elicit strong phenotypic effects by inducing new mutations on a sensitized mutant background. Additionally, the vast allelic diversity present in maize provides potential suppressors or enhancers of branching that have arisen naturally through spontaneous mutation, and which can be identified by genetic mapping techniques. Allelic diversity includes variation in genes for which there is genetic redundancy. In combination, these methods provide a broad-based approach to identify many types of genes functioning within the inflorescence development pathway. Functional characterization of these genes and analysis of their interactions using genome-wide approaches will be helpful in understanding the molecular mechanisms that regulate meristem determinacy and consequently, inflorescence architecture.

Interspecific Diversity of Maize

Maize is a remarkably diverse species with average divergence between cultivars—measured in terms of nucleotide polymorphism within genes—equaling that which is observed between humans and chimpanzees (Buckler et al., 2006). This vast genetic diversity was critical during the domestication of maize from its wild relative, teosinte and throughout the improvement period, during which breeders selected for sturdier plants producing larger, more densely packed ears. In 1877, Dr. William Beal performed the first experiments to evaluate the use of cross-pollinated corn for increased yield through hybrid vigor. Recognizing the importance of diversity for improved heterosis, Beal selected parent lines from sources that were separated by at least one hundred miles and had been maintained in isolation for at least five years. Beal constructed hybrids from these parents and observed that more often than not, the cross-pollinated varieties outperformed their parent lines (Beal, 1876; Beal, 1881). Commercial sale of hybrid seed gained popularity in the 1930's and

breeders ever since have, for the most part, developed inbreds within distinct heterotic breeding groups, which are then tested for their combining ability, as indicated by the degree of heterosis displayed in the F1 lines.

The B73 and Mo17 inbred lines belong to the Reid Yellow Dent and Lancaster Surecrop heterotic groups, respectively, and are among the most widely studied maize varieties to date. The genome of B73 has been sequenced (Schnable et al., 2009) and numerous studies have been undertaken to try to understand the genetic basis for the heterotic pattern observed between these two inbreds (Barber et al., 2012; Paschold et al., 2012; Stupar et al., 2007; Stupar and Springer, 2006; Swanson-Wagner et al., 2006). At the nucleotide level, B73 and Mo17 are quite diverse, with an average of one single nucleotide polymorphism (SNP) for every 300bp of expressed sequence (Barbazuk et al., 2007). Many of these SNPs are inconsequential, being silent or leading to conservative changes in amino acid sequence. On occasion, however, polymorphism within a gene may alter the amino acid sequence in ways that impact protein folding and/or function. Diversity in levels of gene expression has also been observed between B73 and Mo17 (Li et al., 2013; Stupar et al., 2007; Stupar and Springer, 2006). Depending on the tissue, the proportion of genes displaying allelic variation in gene expression levels ranges from 4 to 18% with the majority of differential expression being attributed to cis-regulation (Stupar and Springer, 2006). Interestingly, however, methylation patterns among maize inbreds—assessed by immunoprecipitation of H3K27me3-linked DNA—are mostly conserved (Makarevitch et al., 2013), indicating mutational changes in the sequence of cis-regulatory elements might be responsible for some of the expression differences observed among inbreds.

Besides mutations to promoters or cis-regulatory elements, differential expression between inbred lines can be explained in part by structural variation that exists within their genomes. Having undergone a whole genome duplication roughly 5-12 million years ago, maize is considered an ancient allotetraploid (Gaut and Doebley, 1997; Schnable et al., 2009). Following this duplication event, redundant copies of each gene were present, allowing one homeolog to deviate, through mutation, from its original form (Schnable et al., 2011). Through this process, it is hypothesized that genes may assume a subset of their original functions (sub-functionalize), acquire new functions (neo-functionalize), or may

simply be removed through a mutational process known as fractionation (Woodhouse et al., 2010). These changes occur independently between lines leading to copy number variation (CNV) and presence-absence variation (PAV) (Springer et al., 2009). Variation in gene dosage can also occur through tandem duplication of genes or duplication to non-allelic regions mediated by *Helitron* transposons (Brunner et al., 2005a; Brunner et al., 2005b). Regardless of the source, variation in gene complement or expression between inbreds could be a potential contributor to heterosis in the resulting F1 hybrid. In a recent transcript profiling study of maize roots from B73, Mo17 and reciprocal hybrids, Paschold et al, identified 1124 hybrid-expressed genes that were expressed in only one inbred parent (Paschold et al., 2012). Accordingly, the contingent of expressed genes in hybrid roots was larger than that of either inbred parent. This finding is consistent with the dominance (i.e. complementation) model of heterosis whereby hybrid vigor is caused by the complementation of inferior alleles in one parent by superior or dominant alleles from another.

This diversity is of great agronomic importance as it represents variation that can be exploited by geneticists and breeders for the purpose of improving yield and other agronomic traits. Recent advancements in sequencing technology coupled with rapidly declining costs have facilitated the sequencing of thousands of new genomes and consequently, discovery of a tremendous amount of diversity. For example, the genotype by sequencing (GBS) technology applied to approximately 2,800 accessions of the USA national maize inbred seed bank has generated approximately 680,000 SNPs, which are now available for association mapping, marker development, and allele mining (Romay et al., 2013). Moreover the relationships between inbreds inferred by these data can be used for the selection of parent lines in public breeding programs. Further improvements to sequencing technology will facilitate even greater exploration of maize germplasm and will likely improve our understanding of complex genetic architectures and ability to exploit genetic diversity.

Harnessing Natural Diversity

Most traits of agronomic importance are controlled by the collective actions of multiple genetic factors, known as quantitative trait loci (QTL). For traits that show

quantitative inheritance, the phenotype of an individual depends on the number of QTL present and the magnitude of each QTL effect as well as the allelic interactions at each QTL and epistatic interactions between multiple QTL. In this way, the allelic variance present across several QTL is able to explain much of the phenotypic diversity that is observed between different maize inbreds.

Recent genome wide association studies (GWAS) have identified a number of regions, which through natural variation are able to alter the inflorescence phenotypes of maize varieties (Brown et al., 2011). Interestingly, only a small portion of the regions associated with these effects can be linked to known inflorescence genes. It therefore seems likely that traditional mutagenesis techniques have been able to uncover only a small portion of genes that function in the inflorescence development pathway. Because maize recently experienced a whole genome duplication (WGD), large amounts of genetic redundancy are present in its genome. On average, half of the expressed genes in the maize genome have a homeolog present on a syntenous chromosomal region (Schnable and Freeling, 2011). Recent studies aimed at characterizing the evolution of the two maize subgenomes resulting from WGD have revealed that the majority of the cloned maize mutants are present on the A subgenome of maize, which is expressed at a higher level than the B genome (Schnable and Freeling, 2011). Furthermore, genes that were identified based on their mutant phenotypes are less likely to possess a homeolog than a generic maize gene. These results suggest that previously cloned genes may represent the "low-hanging fruit" of the inflorescence pathway, because detection of their phenotypes was facilitated by mutations in single-copy, large effect genes.

While genetic redundancy often hinders gene discovery through forward genetic approaches, it may be beneficial in the discovery of loci controlling natural variation. For example, retained duplicate genes may experience relaxed selective pressure, allowing one copy to vary in its sequence or level of expression. Over time, these types of changes can lead to phenotypic variation between lines that can subsequently be exploited to map the underlying genes. Numerous studies have utilized natural variation present in maize to identify QTL that alter quantitatively inherited traits and subsequently, a number of the causative genes or sequences have been identified (Table 2). For some of these QTL,

cloning was facilitated by co-localization of the QTL with previously characterized genes, namely those involved in the maize domestication. However, several of the cloned QTL represent novel genetic factors that had not been previously characterized.

Natural variation between maize varieties can also cause the phenotype of mutant alleles to vary according to genetic background. The *ramosa* mutants, for example, display phenotypes that are partially suppressed in Mo17 relative to B73. This indicates that natural variation at one or more loci in these backgrounds is able to influence the branching phenotype of *ramosa* mutants. The genetic factors underlying this effect are likely to be involved, either directly or indirectly, in the regulation of inflorescence branching and therefore it is possible that they represent undiscovered components of the branching pathway. Identification of these loci using approaches developed for mapping quantitative traits could further our understanding of the genetic network involved in controlling inflorescence architecture.

Mapping Quantitative Trait Loci (QTL)

QTL mapping typically begins with the selection of diverse inbred parents. If a particular trait is of interest, a researcher might select parents that differ widely for that trait, although this is not necessary as transgressive segregation in the filial generations may reveal effects from loci that were undetected in the parent lines due to epistasis or the coupling of QTL with competing effects. Once an F1 has been generated, standard mating schemes (BC1, F2, etc) can be used to generate segregating progeny, which are then genotyped at markers spanning the genome. Depending on the heritability of the trait, phenotyping can be performed on the genotyped individuals or on their progeny, ($F_{2:3}$ lines for example.) Over the last decade, the use of recombinant inbred lines (RILs) for QTL mapping has become quite popular. RILs are generated by crossing two or more parents, randomly mating for several generations and self-pollinating to generate a diverse set of inbred lines, each of which is uniquely mosaic for different segments of the parental genomes. Recently, the use of doubled haploids has gained favor over self-pollination since inbred lines can be generated in a single year rather than over several seasons. In either case, each RIL will be homozygous for one parent allele at almost any given locus, although some residual

heterozygosity can be found in self-pollinated lines, as will be discussed later. Because of this homozygosity, each RIL family will be homogeneous when planted in a field and therefore scoring can be performed on as few as one individual per family, given high heritability for the trait of interest.

Several methods exist for detecting QTL within a population, the simplest of which is single marker analysis. This method fits the data to the simple linear model $y_{ik} = b_0 + b_1 x_i + e_k$ where y_{ik} is the phenotypic value of the k^{th} individual of marker genotype i, b_0 is the population mean (μ), b_1 is the effect of the marker i, x_i is an indicator variable for marker genotype and e_k is the residual error. Single marker analysis is a fast and simple method for QTL detection, but the effects of QTL can be underestimated due to recombination between the marker and the QTL. Interval mapping can be used to more accurately estimate the effect and position of a QTL within an interval. This method places a QTL between two adjacent markers and varies the position of the QTL between them, reporting a LOD score for each test position. Interval mapping gives increased power for detecting QTL, but it is not able to account for multiple QTL within an interval, or elsewhere in the genome, which may introduce significant variation within genotypic classes of the marker being considered. Composite Interval Mapping (CIM) (Jansen and Stam, 1994; Zeng, 1994) tackles this problem by including markers linked to background QTL as cofactors in the model. These cofactors partition variation that would otherwise be considered residual into the model.

The results of these regression analyses are expressed as logarithm of the odds (LOD) scores, which compare the likelihood of the null hypothesis (no QTL) with that of the alternative hypothesis (QTL present). Regions of the genome that co-segregate with the measured trait will exhibit a significant peak in the LOD score near the most closely linked markers. Typically, a confidence interval is delineated by noting the points along the significance peak where the LOD score is 1 unit below its maximum for the interval. Also important are the effect estimates for each QTL, which are calculated by comparing the means for the genotypic classes of a given marker and estimating additive and dominance effects based on the mean of the heterozygote. Finally, the square of the partial correlation coefficient (R^2) is used to estimate the proportion of phenotypic variance explained by a given QTL.

Confirming QTL and Identifying Causative Genetic Factors

Regression mapping is a powerful method for detecting QTL within a population, however the magnitude of the effects and their significance must ultimately be confirmed by examining each QTL in isolation. One way to achieve this is through the use of heterozygous inbred families (HIFs). As previously mentioned, RILs that are generated by random mating and subsequent selfing are homozygous for most loci in the genome. However, residual heterozygosity is present at a low frequency for some loci. By screening for rare heterozygotes at a closely linked marker, it may be possible to identify RIL families that are segregating for a QTL of interest, but remain fixed elsewhere, making it possible to examine the QTL effect in a homogeneous background. When HIFs are not available, QTL isolation can be achieved by repeatedly backcrossing to a parent line in order to generate near isogenic lines (NILs) that segregate for the QTL region, while being fixed elsewhere for genome of the recurrent parent. Both HIFs and NILs are useful for validating QTL effects and both can be used to generate additional recombination in a QTL region, which can be used for fine-mapping of the QTL.

Once a QTL effect has been narrowed to a region containing a small number of genes, it is of interest to identify the specific polymorphism that is responsible for the QTL effect. If the phenotypic effect is thought to result from a non-conservative substitution in the candidate gene, reverse genetics approaches such as transposon tagging or TILLING might be useful for identifying alleles that mimic the phenotype. However, as previously mentioned, many maize genes are redundant and therefore loss-of-function alleles may not elicit visible phenotypes. In this case, transgenic methods might provide the key to proving a causative gene. Numerous transgenic methods exist and determining which approach is most suitable depends on the nature of the candidate gene, allelic interactions at the locus, and interactions with redundant loci or other QTL. In general, however, RNA knockdown has been successfully used in rice to clone QTL that result from the overexpression of respective candidate gene (Ashikari et al., 2005; Huang et al., 2009). Similarly, QTL effects resulting from null mutations or expression differences can be verified by transgenic complementation (Xue et al., 2008). Finally, the growing success of genome editing techniques such as ZF nucleases, TALENs, and CRISPR/Cas might soon provide the opportunity to produce allelic

substitutions (Zu et al., 2013) for candidate genes or generate tailor-made mutations (Ma et al., 2013) that specifically mimic the natural variation. Phenotypic responses elicited by these induced mutations would provide conclusive evidence for a causal variant, which sometimes cannot be achieved through simple transgenic complementation when multiple mutations are present in tight linkage.

QTL resulting from changes to cis-regulatory elements (CREs) or promoters are slightly more difficult to pinpoint, however some methods do exist. As mentioned above, genome-editing techniques are a useful tool for generating alterations to endogenous sequences and techniques such as these could theoretically be used to induce mutations in CREs that mimic those observed in the parent lines. This is only feasible, however, if the CRE has enough unique sequence to exclude off-target effects at the CREs of other genes. With the same caveat, promoter hairpins could be used to generate RNAi-mediated silencing of targeted upstream elements (Cigan and Unger-Wallace, 2012). It is important to note that maize transformation is usually performed using an inbred or hybrid line with an improved transformation efficiency (Frame et al., 2002) and therefore the genomic context of that particular line must be taken into consideration. The recent sequencing of 2800 maize accessions has facilitated the use of association mapping for identifying potential causative SNPs. Association mapping utilizes historical recombination to identify SNPs that are associated with traits of interest. Once a candidate region has been identified, it may be possible to sequence that region across a large set of diverse inbred lines and identify which SNPs are associated with the phenotype. However, even with the high rates of linkage disequilibrium (LD) decay in maize, association analysis may be unable to identify the causal variant from a group of tightly linked polymorphisms (Hung et al., 2012).

RESEARCH GOALS

The identification and mapping of genes that alter inflorescence development has been helpful in understanding the processes regulating inflorescence architecture, however the small overlap between these genes and QTL influencing the inflorescence traits of maize inbreds suggests that many more genes may be involved in this network. The *ramosa* genes, through regulating meristem determinacy, are able to impart novel phenotypes, especially to

the female inflorescence. Furthermore, the phenotypes of these mutants are background-dependent indicating that natural genetic variation plays a role in determining the ultimate phenotype of the individual and signaling that there are other genes involved in regulating inflorescence branching. Therefore, the first research goal was to determine whether alternative methods such as suppressor/enhancer screens and QTL mapping would be able to identify novel loci involved in regulating the inflorescence branch number of *ramosa* mutants. The second objective, as an extension of the first, was to examine the overlap of these loci with known inflorescence genes and QTL identified for tassel branch number in previous studies. Finally, for a few of these loci, we sought to fine-map the loci in order to identify candidate genes that might be responsible for the phenotypic effects.

LITERATURE CITED

Ashikari, M., Sakakibara, H., Lin, S., Yamamoto, T., Takashi, T., Nishimura, A., Angeles, E. R., Qian, Q., Kitano, H. and Matsuoka, M. (2005). Cytokinin oxidase regulates rice grain production. *Science* **309**, 741-5.

Barbazuk, W. B., Emrich, S. J., Chen, H. D., Li, L. and Schnable, P. S. (2007). SNP discovery via 454 transcriptome sequencing. *Plant J* **51**, 910-8.

Barber, W. T., Zhang, W., Win, H., Varala, K. K., Dorweiler, J. E., Hudson, M. E. and Moose, S. P. (2012). Repeat associated small RNAs vary among parents and following hybridization in maize. *Proc Natl Acad Sci U S A* **109**, 10444-9.

Beal, W. J. (1876). In *Report of the Michigan Board of Agriculture*, (ed., pp. 212-213. East Lansing, MI: Michigan State Agricultural College.

Beal, W. J. (1881). In *Report of the Michigan Board of Agrilculture*, (ed., pp. 98-153. East Lansing, MI: Michigan State Agricultural College.

Bortiri, E., Chuck, G., Vollbrecht, E., Rocheford, T., Martienssen, R. and Hake, S. (2006). ramosa2 encodes a LATERAL ORGAN BOUNDARY domain protein that determines the fate of stem cells in branch meristems of maize. *Plant Cell* **18**, 574-85.

Brown, P. J., Upadyayula, N., Mahone, G. S., Tian, F., Bradbury, P. J., Myles, S., Holland, J. B., Flint-Garcia, S., McMullen, M. D., Buckler, E. S. et al. (2011). Distinct genetic architectures for male and female inflorescence traits of maize. *PLoS Genet* **7**, e1002383.

Brunner, S., Fengler, K., Morgante, M., Tingey, S. and Rafalski, A. (2005a). Evolution of DNA sequence nonhomologies among maize inbreds. *Plant Cell* **17**, 343-60.

Brunner, S., Pea, G. and Rafalski, A. (2005b). Origins, genetic organization and transcription of a family of non-autonomous helitron elements in maize. *Plant J* **43**, 799-810.

Buckler, E. S., Gaut, B. S. and McMullen, M. D. (2006). Molecular and functional diversity of maize. *Curr Opin Plant Biol* **9**, 172-6.

Chuck, G. and Bortiri, E. (2010). The unique relationship between tsh4 and ra2 in patterning floral phytomers. *Plant Signal Behav* **5**, 979-81.

Cigan, A. M. and Unger-Wallace, E. (2012). Method for identifying gene function, (ed. U.S.A: Pioneer Hi Bred International Inc.

Duvick, D. N. (1997). What is yield? In *Developing Drought- and Low N-Tolerant Maize*, (ed. G. O. Edmeades M. Banziger and H. R. Mickelson), pp. 332-335. El Batan, Mexico: CIMMYT, Mexico D.F.

Fan, C., Xing, Y., Mao, H., Lu, T., Han, B., Xu, C., Li, X. and Zhang, Q. (2006). GS3, a major QTL for grain length and weight and minor QTL for grain width and thickness in rice, encodes a putative transmembrane protein. *Theor Appl Genet* **112**, 1164-71.

Fonseca, A. E., Westgate, M. E., Grass, L. and Dornbos, D. L. (2003). Tassel morphology as an indicator of potential pollen production in maize. *Crop Management* **Online**.

Frame, B. R., Shou, H., Chikwamba, R. K., Zhang, Z., Xiang, C., Fonger, T. M., Pegg, S. E., Li, B., Nettleton, D. S., Pei, D. et al. (2002). Agrobacterium tumefaciens-mediated transformation of maize embryos using a standard binary vector system. *Plant Physiol* **129**, 13-22.

Gallavotti, A., Long, J. A., Stanfield, S., Yang, X., Jackson, D., Vollbrecht, E. and Schmidt, R. J. (2010). The control of axillary meristem fate in the maize ramosa pathway. *Development* **137**, 2849-56.

Gaut, B. S. and Doebley, J. F. (1997). DNA sequence evidence for the segmental allotetraploid origin of maize. *Proc Natl Acad Sci U S A* **94**, 6809-14.

Geraldi, I. O., Miranda Filho, J.B. Vencovski, R. (1978). Prospects of breeding maize (Zea mays L.) with reference to tassel characters. In *Brazilian Sociey for Scientific Progress*, vol. 30 (ed., pp. 533-534.

Geraldi, I. O., Miranda Filho, J.B. Vencovski, R. (1985). Estimates of ggenetic parameters for tassel characters in maize (Zea mays L.) and breeding perspectives. *Maydica*, 1-14.

Huang, X., Qian, Q., Liu, Z., Sun, H., He, S., Luo, D., Xia, G., Chu, C., Li, J. and Fu, X. (2009). Natural variation at the DEP1 locus enhances grain yield in rice. *Nat Genet* **41**, 494-7.

Hung, H. Y., Shannon, L. M., Tian, F., Bradbury, P. J., Chen, C., Flint-Garcia, S. A., McMullen, M. D., Ware, D., Buckler, E. S., Doebley, J. F. et al. (2012). ZmCCT and the genetic basis of day-length adaptation underlying the postdomestication spread of maize. *Proc Natl Acad Sci U S A* **109**, E1913-21.

Hunter, R. B., T.B. Daynard, D.J. Hume, J.W.Tanner, J.D. Curtis, and L.W. Kannenberg. (1969). Effect of tassel removal on grain yield of corn (Zea mays L.). *Crop Sci.* **9**, 405-406.

Jansen, R. C. and Stam, P. (1994). High resolution of quantitative traits into multiple loci via interval mapping. *Genetics* **136**, 1447-55.

Jiao, Y., Wang, Y., Xue, D., Wang, J., Yan, M., Liu, G., Dong, G., Zeng, D., Lu, Z., Zhu, X. et al. (2010). Regulation of OsSPL14 by OsmiR156 defines ideal plant architecture in rice. *Nat Genet* **42**, 541-4.

Jin, J., Huang, W., Gao, J. P., Yang, J., Shi, M., Zhu, M. Z., Luo, D. and Lin, H. X. (2008). Genetic control of rice plant architecture under domestication. *Nat Genet* **40**, 1365-9.

Kellogg, E. A., Camara, P. E., Rudall, P. J., Ladd, P., Malcomber, S. T., Whipple, C. J. and Doust, A. N. (2013). Early inflorescence development in the grasses (Poaceae). *Front Plant Sci* **4**, 250.

Ku, L., Wei, X., Zhang, S., Zhang, J., Guo, S. and Chen, Y. (2011). Cloning and Characterization of a Putative TAC1 Ortholog Associated with Leaf Angle in Maize (Zea mays L.). *PLoS One* **6**.

Li, L., Li, H., Li, Q., Yang, X., Zheng, D., Warburton, M., Chai, Y., Zhang, P., Guo, Y., Yan, J. et al. (2011a). An 11-bp Insertion in Zea mays fatb Reduces the Palmitic Acid Content of Fatty Acids in Maize Grain. *PLoS One* **6**.

Li, L., Petsch, K., Shimizu, R., Liu, S., Xu, W. W., Ying, K., Yu, J., Scanlon, M. J., Schnable, P. S., Timmermans, M. C. et al. (2013). Mendelian and non-Mendelian regulation of gene expression in maize. *PLoS Genet* **9**, e1003202.

Li, Y., Fan, C., Xing, Y., Jiang, Y., Luo, L., Sun, L., Shao, D., Xu, C., Li, X., Xiao, J. et al. (2011b). Natural variation in GS5 plays an important role in regulating grain size and yield in rice. *Nat Genet* **43**, 1266-9.

Liu, S., Wang, X., Wang, H., Xin, H., Yang, X., Yan, J., Li, J., Tran, L. S. P., Shinozaki, K., Yamaguchi-Shinozaki, K. et al. (2013). Genome-Wide Analysis of ZmDREB Genes

and Their Association with Natural Variation in Drought Tolerance at Seedling Stage of Zea mays L. *PLoS Genet* **9**.

Ma, N., Liao, B., Zhang, H., Wang, L., Shan, Y., Xue, Y., Huang, K., Chen, S., Zhou, X., Chen, Y. et al. (2013). TALEN-mediated gene correction in integration-free beta-thalassemia iPSCs. *J Biol Chem*.

Makarevitch, I., Eichten, S. R., Briskine, R., Waters, A. J., Danilevskaya, O. N., Meeley, R. B., Myers, C. L., Vaughn, M. W. and Springer, N. M. (2013). Genomic distribution of maize facultative heterochromatin marked by trimethylation of H3K27. *Plant Cell* **25**, 780-93.

Meghji, M. R., Dudley, J. W., Lambert, R. J. and Sprague, G. F. (1984). Inbreeding depression, inbred and hybrid grain yields, and other traits of maize genotypes representing three eras. *Crop Sci.* **24**, 545-549.

Miura, K., Ikeda, M., Matsubara, A., Song, X. J., Ito, M., Asano, K., Matsuoka, M., Kitano, H. and Ashikari, M. (2010). OsSPL14 promotes panicle branching and higher grain productivity in rice. *Nat Genet* **42**, 545-9.

Paschold, A., Jia, Y., Marcon, C., Lund, S., Larson, N. B., Yeh, C. T., Ossowski, S., Lanz, C., Nettleton, D., Schnable, P. S. et al. (2012). Complementation contributes to transcriptome complexity in maize (Zea mays L.) hybrids relative to their inbred parents. *Genome Res* **22**, 2445-54.

Qi, P., Lin, Y. S., Song, X. J., Shen, J. B., Huang, W., Shan, J. X., Zhu, M. Z., Jiang, L., Gao, J. P. and Lin, H. X. (2012). The novel quantitative trait locus GL3.1 controls rice grain size and yield by regulating Cyclin-T1;3. *Cell Res* **22**, 1666-80.

Riedel, C., Habekuss, A., Schliephake, E., Niks, R., Broer, I. and Ordon, F. (2011). Pyramiding of Ryd2 and Ryd3 conferring tolerance to a German isolate of Barley yellow dwarf virus-PAV (BYDV-PAV-ASL-1) leads to quantitative resistance against this isolate. *Theor Appl Genet* **123**, 69-76.

Romay, M. C., Millard, M. J., Glaubitz, J. C., Peiffer, J. A., Swarts, K. L., Casstevens, T. M., Elshire, R. J., Acharya, C. B., Mitchell, S. E., Flint-Garcia, S. A. et al. (2013). Comprehensive genotyping of the USA national maize inbred seed bank. *Genome Biol* **14**, R55.

Salvi, S., Sponza, G., Morgante, M., Tomes, D., Niu, X., Fengler, K. A., Meeley, R., Ananiev, E. V., Svitashev, S., Bruggemann, E. et al. (2007). Conserved noncoding genomic sequences associated with a flowering-time quantitative trait locus in maize. *Proc Natl Acad Sci U S A* **104**, 11376-81.

Satoh-Nagasawa, N., Nagasawa, N., Malcomber, S., Sakai, H. and Jackson, D. (2006). A trehalose metabolic enzyme controls inflorescence architecture in maize. *Nature* **441**, 227-30.

Schnable, J. C. and Freeling, M. (2011). Genes identified by visible mutant phenotypes show increased bias toward one of two subgenomes of maize. *PLoS One* **6**, e17855.

Schnable, J. C., Springer, N. M. and Freeling, M. (2011). Differentiation of the maize subgenomes by genome dominance and both ancient and ongoing gene loss. *Proc Natl Acad Sci U S A* **108**, 4069-74.

Schnable, P. S. Ware, D. Fulton, R. S. Stein, J. C. Wei, F. Pasternak, S. Liang, C. Zhang, J. Fulton, L. Graves, T. A. et al. (2009). The B73 maize genome: complexity, diversity, and dynamics. *Science* **326**, 1112-5.

Sharma, P. P. a. N. L. D. (1968). Correlation between tassel and ear characters and yield in maize. *Indian J. Genet. Plant Breed.* **28**, 196-204.

Shomura, A., Izawa, T., Ebana, K., Ebitani, T., Kanegae, H., Konishi, S. and Yano, M. (2008). Deletion in a gene associated with grain size increased yields during rice domestication. *Nat Genet* **40**, 1023-8.

Sigmon, B. and Vollbrecht, E. (2010). Evidence of selection at the ramosa1 locus during maize domestication. *Mol Ecol* **19**, 1296-311.

Song, X. J., Huang, W., Shi, M., Zhu, M. Z. and Lin, H. X. (2007). A QTL for rice grain width and weight encodes a previously unknown RING-type E3 ubiquitin ligase. *Nat Genet* **39**, 623-30.

Springer, N. M., Ying, K., Fu, Y., Ji, T., Yeh, C. T., Jia, Y., Wu, W., Richmond, T., Kitzman, J., Rosenbaum, H. et al. (2009). Maize inbreds exhibit high levels of copy number variation (CNV) and presence/absence variation (PAV) in genome content. *PLoS Genet* **5**, e1000734.

Studer, A., Zhao, Q., Ross-Ibarra, J. and Doebley, J. (2011). Identification of a functional transposon insertion in the maize domestication gene tb1. *Nat Genet* **43**, 1160-3.

Stupar, R. M., Hermanson, P. J. and Springer, N. M. (2007). Nonadditive expression and parent-of-origin effects identified by microarray and allele-specific expression profiling of maize endosperm. *Plant Physiol* **145**, 411-25.

Stupar, R. M. and Springer, N. M. (2006). Cis-transcriptional variation in maize inbred lines B73 and Mo17 leads to additive expression patterns in the F1 hybrid. *Genetics* **173**, 2199-210.

Swanson-Wagner, R. A., Jia, Y., DeCook, R., Borsuk, L. A., Nettleton, D. and Schnable, P. S. (2006). All possible modes of gene action are observed in a global comparison of gene

expression in a maize F1 hybrid and its inbred parents. *Proc Natl Acad Sci U S A* **103**, 6805-10.

Tan, L., Li, X., Liu, F., Sun, X., Li, C., Zhu, Z., Fu, Y., Cai, H., Wang, X., Xie, D. et al. (2008). Control of a key transition from prostrate to erect growth in rice domestication. *Nat Genet* **40**, 1360-4.

Tanaka, W., Pautler, M., Jackson, D. and Hirano, H. Y. (2003). Grass meristems II: inflorescence architecture, flower development and meristem fate. *Plant Cell Physiol* **54**, 313-24.

Terao, T., Nagata, K., Morino, K. and Hirose, T. (2010). A gene controlling the number of primary rachis branches also controls the vascular bundle formation and hence is responsible to increase the harvest index and grain yield in rice. *Theor Appl Genet* **120**, 875-93.

Upadyayula, N., da Silva, H. S., Bohn, M. O. and Rocheford, T. R. (2006). Genetic and QTL analysis of maize tassel and ear inflorescence architecture. *Theor Appl Genet* **112**, 592-606.

Vollbrecht, E. and Schmidt, R. (2009). Development of the Inflorescences. In *Handbook of Maize: Its Biology*, (ed. J. L. Bennetzen and S. Hake), pp. 13-40: Springer.

Vollbrecht, E., Springer, P. S., Goh, L., Buckler, E. S. t. and Martienssen, R. (2005). Architecture of floral branch systems in maize and related grasses. *Nature* **436**, 1119-26.

Wang, E., Wang, J., Zhu, X., Hao, W., Wang, L., Li, Q., Zhang, L., He, W., Lu, B., Lin, H. et al. (2008). Control of rice grain-filling and yield by a gene with a potential signature of domestication. *Nat Genet* **40**, 1370-4.

Wang, H., Nussbaum-Wagler, T., Li, B., Zhao, Q., Vigouroux, Y., Faller, M., Bomblies, K., Lukens, L. and Doebley, J. F. (2005). The origin of the naked grains of maize. *Nature* **436**, 714-9.

Wei, X., Xu, J., Guo, H., Jiang, L., Chen, S., Yu, C., Zhou, Z., Hu, P., Zhai, H. and Wan, J. (2010). DTH8 suppresses flowering in rice, influencing plant height and yield potential simultaneously. *Plant Physiol* **153**, 1747-58.

Wills, D. M., Whipple, C. J., Takuno, S., Kursel, L. E., Shannon, L. M., Ross-Ibarra, J. and Doebley, J. F. (2013). From many, one: genetic control of prolificacy during maize domestication. *PLoS Genet* **9**, e1003604.

Woodhouse, M. R., Schnable, J. C., Pedersen, B. S., Lyons, E., Lisch, D., Subramaniam, S. and Freeling, M. (2010). Following tetraploidy in maize, a short deletion mechanism removed genes preferentially from one of the two homologs. *PLoS Biol* **8**, e1000409.

Xue, W., Xing, Y., Weng, X., Zhao, Y., Tang, W., Wang, L., Zhou, H., Yu, S., Xu, C., Li, X. et al. (2008). Natural variation in Ghd7 is an important regulator of heading date and yield potential in rice. *Nat Genet* **40**, 761-7.

Yan, W. H., Wang, P., Chen, H. X., Zhou, H. J., Li, Q. P., Wang, C. R., Ding, Z. H., Zhang, Y. S., Yu, S. B., Xing, Y. Z. et al. (2011). A major QTL, Ghd8, plays pleiotropic roles in regulating grain productivity, plant height, and heading date in rice. *Mol Plant* **4**, 319-30.

Zeng, Z. B. (1994). Precision mapping of quantitative trait loci. *Genetics* **136**, 1457-68.

Zha, X., Luo, X., Qian, X., He, G., Yang, M., Li, Y. and Yang, J. (2009). Over-expression of the rice LRK1 gene improves quantitative yield components. *Plant Biotechnol J* **7**, 611-20.

Zhang, B., Shi, W., Li, W., Chang, X. and Jing, R. (2013). Efficacy of pyramiding elite alleles for dynamic development of plant height in common wheat. *Mol Breed* **32**, 327-338.

Zheng, P., Allen, W. B., Roesler, K., Williams, M. E., Zhang, S., Li, J., Glassman, K., Ranch, J., Nubel, D., Solawetz, W. et al. (2008). A phenylalanine in DGAT is a key determinant of oil content and composition in maize. *Nat Genet* **40**, 367-72.

Zu, Y., Tong, X., Wang, Z., Liu, D., Pan, R., Li, Z., Hu, Y., Luo, Z., Huang, P., Wu, Q. et al. (2013). TALEN-mediated precise genome modification by homologous recombination in zebrafish. *Nat Methods* **10**, 329-31.

TABLE 1

Cloned grain yield related QTL in rice

Yield component[a]	QTL/Gene	Causal mutation	Location	Reference
GN*	*Gn1a***	Deletion, substitution	CDS	(Ashikari et al., 2005)
GN*	*Ghd7*	Deletion	CDS	(Xue et al., 2008)
GN*	*Ghd8/DTH8*	Frameshift	CDS	(Wei et al., 2010; Yan et al., 2011)
GN*	*DEP1***	Premature stop	CDS	(Huang et al., 2009)
GN*	*APO1***	Substitution	Upstream	(Terao et al., 2010)
GN/TN*	*LRK1*	Over-expression	Unknown	(Zha et al., 2009)
GN/TN*	*PROG1*	Substitution	CDS	(Jin et al., 2008; Tan et al., 2008)
GN/TN*	*IPA1/WFP1***	Substitution	MiR binding site	(Jiao et al., 2010; Miura et al., 2010)
GW	*GIF1*	Premature stop	CDS	(Wang et al., 2008)
GW	*GW2*	Premature stop	CDS	(Song et al., 2007)
GW	*GS3*	Premature stop	CDS	(Fan et al., 2006)
GW	*GS5*	Substitution	Upstream	(Li et al., 2011b)
GW	*qSW5/GW5*	Deletion	CDS	(Shomura et al., 2008; Wang et al., 2008)
GW	*GL3.1*	-	-	(Qi et al., 2012)

[a] GN, Grain number per tiller; TN, Tiller number; GW, Grain weight

* Panicle branching affected

** Functions in inflorescence development pathway

TABLE 2

Cloned QTL in maize

QTL/Gene	Trait	Variant location	Reference
*tb1**	Plant architecture	Upstream	(Studer et al., 2011)
*gt1**	Plant architecture	Upstream	(Wills et al., 2013)
*tga1**	Kernel enclosure	CDS	(Wang et al., 2005)
vgt1	Flowering Time	Upstream	(Salvi et al., 2007)
ZmCCT	Flowering time	CDS	(Hung et al., 2012)
DGAT	Kernel oil content	CDS	(Zheng et al., 2008)
fatb	Kernel oil content	Upstream	(Li et al., 2011a)
ZmTAC1	Leaf angle	UTR	(Ku et al., 2011)
ZmDREB2.7	Drought tolerance	Upstream	(Liu et al., 2013)

* Domestication QTL

FIGURE LEGEND

Figure 1. Development of maize inflorescences. A) Mature male inflorescence, or tassel. B) Immature maize tassel (1mm length), C) Mature female inflorescence, or ear, D) Immature maize ear (1mm length), E) Diagram of inflorescence development in maize, starting with the vegetative meristem and ending with the floral meristem. The formation of long branches is normally specific to the tassel. The figure illustrates the striking similarities between the development of male and female inflorescences.

Figure 1 Weeks

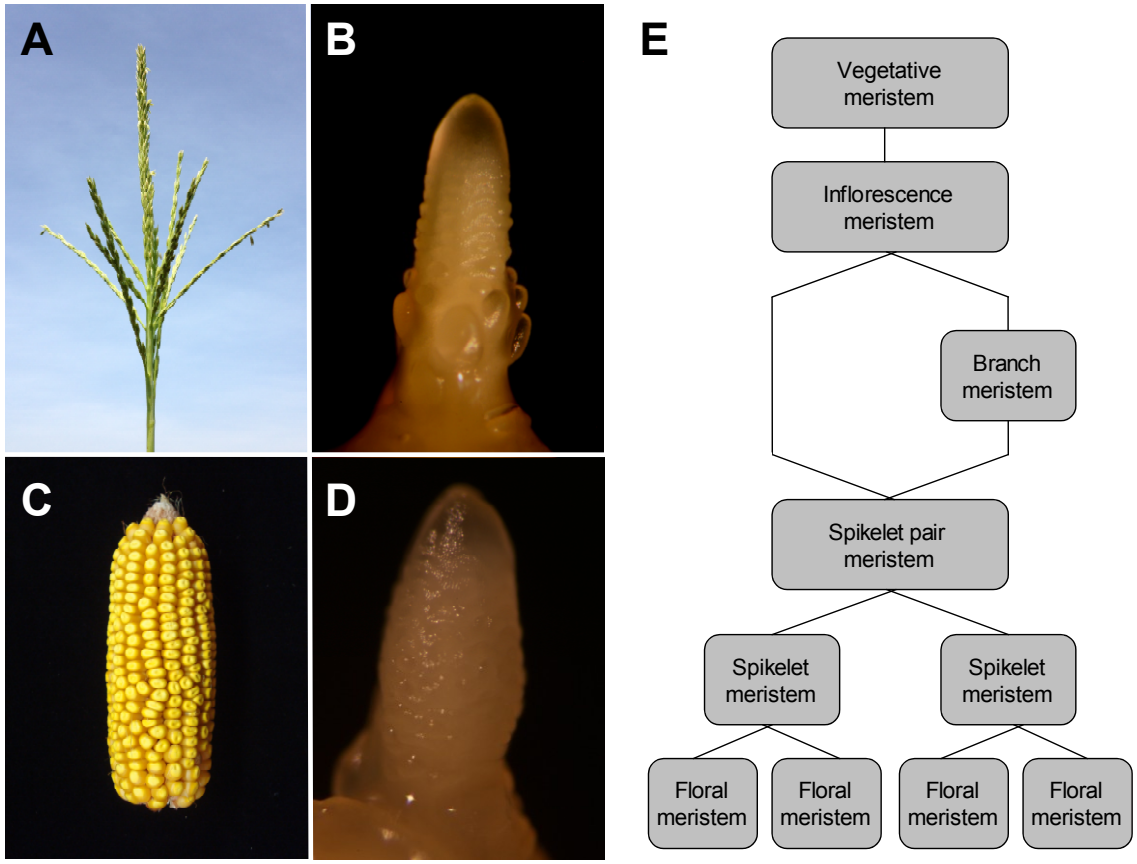

CHAPTER 2. IDENTIFICATION AND MAPPING OF EMS-INDUCED MODIFIERS OF BRANCHING IN *RAMOSA* MUTANTS

A manuscript to be submitted to *G3*

Rebecca Weeks, Erica Unger-Wallace, Stacey Barnes and Erik Vollbrecht

ABSTRACT

Inflorescence branching in maize has long been recognized as an important factor impacting grain yield. The isolation and characterization of maize mutants with perturbed inflorescence branching is helping to understand genetic pathways through which inflorescence branch number is determined. Among mutants that have been isolated, those in the the *ramosa* class display a loss in determinacy of spikelet pair meristems leading to an increase in branch number in the tassel and ear. To uncover additional factors impacting inflorescence branching, we performed suppressor/enhancer screens using *ramosa1* and *ramosa2* mutants and uncovered a number of extragenic mutations that altered the phenotypes of *ramosa* tassels and ears. Bulked segregant mapping (BSA) was used to determine the rough location of each gene. While several of the mutations mapped to genes previously noted for their roles in inflorescence development, a number of the putative mutants mapped to areas of the genome not known for harboring inflorescence branching genes. Fine-mapping is currently underway for several of these novel inflorescence branching mutants.

INTRODUCTION

The architecture of the maize inflorescence can be explained, in large part, by the fate of lateral meristems borne along its central rachis. In the male inflorescence, a few of these meristems are indeterminant and will go on to produce long branches at the base of the tassel. The lateral meristems of the female inflorescence, however, are determinant, resulting in unbranched ears with tightly packed kernels. The *ramosa* genes (*ra1, ra2, ra3*) have been characterized as key players controlling the determinacy of lateral meristems in the

inflorescences of maize. Tassels of *ramosa* mutants display increased branching and mutant ears exhibit unorganized rows and/or lateral branching. All three *ramosa* genes have been cloned; *ra1* encodes a cys2-his2 zinc finger transcription factor (Vollbrecht et al., 2005), *ra2* encodes a LATERAL ORGAN BOUNDARY (LOB) domain transcription factor (Bortiri et al., 2006), and *ra3* encodes a trehalose-6-phosphate phosphatase metabolic enzyme (Satoh-Nagasawa et al., 2006). Expression and double mutant analyses suggest a pathway where *ra2* and *ra3* function in parallel to stimulate the expression of *ra1* and ultimately impose determinacy on lateral meristems of the inflorescence. In addition, the *TOPLESS*-like gene *ramosa enhancing locus2* (*rel2*) has been shown to physically interact with *ra1* and plays an important role in suppression of branch formation in inflorescences (Gallavotti et al., 2010).

For decades, forward mutagenesis has proven to be an effective tool for generating novel maize mutants whose phenotypes can then be meticulously characterized so that the function of causative genes may be deduced. With the advent of genomics tools and positional cloning, gene function has also been readily linked to molecular mechanism. In recent years, however, it has become increasingly difficult to identify novel genes involved in inflorescence branching. Attempts to generate new mutants frequently turn up new alleles of previously cloned genes and very few novel inflorescence branching mutants. Any number of possible explanations might account for the deficiency of new mutants to emerge from forward genetic screens. It is possible, for example, that most of the major genes in this pathway have already been discovered or that the remaining players are recalcitrant to mutagenesis, either because their chemical structure is resistant to traditional mutagenesis techniques or because redundant genes in the genome compensate for the loss of the mutated gene. It is also possible that when mutated, some pathway genes confer phenotypes that are difficult to detect, either because they lead to lethality or because they are so subtle that they go unnoticed.

Suppressor/enhancer screens are one method of identifying mutants whose phenotypes are subtle or undetectable through traditional forward mutagenesis. The approach of such a screen is to establish conditions under which these mutations might have a strong phenotypic effect. Seminal enhancer screen experiments were successfully executed decades ago in Drosophila, to identify components in the signal-transduction pathway

downstream of the receptor tyrosine kinase *sevenless* (*sev*), that controls cell fate decisions between photoreceptor cells and non-neuronal cone cells of the compound eye (reviewed in (Simon, 1994)). In these early screens, a weak mutant allele of *sev* provided a sensitized background on which the phenotypes of second site, novel mutations could easily be detected (Simon et al., 1991). This method of screening proved especially useful because mutagenized flies could be screened directly since hypomorphic alleles behaved as dominants on the sensitized background. Additionally, lethal mutations in essential genes could be identified since the sensitized background only affected the R7 cell of the ommatidia, the structural units that make up the compound eye of arthropods. Using this method, Simon et al. were able to identify seven mutant genes that attenuated signaling by *sevenless*. The novel mutations were called *Enhancers of sevenless* because they exacerbated the mutant phenotype of the *sevenless* allele. Rogge et al. used a stronger *sev* hypomorphic mutation to identify mutants that increased the number of R7 cells (Rogge et al., 1991). Alleles isolated from this screen were called *Suppressors of sevenless* because they ameliorated the *sevenless* phenotype. Finally, Olivier et al. were able to identify still more components of the *Sev* pathway by screening for suppression of the rough-eye phenotype conferred by the gain-of-function Sev^{S11} allele (Olivier et al., 1993). Taken together, these studies successfully identified twenty-one novel components of the *sevenless* signaling pathway, many of which were essential for viability and thus would have otherwise gone undiscovered.

We employed a similar approach to identify additional components of the inflorescence branching pathway. Suppressor/enhancer screens were performed using the *ra1-63.3359* and *ra2-R* alleles. Backgrounds were chosen in order to facilitate easy identification of enhanced phenotypes. For example, in the Mo17 background, the tassels of *ra1-63.3359* mutants display a subtle phenotype (Figure 1A), with only a few extra branches present in the transition zone, the area of the tassel where lateral meristems switch from making the long branches to short spikelet pairs. The phenotype of *ra1-63.3359* ears in Mo17 is even more subtle (Figure 1G), with mutants displaying somewhat crooked rows and rarely a branch. For the *ra2-R* allele, the A619 background was chosen because of its weak ear phenotype (Figure 2G). While mutant ears can be characterized by their long staminate

tips, row disorganization is uncommon and branching is very rare. Using these weak baselines, extragenic mutations that enhance branch number should be easily detected by observing tassel branch number (TBN) and dissecting ears to screen for increased ear branch number (EBN.)

To facilitate the identification of branching suppressors, the Illinois High Oil population was used. This population was derived from the long-term selection experiment performed at the University of Illinois, during which mass selection was performed for high or low kernel oil content (IHO and ILO, respectively) and high or low protein (IHP and ILP, respectively) (Alrefai et al., 1995; Dudley, 2004). Within the IHO and ILO populations, divergence in oil content has been accompanied by changes in tassel branch number and angle, and total tassel weight (Berke and Rocheford, 1999). In particular, recent selections of IHO have developed highly branched tassels, often resembling a strong *ra1* mutant (Figure 3A). While IHO possesses a common *ra1* haplotype (Vollbrecht, unpublished), allele tests with the mutant allele *ra1-R* result in non-complementation (Figure 3E-H) and preliminary expression analyses suggest a later onset of *ra1* expression in IHO individuals (Vollbrecht, unpublished), which might explain the presence of an elongated branch zone. Furthermore, mapping of inflorescence traits in IHO vs ILO populations has revealed significant QTL for branch number and angle on chromosome 7 near the genetic location of *ra1* (Berke and Rocheford, 1999). Lastly, when introgressed into a B73 background, *ra1-IHO* double mutant analyses with *ra2-R* and *ra3-R* reveal synergistic interactions (Figure 3C,D). Despite this evidence of perturbed *ra1* expression and/or function, the ears of IHO per se are unbranched (Figure 3B), which makes them especially useful for carrying out suppressor screens. Whereas tassels of strong *ra1* mutants might also afford easy scoring of suppressed phenotypes, the highly branched ears invariably associated with strong *ra1* mutants make for poor seed production and thus difficult genetics. IHO, on the other hand, delivers both a useful backdrop for identifying suppressors and a means for relatively unhindered seed production. Furthermore, in the event that an enhancer is found, phenotypes can also be characterized using the ear, which would be difficult in a strong *ra1* mutant background.

Using this approach, we were able to identify twenty-two putative mutants that either suppress or enhance the phenotypes of the sensitized *ramosa* backgrounds. While several of

the identified mutants share genetic locations with previously characterized genes, many appear to be unique. In this study, we present data on the characterization and mapping of these novel inflorescence branching mutants.

MATERIALS AND METHODS

To generate populations segregating for suppressors and enhancers, we used the following alleles: *ra1-63.3359* introgressed into Mo17, *ra2-R* introgressed into A619 (Bortiri et al., 2006), and the 90th cycle of the Illinois High Oil line, which originated from a selection of Burr's White. Pollen was collected from *ra1-63.3359*, *ra2-R* or *IHO* individuals and treated with 0.06% ethyl methanesulfonate (EMS) in paraffin oil according to Neuffer (Neuffer, 1994). The resulting M1s were scored for dominant phenotypes and self-fertilized to generate M2 progeny. For each M2 family, 40 kernels were planted in two adjacent rows of 20 kernels each. Mutants from families segregating for putative suppressors or enhancers of inflorescence branch number were crossed to polymorphic inbred lines and the F1s self-fertilized or backcrossed to generate populations for mapping.

To locate the rough map location of each mutant, bulked segregant mapping (Michelmore et al., 1991) was performed using the Sequenom™ MassARRAY™ (Liu et al., 2010). Plant tissue was collected using a 6mm hole punch to ensure uniformity of individual tissue samples within bulks. Depending on the size of the population and ease of scoring (only confidently scored mutant individuals were chosen for sampling), the number of individuals per bulk ranged from 12-100, with an average of approximately 50 individuals. All plants were punched an equal number of times, with punch count per plant adjusted to achieve a total of at least 150 punches per bulk. The leaf tissue was ground in liquid nitrogen and DNA was extracted using a CTAB-based protocol. Sequenom genotyping was used to compare the segregation of approximately one thousand markers between bulks (Performed by the Genomic Technologies Facility at Iowa State). This technology utilizes multiplex PCR followed by a single base primer extension reaction and finally, product analysis by mass spectrometry. The results can be easily interpreted using an excel spreadsheet like the sample shown in Table. Area1 and Area2 are the mass spectrometer reads for each of the two marker alleles. Dividing them produces the marker segregation ratios for each bulked

sample. Linkage is detected by comparing the segregation ratios of the mutant and wildtype bulks. Markers that are not linked to the gene of interest will segregate at equal ratios in both bulks whereas linked markers will show biased segregation. This bias is reflected in the mutant:wildtype ratio or its inverse, wildtype:mutant. Larger ratios in either of these columns indicate closer linkage with the gene (Figure 5).

To better visualize the results of the BSA analyses, the following transformation was applied; $ratio_{diff}^2 = (mutant{:}wildtype - wildtype{:}mutant)^2$. As previously mentioned, unlinked markers will segregate at roughly a 1:1 ratio in both pools and thus taking a difference of the ratios will yield small number that when squared, trends to zero. Markers linked to the mutation will show biased segregation between pools yielding a difference in ratios that is amplified by squaring. After calculating $ratio_{diff}^2$, a sliding window average was computed on 20 centimorgan (cM) windows with a 1cM step. The results were plotted in Microsoft Excel to aid in visualizing the peaks.

In cases where a map location was revealed through BSA, additional markers were identified (http://www.maizegdb.org; (Schaeffer et al.)) and run on individual mutants from the population. Four leaf punches were collected from each mutant individual and the DNA extracted in 96-well format using the Whatman GF/F UNIFILTER 96-well plates. Primer sequences and protocols for each marker assay were obtained from http://www.maizegdb.org (Schaeffer et al.) and run using the GoTaq® Green PCR kit. Most assays were resolved on 3% MetaPhor™ (Lonza) + 1% agarose gels run at 60 volts for 3-6 hours, depending on the size of the products.

RESULTS

To date we have screened 2,843 M2 families and have identified nineteen putative enhancers and three suppressors from the *ra1-63.3359*, *ra2-R* and IHO populations (Table 2). Photos from a select group of mutants are shown in Figures 1 and 2. Putative enhancers were given the temporary gene identifier *ramosa enhancing locus* (rel*)* and an allele designation composed of the two digit year and the four digit plot number of the M2 from which the mutant phenotype was first observed. Putative suppressors were temporarily named *ramosa suppressing locus* (rsl*)* with the same system used for allele designations. Of the twenty-

two modifiers identified, ten have been mapped using BSA. Five of these mapped to regions known to harbor previously cloned inflorescence genes. *rel*-08.0167* and *rel*-09.5171* mapped to a region on Chr.6 (Figure 5) within which resides a gene named *fasciated4 (fea4)*, which has recently been cloned by a collaborator. Complementation tests between the two *rel** mutants confirmed that they are indeed allelic and sequencing of the *fea4* gene revealed lesions in both alleles. *rel*-09.5171* introduces an early stop codon predicted to generate a truncated protein and *rel*-07.0167* contains a synonomous mutation in the coding sequence of the gene. Because the protein sequence is unaltered, it is unclear how this mutation perturbs gene function, however it is possible that the mutation generates a rare codon or disrupts a regulatory binding site in the mRNA. It is also possible that the causative lesion actually lies outside of the sequenced region, and the synonymous mutation was simply carried along through linkage.

BSA mapping of *rel*-08.0116* yielded a peak on Chr. 7 in close proximity to the genetic location of *ramosa3* (Figure 5). Allelism tests were performed with the mutant allele *ra3-R* and the F1 failed to complement. Next, we self-pollinated individuals from the allele test to confirm that the phenotype was not due to non-allelic non-complementation. Progeny from these crosses all displayed *ramosa3* phenotypes indicating that the phenotype was indeed caused by allelism between *rel*-08.0116* and *ra3-R*.

After closer inspection of the *rel*-09.6823* phenotype in subsequent generations, it was not surprising that it mapped to the long arm of Chr. 7 (Figure 5) very near to the genetic location of the *branched silkless1 (bd1)* gene, which is known to cause indeterminacy in spikelet meristems of the tassel and ear (Chuck et al., 2002). A lesion in *bd1* would explain the sterile phenotype in the ear as mutations in *bd1* cause female spikelets to be replaced by branches. The thick branches observed in the tassels of *rel*-09.6823* mutants are also consistent with the phenotype of the *bd1-ref* tassel in which spikelet meristems become indeteriminate and produce several lateral spikelets causing the tassel to appear thick (Chuck et al., 2002). While the phenotype and general map location of the *rel*-09.6823* mutation seem to suggest allelism with *bd1*, complementation tests have not been performed, nor has the gene been sequenced to confirm the presence of a lesion. Additional work is needed to conclusively determine if the new mutant is indeed an allele of *bd1*.

The upright tassel phenotype of the *rel*-09.6415* mutant led us to wonder if it could be allelic to a recently cloned *ra1* enhancing mutant named *ramosa enhancing locus2 (rel2),* which encodes a *TOPLESS*-like protein that was shown to physically interact with the *ra1* protein (Gallavotti et al., 2010). The *rel*-09.6415* mutant, which was isolated from the IHO suppressor/enhancer screen, was crossed to the inbreds A632, B73 and Mo17. A variety of novel phenotypes, many not yet described in the literature, were observed in these mapping populations. In A632, the mutants had upright tassels, unelongated internodes in the stem, and top leaves lacking midveins. In B73, the tassels were again upright and some mutants displayed unelongated internodes, but many mutants also lacked auricles and in most cases they were earless. Like other backgrounds, mutants in the Mo17 mapping population often had suppressed ears (either absent or very low on the stalk) and compact internodes. However, a portion of the mutants displayed a novel tassel phenotype. These individuals had tassel branches with a seemingly normal branch angle, however the internodes of the tassel were elongated. Some of these elongated internodes were bent, causing the tassel to tilt near the base (not shown). Individuals from these two mutant classes (upright, not upright but internodes elongated) were bulked separately for BSA. All four Mut-WT comparisons (A632 rel*, B73 rel*, Mo17 rel* upright, Mo17 rel* elongated) yielded peaks on Chr. 10, very near the location of *rel2* (Figure 6). A complementation test confirmed allelism between *rel*09.6415* and *rel2*, however DNA sequencing has yet to uncover an underlying lesion despite sequencing all 16 exons of the gene. However, it is possible that the lesion lies in a non-coding region where it alters regulation or splicing, or disrupts binding of a protein or miRNA.

The remaining five genes mapped to regions of the genome not associated with any published inflorescence genes. *rel*-09.5195* mapped to the short arm of chromosome 2 (Figure 6). Using approximately 350 mutant individuals, we mapped the mutant gene to the region between markers idp4437 and umc1635 on chromosome 2. Preliminary analysis of double mutants from the original mapping population suggests varied effects in *ra2-R* and non-*ra2-R* backgrounds. As was originally observed in the M2, the *rel*-09.5195* mutant phenotype enhances tassel branching in *ra2-R* individuals. In the absence of *ra2-R*, however, tassels have fewer branches (Figure 8) and often display barren nodes or thread-like

structures in the place of lateral branches. Recently, a group has reported the cloning of the *barrenstalk2 (ba2)* mutant in maize, which was originally described in the 1920's as having absent ear shoots and erect tassel branches (Hofmeyr, 1931). The genome coordinates presented closely align with the mapped position of *rel*-09.5195* and the allele used in *ba2* cloning reportedly came from the same population as *rel*-09.5195*. The *ba2* gene indeed lies within the mapping interval we identified on chromosome 2, but additional work is needed to confirm if *rel*-09.5195* is actually an allele of *ba2.*

Given the upright tassel phenotype of the *rel*11-7978* mutant, we originally suspected it might be yet another mutant allele of *rel2*. However, BSA mapping revealed a peak on chromosome 9 (Figure 6), not on chromosome10 where *rel2* resides. While there is a putative homeolog of *rel2* on chromosome 9, the peak does not overlap with that location. Fine-mapping is currently being performed on a pool of 130 individuals.

The last of the mapped mutants *rel*-09.5068*, *rel*-11.0327* and *rel*-11.0253* did not yield clear results from BSA (Figure 7). The *rel*09-5068* phenotype was subtle and scoring of mutant and normal individuals was based on a visual classification of tassels as "enhanced" or "non-enhanced". It is likely that this population would have benefited from a more quantitative scoring approach. We suspect the *rel*-11.0253* BSA mapping failed because only twelve mutants were available for sampling. The phenotype of this mutant, however, is quite striking and it appears segregate in a semi-dominant fashion. We intend to plant a larger population in the future and resample for BSA. The failure of the *rel*-11.0327* BSA was perplexing, given the ease of scoring and abundance of individuals used for sampling (N=100/bulk.) However, the mutant/normal bulks were processed on a plate with five other mapping populations all of which yielded poor results. While results can usually be obtained with a mass spectrometer area cutoff of 12 to 15, cutoffs on this plate were necessarily lowered to four, in some cases, before any peaks were observed. We intend to replant this population and resample for additional mapping.

Finally, there was one mutant for which a mapping population was planted, but BSA was not conducted. The *rel*-11.0823* was noted in 2011 as having increased ear branch number with tassels bearing short, pointy branches and some bare nodes, which is often characterized as barren inflorescence or bif-like. We were particularly interested in this

mutant because *ramosa* modifiers tend to have positively correlated tassel and ear branch numbers. *rel*-11.0823* is the only mutant we have observed that displays opposite branching effects in the male and female inflorescences. The challenge in mapping this mutant lies in the subtlety of the inflorescence phenotypes. The reduced tassel branch length and overall bif-like nature of the tassel were obvious in the Mo17 background, however, these elements disappeared in the hybrid Mo17 by B73 mapping population, presumably because they became confounded by the natural bif-like appearance of B73 tassels. Additionally, while the increased branching of the mutant ears was obvious on the backdrop of a weak *ra1* phenotype, the ear phenotype in the mapping population was difficult to score, as the B73 background enhances ear branching in *ra1* mutants. Thus, the phenotypes of *rel** mutants segregating in the population were indistinguishable from *ra1* mutants segregating for one or two B73 modifiers. A different mapping strategy is necessary, in which one can clearly identify the mutants.

DISCUSSION

To identify novel components of the inflorescence branching pathway we performed a suppressor/enhancer screen using the *ramosa* mutants of maize. The screen exploited the sensitized *ramosa* backgrounds in order to uncover novel mutations whose phenotypes might otherwise be too subtle to detect in a traditional forward genetics screen. In total, twenty-two mutants were identified, ten of which were subsequently mapped by bulked segregant analysis. These ten mutants represent four novel and six previously cloned inflorescence mutants, three of which have been cloned only recently.

The suppressor/enhancer screen is a method that identifies subtle mutant phenotypes by placing them in conditions under which weak mutations might have strong phenotypic consequences. The use of weak alleles such as *ra1-63* and *ra2-R* was essential to identifying enhancers of inflorescence branching because the phenotypes of these mutations are subtle and thus mutations that exacerbate their phenotypes can easily be identified. By contrast, the IHO background was useful for identifying suppressors of inflorescence branching because it allowed for the identification of mutants that suppressed the highly branched phenotype of the IHO tassel.

The goal of this study was to identify novel components of the inflorescence development pathway. However, in any untargeted forward genetics screen, it is to be expected that new alleles of previously characterized genes will be identified. The key in dealing with this issue is to recognize and cull such mutants before too many resources are expended to map them. This can be accomplished either by sequencing candidate genes from mutant M2 individuals or by running markers linked to a panel of candidate genes in the F2 mapping phase. The latter strategy is likely to be the most comprehensive and cost-effective strategy for identifying which mutants represent new alleles of previously cloned genes.

While the identification of known inflorescence mutants, and subsequent time spent mapping them, distracts from the goal of identifying novel genes in the inflorescence branching pathway, the detection of mutants such as *ra3* and *rel2*, both of which have weak phenotypes alone, demonstrates the utility of the suppressor/enhancer screen. Only when *ra1* is mutated, does *ra3* bear a striking inflorescence branching phenotype. Likewise with the gene *rel2*, whose reference allele was also identified from a suppressor/enhancer screen using the allele *ra1-RS* (Gallavotti et al., 2010). By creating a suitable backdrop for weak mutations such as these, one can facilitate conditions under which these phenotypes become apparent and are easily identified.

Positional cloning is typically performed by crossing a mutant to a distantly-related line and self-pollinating or backcrossing to generate a population segregating for the mutant phenotype. In distant crosses, however, parent lines may differ at many loci, causing the F2 phenotypic to follow a Gaussian rather than a discrete distribution (Baulcombe, 2010). This is of little consequence for monogenic phenotypes with strong phenotypic effects. However, the mapping of polygenic traits can be confounded by the segregation of additional loci that are polymorphic in the parent lines. The presence of these loci reduces the total number of individuals that can be classified since only the tails of the distribution can be confidently scored as mutant or wild-type. Moreover, because half of the F2 will be heterozygous for a given locus, heterosis may further impede mapping by altering the expressivity of the mutant phenotype.

These considerations are especially important when mapping inflorescence branching mutants as inflorescence branch number is polygenic (Berke and Rocheford, 1999; Mickelson et al., 2002; Upadyayula et al., 2006) and has a known heterotic effect (Yao et al., 2013). Two of our mutants showed striking effects in the Mo17 parent line that were obscured once crossed to B73. This was not surprising since natural modifiers of *ra1* are known to be present in B73 and efforts to map them are currently underway (Chapter 3). However, the difficulty in mapping these mutants illustrates the need for a better strategy to isolate the causal mutations underlying inflorescence branching phenotypes. Recently, several groups have utilized whole genome resequencing to isolate the mutations responsible for complex or polygenic traits (Abe et al., 2012; Austin et al., 2011; Lindner et al., 2012; Schneeberger et al., 2009). In this method, an EMS-induced mutant is backcrossed to the non-mutagenized cultivar from which it was derived. The resulting F1 is self-fertilized and the F2 population scored for the mutant phenotype. Because the mapping occurs within a single cultivar, polymorphism is limited to the causal mutation and any background mutations that arose through mutagenesis. Mapping is performed by observing the segregation of SNPs present in the mutant and wild-type bulks. Like conventional BSA, SNPs linked to the causal mutation will deviate from the 1:1 segregation ratio expected for unlinked regions. By generating clusters of 4-5 consecutive SNPs, genome coverage can be reduced to 10-15X without increasing the rate of false positives, due largely to the fact that the probability of observing a cluster of SNPs not linked to the causal mutation, but each displaying biased segregation approaches zero as the number of number of SNPs in the cluster increases. The benefits of this method are many, including reduced ambiguity of F2 phenotypes, increased resolution of map results and faster identification of causal genes. In cases where sufficient seed can be produced from a single M1 plant, mapping may even be possible in the M2 per se. With success stories of sequencing-based cloning approaches mounting, the use of this method for future suppressor/enhancer cloning efforts is being taken under serious consideration.

The novel inflorescence mutants that have emerged from this study give proof to the effectiveness of suppressor/enhancer screens in bringing about conspicuous phenotypes from subtle mutations. As we continue to explore the gene space of maize, methods such as these

are vital to further expand our understanding of the functional roles that these genes play throughout development. It is important to note, however, that while progress can be made through the mapping and isolation of novel mutants, the continued presence of mutants whose phenotypes are still too subtle for traditional mapping highlights the need for a more quantitative approach to identifying and mapping inflorescence genes in maize.

LITERATURE CITED

Abe, A., Kosugi, S., Yoshida, K., Natsume, S., Takagi, H., Kanzaki, H., Matsumura, H., Mitsuoka, C., Tamiru, M., Innan, H. et al. (2012). Genome sequencing reveals agronomically important loci in rice using MutMap. *Nature Biotechnology* **30**, 174-8.

Alrefai, R., Berke, T. G. and Rocheford, T. R. (1995). Quantitative trait locus analysis of fatty acid concentrations in maize. *Genome* **38**, 894-901.

Austin, R. S., Vidaurre, D., Stamatiou, G., Breit, R., Provart, N. J., Bonetta, D., Zhang, J., Fung, P., Gong, Y., Wang, P. W. et al. (2011). Next-generation mapping of Arabidopsis genes. *Plant J* **67**, 715-25.

Baulcombe, D. (2010). Reaping benefits of crop research. *Science* **327**, 761.

Berke, T. G. and Rocheford, T. R. (1999). Quantitative Trait Loci for Tassel Traits in Maize. *Crop Sci.* **1999**, 1439-1443.

Bortiri, E., Chuck, G., Vollbrecht, E., Rocheford, T., Martienssen, R. and Hake, S. (2006). ramosa2 encodes a LATERAL ORGAN BOUNDARY domain protein that determines the fate of stem cells in branch meristems of maize. *Plant Cell* **18**, 574-85.

Chuck, G., Muszynski, M., Kellogg, E., Hake, S. and Schmidt, R. J. (2002). The control of spikelet meristem identity by the branched silkless1 gene in maize. *Science* **298**, 1238-41.

Dudley, R. J. L. (2004). 100 Generations of selection for oil and protein in corn. In *Plant Breeing Rev.*, vol. Pt. 1, pp. 79-110.

Gallavotti, A., Long, J. A., Stanfield, S., Yang, X., Jackson, D., Vollbrecht, E. and Schmidt, R. J. (2010). The control of axillary meristem fate in the maize ramosa pathway. *Development* **137**, 2849-56.

Hofmeyr, J. D. J. (1931). The Inheritance and Linkage Relationships of barren stalk-1 and barren stalk-2, Two Mature-Plant Characters of Maize. *Ithaca, NY: Cornell University*.

Lindner, H., Raissig, M. T., Sailer, C., Shimosato-Asano, H., Bruggmann, R. and Grossniklaus, U. (2012). SNP-Ratio Mapping (SRM): identifying lethal alleles and

mutations in complex genetic backgrounds by next-generation sequencing. *Genetics* **191**, 1381-6.

Liu, S., Chen, H. D., Makarevitch, I., Shirmer, R., Emrich, S. J., Dietrich, C. R., Barbazuk, W. B., Springer, N. M. and Schnable, P. S. (2010). High-throughput genetic mapping of mutants via quantitative single nucleotide polymorphism typing. *Genetics* **184**, 19-26.

Michelmore, R. W., Paran, I. and Kesseli, R. V. (1991). Identification of markers linked to disease-resistance genes by bulked segregant analysis: a rapid method to detect markers in specific genomic regions by using segregating populations. *Proc Natl Acad Sci U S A* **88**, 9828-32.

Mickelson, S. M., Stuber, C. S., Senior, L. and Kaeppler, S. M. (2002). Quantitative Trait Loci Controlling Leaf and Tassel Traits in a M73 x Mo17 Population of Maize. *Crop Sci.*, 1902-1909.

Neuffer, M. G. (1994). The Maize Handbook. New York: Springer-Verlang.

Olivier, J. P., Raabe, T., Henkemeyer, M., Dickson, B., Mbamalu, G., Margolis, B., Schlessinger, J., Hafen, E. and Pawson, T. (1993). A Drosophila SH2-SH3 adaptor protein implicated in coupling the sevenless tyrosine kinase to an activator of Ras guanine nucleotide exchange, Sos. *Cell* **73**, 179-91.

Rogge, R. D., Karlovich, C. A. and Banerjee, U. (1991). Genetic dissection of a neurodevelopmental pathway: Son of sevenless functions downstream of the sevenless and EGF receptor tyrosine kinases. *Cell* **64**, 39-48.

Satoh-Nagasawa, N., Nagasawa, N., Malcomber, S., Sakai, H. and Jackson, D. (2006). A trehalose metabolic enzyme controls inflorescence architecture in maize. *Nature* **441**, 227-30.

Schaeffer, M. L., Harper, L. C., Gardiner, J. M., Andorf, C. M., Campbell, D. A., Cannon, E. K., Sen, T. Z. and Lawrence, C. J. (2011). MaizeGDB: curation and outreach go hand-in-hand. *Database (Oxford)* **2011**, bar022.

Schneeberger, K., Ossowski, S., Lanz, C., Juul, T., Petersen, A. H., Nielsen, K. L., Jorgensen, J. E., Weigel, D. and Andersen, S. U. (2009). SHOREmap: simultaneous mapping and mutation identification by deep sequencing. *Nat Methods* **6**, 550-1.

Simon, M. A. (1994). Signal transduction during the development of the Drosophila R7 photoreceptor. *Dev Biol* **166**, 431-42.

Simon, M. A., Bowtell, D. D., Dodson, G. S., Laverty, T. R. and Rubin, G. M. (1991). Ras1 and a putative guanine nucleotide exchange factor perform crucial steps in signaling by the sevenless protein tyrosine kinase. *Cell* **67**, 701-16.

Upadyayula, N., da Silva, H. S., Bohn, M. O. and Rocheford, T. R. (2006). Genetic and QTL analysis of maize tassel and ear inflorescence architecture. *Theor Appl Genet* **112**, 592-606.

Vollbrecht, E., Springer, P. S., Goh, L., Buckler, E. S. t. and Martienssen, R. (2005). Architecture of floral branch systems in maize and related grasses. *Nature* **436**, 1119-26.

Yao, H., Dogra Gray, A., Auger, D. L. and Birchler, J. A. (2013). Genomic dosage effects on heterosis in triploid maize. *Proc Natl Acad Sci U S A* **110**, 2665-9.

TABLE 1

Sample BSA result table

Pool	Assay Id	Area1	Area 2	*mut* ratio	*wt* ratio	$\frac{mut}{wt}$	$\frac{wt}{mut}$
Mutant	101072W47	36.7	41.8	1.14	-	-	-
Normal	101072W47	53.8	42.6	-	0.79	0.69	1.44
Mutant	8999W44	79.9	40.3	0.50	-	-	-
Normal	8999W44	29.2	42.2	-	1.44	2.86	0.35
Mutant	112436W11	78.6	28.8	0.37	-	-	-
Normal	112436W11	22.7	28.2	-	1.24	3.40	0.29
Mutant	64459W34	117.6	56.8	0.48	-	-	-
Normal	64459W34	46.3	66.7	-	1.44	2.98	0.34
Mutant	32158W19	87.3	4.9	0.06	-	-	-
Normal	32158W19	82.8	5.7	-	0.07	1.24	0.80

TABLE 2

Descriptions of new mutants

Mutant ID[a]	Population	Description of phenotype[b]
rel-07.0167*	*ra2-R*	Increased tassel branch number? Ear is branched at the tip.
rel-08.0116*	*ra2-R*	Increased TBN. Increased EBN.
rel-09.5068*	*ra2-R*	Increased TBN. Ears appear normal.
rel-09.5171*	*ra2-R*	Central spike of the tassel forked. Ears have some branching at tip.
rel-09.5195*	*ra2-R*	Increased TBN. Earless.
rel-09.6823*	*ra1-63*	Ears are highly branched and sterile. Tassels appear thickened. Increased TBN?
rel-09.6415*	IHO	Upright tassels. Branched ear.
rel-11.7978*	IHO	Upright tassels. Ears appear normal.
rel-11.0253*	*ra1-63*	Increased TBN appears to segregate in a semidominant fashion. Ears appear normal.
rel-11.0327*	*ra1-63*	Increased TBN. Increased EBN.
rel-11.0823*	*ra1-63*	Tassels have short branches and some bare nodes. Increased EBN. Mutants mature faster.
rsl-11.0243*	*ra1-63*	4/21 consumed meristem. 5/21 reduced tassels with fewer branches and missing spikelets. Ears are silkless and/or slow.
rel-11.0419*	*ra1-63*	Short with broad leaves. Some male sterile with brown anthers. Dominant? Increased TBN?
rsl-11.0625*	*ra1-63*	Male sterile. Female fertile? Reduced rows on ear. Some brown color in glume margin.
rel-11.0279*	*ra1-63*	Increased TBN. Tassel branches near base point down. Short, thick central spike. Kinked stalk with missing leaves.
rel-11.0811*	*ra1-63*	Increased TBN. Leaning tassel. Some with increased branching in the ear. Some earless.
rel-11.0835*	*ra1-63*	Increased BN. Increased EBN.
rel-12.2981*	*ra1-63*	Increased TBN. Kinky stalk. 16 branches on one ear. Ears small/behind?
rsl-12.2995*	*ra1-63*	Compressed internodes throughout. Decreased TBN? One ear unbranched.
rel-12.3019*	*ra1-63*	Upper internodes unelongated with short leaves. Increased TBN? Sterile kinky tassel. Small, fertile, unbranched ears.
rel-12.3103*	*ra1-63*	Upright tassel is male sterile. Ears look normal.
rel-12.3231*	*ra1-63*	TBN suppressor. Fewer long branches. Single spikelets. Earless.

[a] *rel*, ramosa enhancing locus; rsl*, ramosa suppressing locus*

[b] TBN, tassel branch number; EBN, ear branch number

TABLE 3

Number of M2s screened and mutants discovered

	Total M2 families screened (Mutants identified)		
Year	*ra2-R*	*ra1-63*	IHO
2007	120 (1)	0	0
2008	197 (1)	0	0
2009	379 (3)	208 (1)	208 (1)
2010	177	535	0
2011	65	552 (9)	183 (1)
2012	0	219 (5)	0
Total	938 (5)	1514 (15)	391

FIGURE LEGENDS

Figure 1. Phenotypes of *ra1-63.3359* suppressor/enhancer mutants. (A) Tassel of a *ra1-63.3359* homozygote in Mo17. (B) Suppressed tassel branching phenotype of *rsl*-11.0243*. (C) Suppressed tassel branching phenotype of *rsl*-11.0625*. (D) Enhanced tassel branching phenotype of *rel*-11.0811*. (E) Enhanced tassel branching phenotype of *rel*-11.0327*. (F) Enhanced tassel branching phenotype of *rel*-11.0823*. (G) Ear of a ra1-63.3359 homozygote. (H) Suppressed ear branching and sterile phenotype of *rsl*-11.0243*. (I) Suppressed ear branching phenotype of *rsl*-11.0625*. (J) Enhanced ear branching and sterile phenotype of *rel*-11.0811*. (K) Enhanced ear branching phenotype of *rel*-11.0327*. (L) Enhanced ear branching phenotype of *rel*-11.0823*.

Figure 2. Phenotypes of *ra2-R* and IHO suppressor/enhancer mutants. (A) Tassel of *ra2-R* homozygote in A619. (B) Enhanced tassel branching phenotype of *rel*-07.0116*. (C) Enhanced tassel branching phenotype of *rel*-08.0167*. (D) Enhanced tassel branching phenotype of *rel*-09.5068*. (E) Tassel of IHO. (F) Enhanced tassel branching phenotype of *rel*-09. 6415*. (G) Ear phenotype of *ra2-R* homozygote in A619. (H) Enhanced ear branching phenotype of *rel*-07.0116*. (I) Enhanced ear branching of *rel*-08.0167*. Note branching occurs mostly at the tip. (J) Ear phenotype of *rel*-09.5068*. (K) Ear of IHO. (L) Enhanced ear branching phenotype of *rel*-09.6415*.

Figure 3. Inflorescences phenotypes and *ramosa1* non-complementation of the Illinois High Oil (IHO) line. (A) Highly-branched tassel of IHO. (B) Unbranched ear of IHO. (C) B73 introgression of *ra2-R* segregating for *ra1-IHO*. (D) B73 introgression of *ra3-R* segregating for *ra1-IHO*. (E) Tassel phenotype indicating complementation of *ra1-R* mutant with B73. (F) Tassel phenotype indicating complementation of *ra1-IHO* with B73. (G) Tassel phenotype of *ra1-R* homozygote. (H) Tassel phenotype indicating non-complementation of *ra1-IHO* with *ra1-R* mutant.

Figure 4. Bulked segregant mapping (BSA) methodology. Adapted from a presentation by the Genomic Technologies Facility at Iowa State University. (A) Linkage between a marker

and causal mutation produces biased parental:non-parental SNP ratios in mutant and wild-type bulks. (B) Independent segregation of unlinked markers leads to equal parental:non-parental SNP ratios in mutant and wild-type bulks. (C) Comparisons of ratios in mutant and wild-type bulks can be used to estimate genetic distance between the SNP marker and the causal mutation. Tight linkages are indicated by large wild-type to mutant ratios.

Figure 5. Bulked segregant mapping (BSA) results. Transformed ratios plotted against genetic position on a sliding window of 20cM with 1cM steps. Genetic locations of previously characterized mutants indicated in red. (top) The results for *rel*-08.0167* align closely with recently-cloned mutant *fea4*. (middle) Peak for *rel*08.116* indicates possible allelism with *ra3*. (C) Overlap of *rel*-09.6823* with genetic location of *bd1*.

Figure 6. Bulked segregant mapping (BSA) results. Transformed ratios plotted against genetic position on a sliding window of 20cM with 1cM steps. Genetic locations of previously characterized mutants indicated in red. (top) Results for *rel*-09.6415* suggest linkage with *rel2*. (middle) BSA mapping results for *rel*-09.5195*. (bottom) BSA mapping results for *rel*-09.7978*.

Figure 7. Bulked segregant mapping (BSA) results. Transformed ratios plotted against genetic position on a sliding window of 20cM with 1cM steps. (top) *rel*-09.5068* (middle) *rel*-11.0253* (bottom) *rel*-11.0327*. Results do not point to a single location for any of these genes. Additional mapping populations have been constructed for re-mapping of *rel*-11.0327.*

Figure 8. Tassel branch number in *rel*-09.5195* F2 mapping populations. *rel*-09.5195* originated in the A619 background and was crossed to B73 (gray) or Mo17 (red) for mapping. TBN was scored on a subset of individuals from each F2 population. Tassels of *rel*09.5195* mutants were fewer branched relative to normal siblings. However, when *ra2-R* was present in the background, *rel*09.5195* appeared to increase tassel branching relative to *ra2-R/ra2-R*; +/+ siblings.

Figure 1 Weeks *et al.*

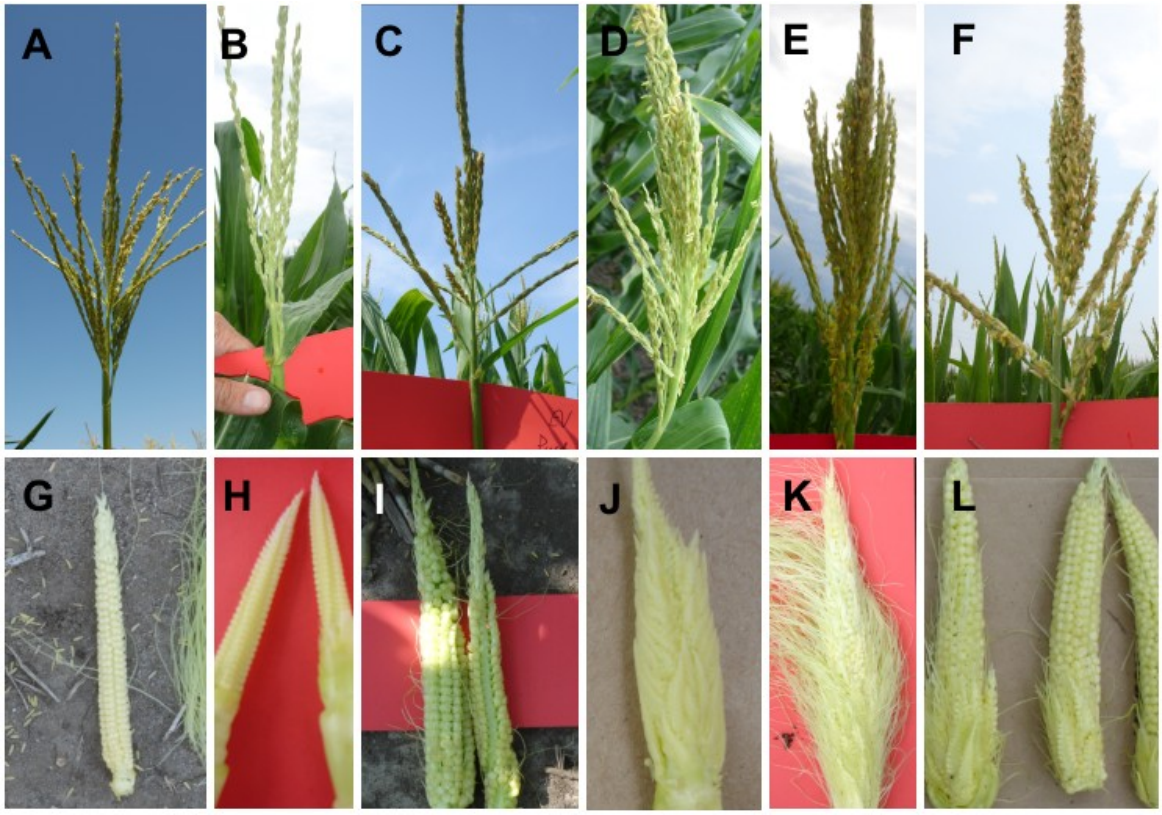

Figure 2 Weeks *et al.*

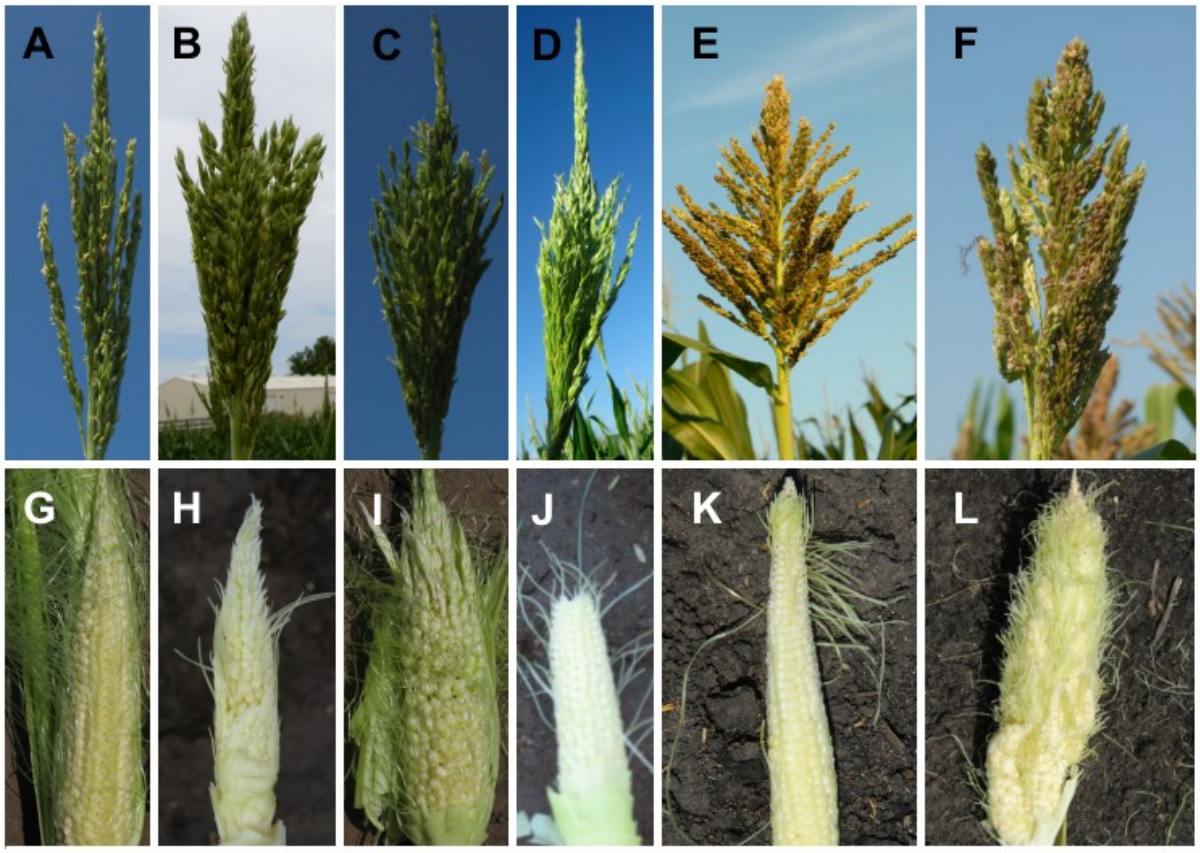

Figure 3 Weeks *et al.*

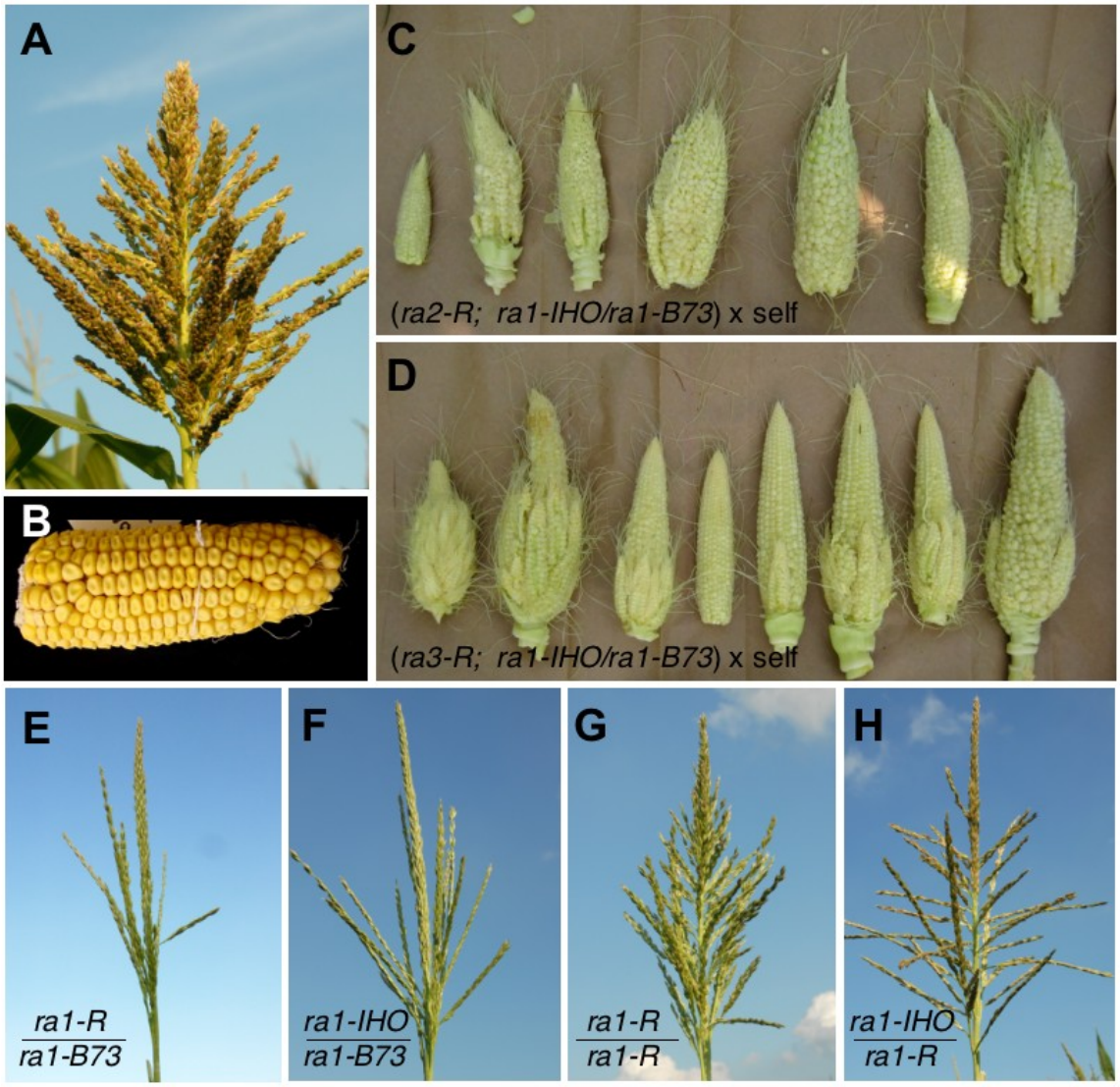

Figure 4 Weeks *et al.*

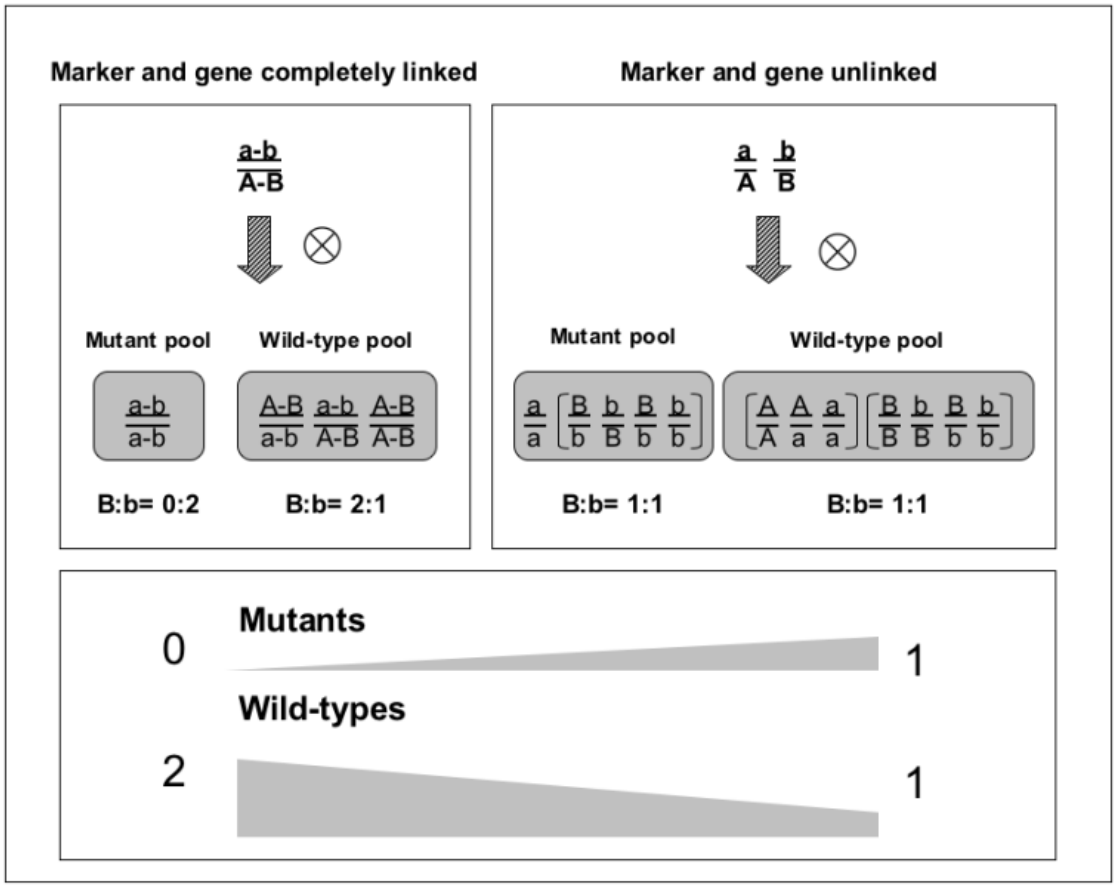

Figure 5 Weeks *et al.*

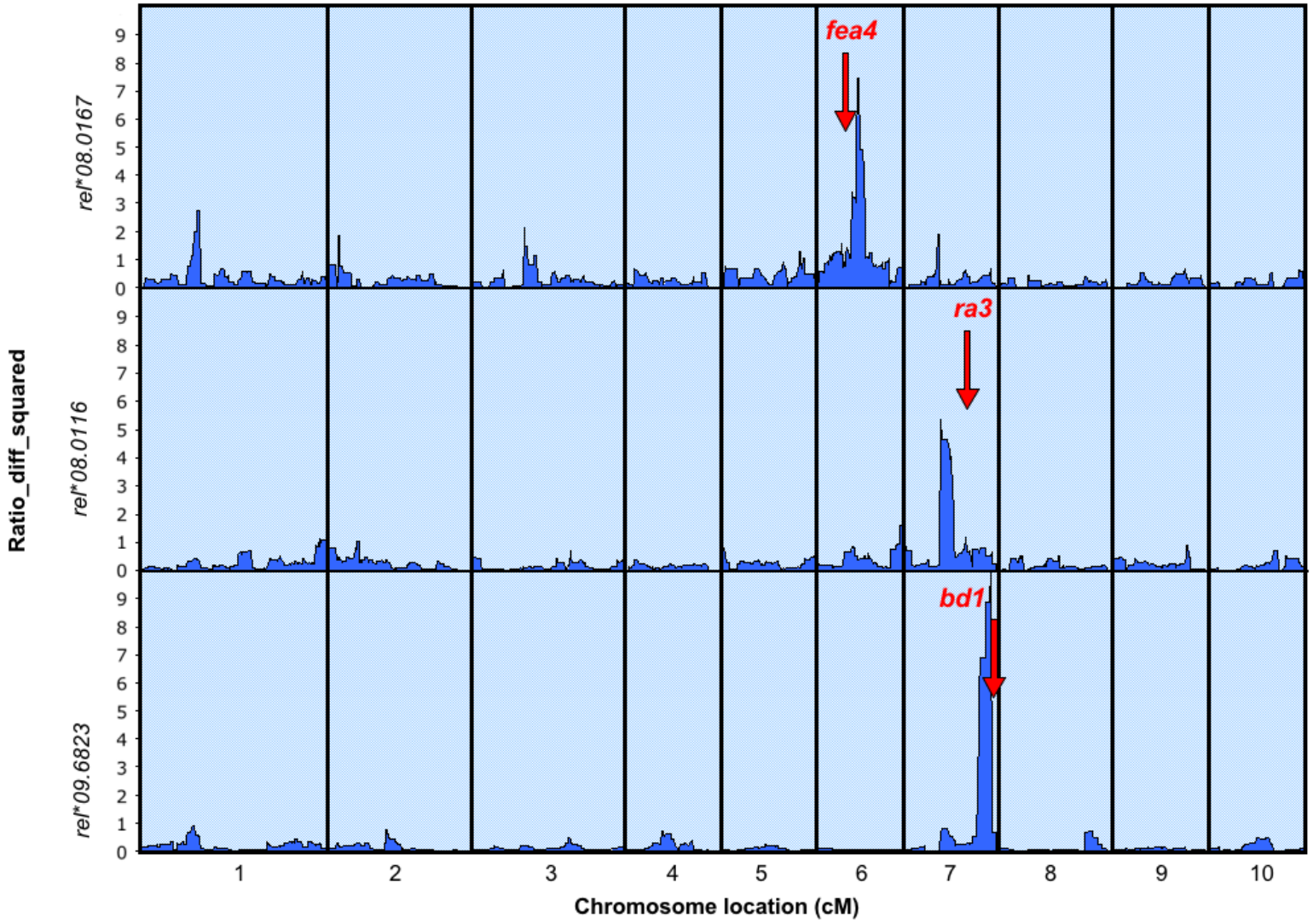

Figure 6 Weeks *et al.*

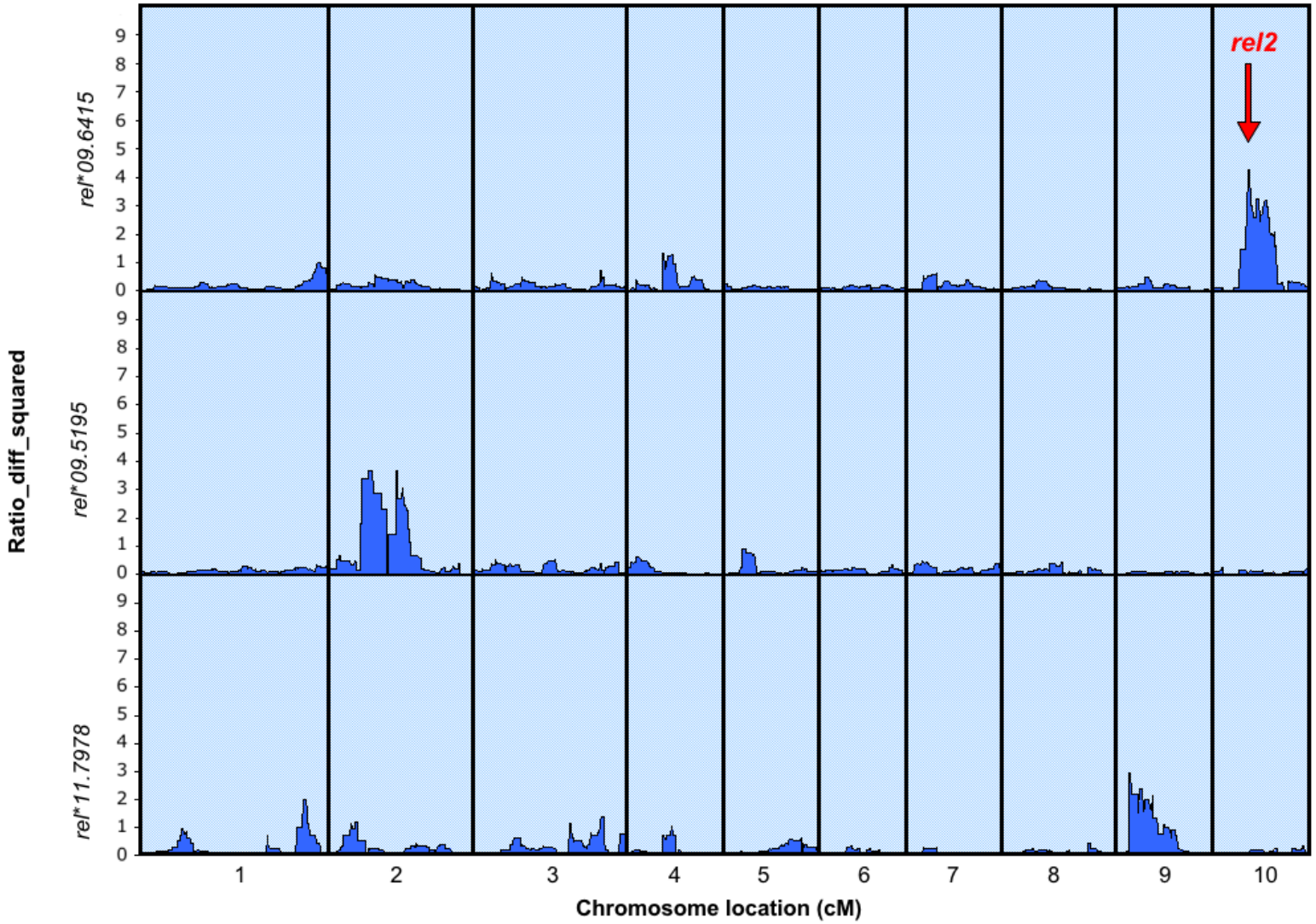

Figure 7 Weeks *et al.*

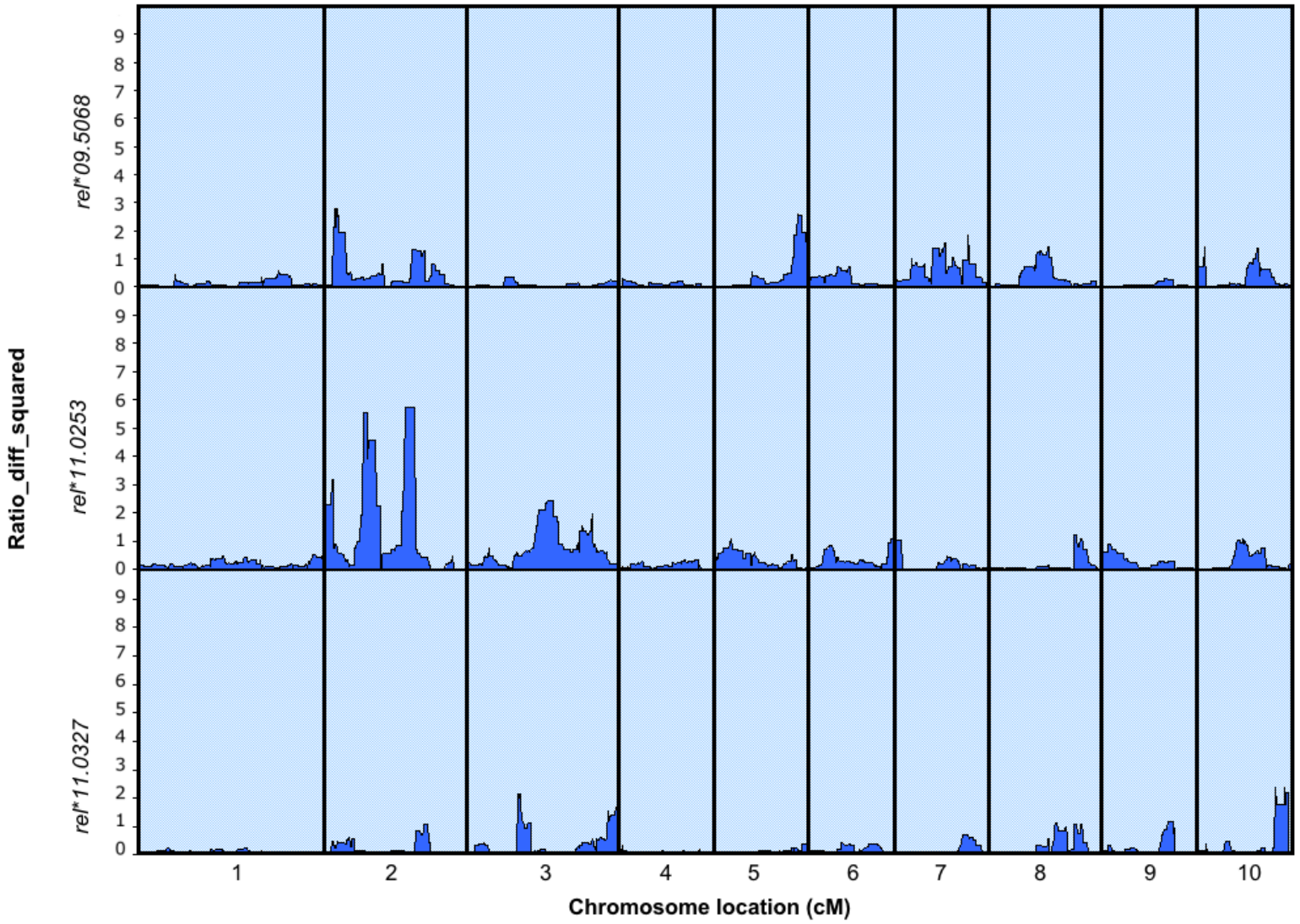

Figure 8 Weeks *et al.*

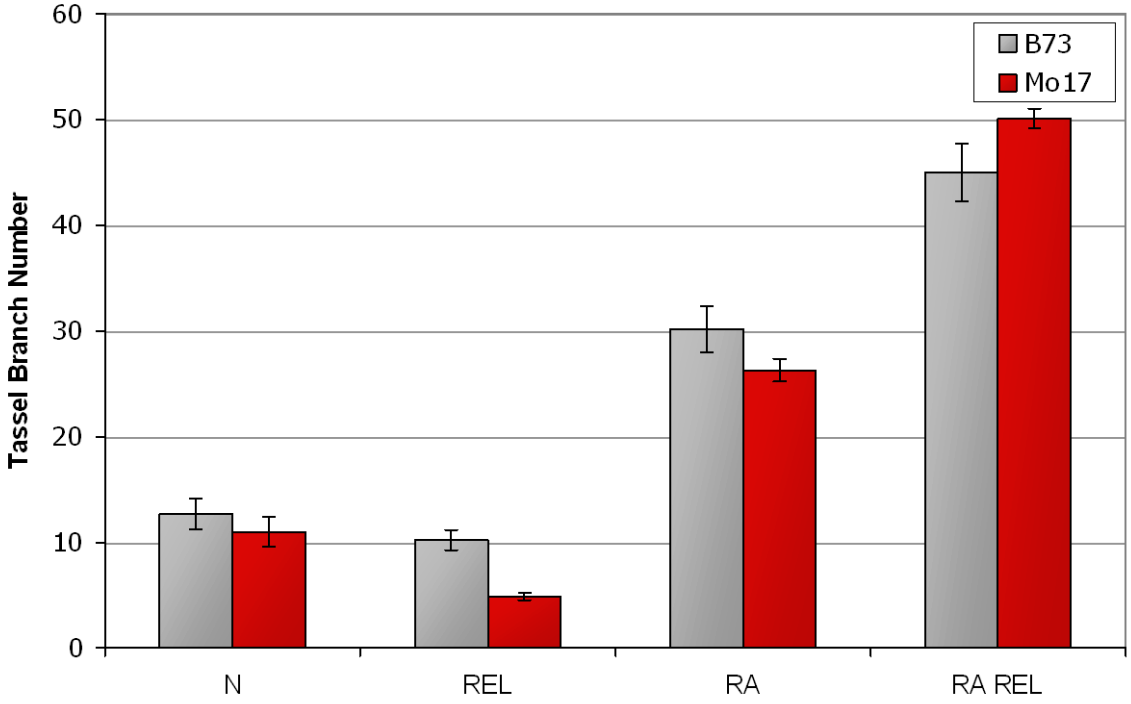

CHAPTER 3. QUANTITATIVE TRAIT LOCI FOR EAR BRANCH NUMBER IN *RA1-63.3359* MUTANTS

A manuscript to be submitted to *Genetics*

Rebecca Weeks, Maria Mateos-Hernandez, Kokulapalan Wimalanathan, Torbert Rocheford and Erik Vollbrecht

ABSTRACT

The *ramosa1* (*ra1*) gene controls maize inflorescence architecture by imposing determinate or short branch identity on the lateral meristems of developing ears and tassels. Thus, tassels of *ramosa1* mutants display increased branching, while ears exhibit unorganized rows and/or lateral branching. The severity of the *ra1* mutant phenotype varies widely according to genetic background. In a B73 introgression, for example, the mutant allele *ra1-63.3359* conditions highly branched tassels and ears. In Mo17 introgressions, however, *ra1-63.3359* displays relatively mild effects including a few additional branches in the tassel and ears with crooked rows and an occasional branch. We exploited these phenotypic differences by using the IBM population to identify loci that affect the number of ear branches in *ra1-63.3359* mutants. Each RIL in the IBM-94 population was backcrossed to Mo17- and B73-introgressed *ra1-63.3359,* resulting in two sets of F1BC1 populations. We then mapped modifiers of branching from the B73 and Mo17 backgrounds, and identified several putative modifier QTL. In the B73 backcross population, a particularly significant peak was identified on chromosome 1 with an effect of approximately 1.75 branches. Near isogenic lines (NILs) were used to generate additional recombinants within the QTL region, which were then backcrossed to B73 introgressions to create lines fixed for *ra1-63.3359* and segregating for the new recombinant chromosome. Using this technique, we were able to narrow down the region to a 750 kb interval containing nine candidate genes.

INTRODUCTION

Cross-pollination in maize is facilitated by the presence of separate male and female inflorescences, each bearing unique architecture and sex-specific flowers. Despite their

obvious physical dissimilarity at maturity, the underlying organization and development of these structures is remarkably similar. In fact, examined at the earliest stages of development, incipient male and female inflorescences are nearly indistinguishable until a few branch primordia appear at the base of the male inflorescence. These nascent structures signal the beginning of long-branch development, a process that is normally exclusive to the tassel. Although long branches are not formed in the ear, short branches are present beneath each pair of kernels and under certain conditions these can be converted to long branches, as is the case with the *ramosa* mutants of maize. Characterized by their branched ears and poor kernel organization, *ramosa* inflorescences display pronounced defects in branch identity resulting from a conversion of short branches, which would normally produce spikelet pairs, to long branches. Additionally, some branches are converted to an intermediate fate, producing extra spikelets, which in the ear cause rows to appear crooked or disorganized (Sigmon and Vollbrecht, 2010). Intermediate branches are also present in the tassel and are called mixed branches because they produce spikelets both singly and in pairs.

The *ramosa* phenotype can be explained, in large part, by a loss of determinacy in second order meristems of the inflorescence. Determinacy is an attribute of the meristem that specifies its potential for indefinite growth. Spikelet pair meristems (SPMs) are said to be determinate because they will terminate following the production of a pair of spikelet primordia. Branch meristems (BMs), on the other hand, are indeterminate and will go on to produce an undefined number of third order spikelet pair meristems along their flanks. The conversion of second order meristems in *ramosa* mutants to a less-determinate fate suggests that the *ramosa* genes may have a molecular role in regulating meristem determinacy. All three *ramosa* genes have been cloned; *ra1* encodes a cys2-his2 zinc finger transcription factor (Vollbrecht et al., 2005), *ra2* encodes a LATERAL ORGAN BOUNDARY (LOB) domain transcription factor (Bortiri et al., 2006), and *ra3* encodes a trehalose-6-phosphate phosphatase metabolic enzyme (Satoh-Nagasawa et al., 2006). An additional factor called *ramosa1 enhancer locus2* (*rel2*) encodes a *TOPLESS*-like co-repressor and has been shown to physically interact with the *ramosa1* protein (Gallavotti et al., 2010). The *ramosa* genes are co-expressed in overlapping domains near the base of developing SPMs and mutation of *ra2* or *ra3* leads to reduced *ra1* expression indicating that they function upstream of *ramosa1*

and promote its expression (Bortiri et al., 2006; Satoh-Nagasawa et al., 2006; Vollbrecht et al., 2005).

The phenotypes of *ramosa* mutants vary according to genetic background. For example, the *ra1-63.3359* mutant allele displays strong phenotypic effects in B73, with tassels producing extra long branches and ears displaying branching and crooked rows (Figure 1A,C). In Mo17, however, both tassels and ears display relatively mild effects including a few extra branches in the transition zone of the tassel and ears with crooked rows and an occasional branch (Figure 1B,D)(Sigmon and Vollbrecht, 2010). Similar phenotypic disparity between B73 and Mo17 introgressions has been observed for all *ramosa1* alleles tested to date (Figure 1E), indicating that natural variation at one or more loci is able alter the inflorescence branching phenotype of *ramosa1* mutants. The genetic factors underlying these effects are likely to be involved, either directly or indirectly, in the regulation of meristem determinacy and therefore it is possible that they represent undiscovered components of the inflorescence branching pathway. Identification of these loci using approaches developed for mapping quantitative traits could further our understanding of the genetic network involved in controlling inflorescence architecture.

In order to map loci influencing inflorescence branch number in *ra1-63.3359* mutants, we conducted a quantitative trait loci (QTL) mapping experiment using the intermated B73 × Mo17 (IBM) population of maize. Through this approach we were able to identify five putative loci that either suppress or enhance the ear branching phenotype of *ra1-63.3359* mutants. For one of these QTL, we confirmed the phenotypic effect by generating near-isogenic lines (NILs) that segregated for the QTL region while remaining mostly fixed for background effects. Recombinants derived from the NIL were used to narrow the QTL to a smaller interval containing twenty-one genes. Seven of these genes are not expressed in inflorescences and five encode proteins involved in basic cellular processes, therefore we have focused on the nine remaining genes for further analysis.

MATERIALS AND METHODS

A subset of 88 lines originating from the IBM-94 population was used to identify modifiers of branching in *ra1-63.3359* mutants. B73 and Mo17 4X introgressions of *ra1-*

63.3359 were used as recurrent backcross parents to generate two F1-BC1 populations for each recombinant inbred line (RIL); each population is henceforth referred to as a treatment. The resulting collection of treatments was planted in the summer of 2008 in a randomized complete block design (RCBD) with four blocks and each experimental unit consisting of a single row of six kernels. Because two doses of the recessive allele *ra1-63.3359* are required to observe branching in the ear, only half of the F1-BC1 individuals within each treatment could produce an ear branching phenotype. Furthermore, F1-BC1 individuals also segregated for the RIL chromosome, so only one quarter of the F1-BC1 carried both a homozygous *ra1-63.3359* genotype and a RIL allele at a given locus. Due to the large size of the population and lack of an inexpensive and robust genotyping assay for *ra1-63.3359*, uninformative individuals were not eliminated and all individuals were scored. Scoring was performed by harvesting the mature to ear, husking it, and counting branches as they were removed from the ear.

The SAS 9.3 statistical package (SAS Institute, 2012) was used to estimate block effects and compute least squared means for each treatment. Upon preliminary analysis, however, it became apparent that the blocking design had failed to capture a significant amount of the phenotypic variation ($p=0.37$) so the blocking factor was removed and treatment means were computed across all four replicates. The distribution of phenotypes based on means of treatments across replicates was not normal as tested for normality by the Shapiro-Wilk test statistic in the SAS univariate procedure (SAS Institute, 2012). Transformations using natural log, log 10, square root, and Box-Cox failed to confer normality to the distribution of phenotypes, so analyses were performed using untransformed data. Heritability, defined as the proportion of the phenotypic variance explained by the genotype, was estimated by performing a one-way ANOVA of treatments on mean ear branch number between replicates. Transgressive segregation was investigated by making pairwise comparisons of treatments with parent lines and testing for significance using LSD0.05. Comparison of *ra1*-63.3359 B73 and Mo17 treatment means was performed using the Spearman rank-order and Pearson correlation tests in SAS (SAS_Institute, 2012).

The IBM-94 population (Lee et al., 2002) has been genotyped for ~4000 markers across the maize genome, of which we used 2,025 framework markers to perform the QTL

analysis. Composite Interval mapping (Jansen and Stam, 1994; Zeng, 1994) was performed on treatment means for each backcross experiment using WinQTLCart version 2.5 (Wang et al., 2012). Cofactors were selected by stepwise regression using the forward selection, backward elimination method with a cutoff of 0.05 for cofactor selection and elimination. A LOD threshold of 3.55 was applied on a per chromosome basis (Van Ooijen, 1999). This threshold corresponds to a chromosome-wise error rate of 0.005 and a genome-wise error rate of 0.05. It is important to note that this method uses an average chromosome length, 250cM in this case, to determine LOD thresholds. Therefore, smaller chromosomes will experience a slightly more stringent threshold relative to larger chromosomes. QTL support intervals were calculated as the position along the significance peak at which the LOD score is 1.0 unit less than the peak LOD score. Estimates of additive effects and phenotypic variance explained by each QTL were calculated by fitting the final model including all putative QTL using the Multiple Interval Mapping function of WinQTLCartographer. The additive effect of a given marker was calculated as one half of the difference between the homozygous B73 and Mo17 class means, whereby a positive effect corresponds to an increase in the B73 class mean relative to Mo17. The proportion of phenotypic variance explained by each QTL and covariance estimates between QTL were used to calculate the total phenotypic variance explained by the model. Genotypic variance explained by the model was calculated by dividing the model R^2 by the trait heritability (Schön et al., 1994).

Near-isogenic lines (NILs) were generated to isolate the region responsible for the chromosome 1 QTL effect. In order to further minimize effects from background QTL we screened for RILs that possessed a Mo17 genotype across the chromosome 1 QTL and were fixed as B73 for most other QTL. This analysis identified RIL M0040 as the best line for introgression. With B73-introgressed *ra1-63.3359* as the recurrent parent, we performed four generations of marker-assisted backcrossing using the markers idp7478 and idp7413, which flank the 1.5LOD interval. At this point, we screened for recombination between the flanking markers and identified a number of putative recombinants; however, due to poor greenhouse conditions, we were only able to generate seed from 12 recombinant individuals.

In summer 2012, a high-throughput approach was employed to identify additional recombinants within the QTL region. The Panzea/HapMap project portal (www.panzea.org)

was used to identify 15 B73-Mo17 SNPs within the 1.5 LOD interval, which were subsequently converted into KASP assays (Kbioscience-LGC Genomics) (Table 1). A total of 1872 individuals derived from a self of a NIL heterozygote were screened for recombination within the QTL region (Figure 3). To accomplish this, two 6mm round punches were collected from each individual and the DNA extracted using the Promega Wizard® Magnetic 96 DNA Plant System. KASP™ genotyping reagents were used to genotype each individual at six markers spanning the QTL region (Figure 3). Recombinant individuals were tagged and later crossed by B73-introgressed *ra1-63.3359*. At maturity, the top ears of both recombinant and non-recombinant individuals were scored for ear branch number. Ear branch numbers from non-recombinant individuals were used to calculate the phenotypic effect of the QTL region and phenotypes from all individuals were used to estimate the rough location of the QTL effect. This was performed by regressing ear branch number on genotype at each of the six markers. Segregation distortion was observed for each of the six markers. To determine whether this distortion was the result of bias in the KASP assay, we genotyped 96 individuals at idp8570, which is tightly linked with the KASP marker RA1MOD-8, using a conventional gel-based method. Only one instance of non-concordance was observed between the two markers indicating that the distortion observed in the KASP dataset is likely due to a higher failure rate for Mo17 SNP detection rather than incorrect calling of genotypes.

For a select set of recombinant lines, an additional round of backcrossing was performed, indiscriminate of genotype at the chromosome 1 QTL. This resulted in two subsets of lines for each recombinant treatment, one of which segregated for the recombinant chromosome from the NIL while the other segregated for the parental chromosome. These subclasses were identified based on genotyping of the QTL region and were subsequently selected for further phenotyping.

In summer 2013, a total of 37 recombinant treatments and 5 checks were planted in a 6x7 alpha lattice with three replicates. Within each treatment, two 20 kernel rows of the recombinant subclass were planted aside two 20 kernel rows of the parental subclass, which permitted adjustments for background effects. Three weeks after sowing, rows were thinned to 16 plants in order to generate a more uniform stand count. This was important because the

branching phenotype of *ramosa1* mutants is susceptible to density effects (data not shown). At maturity, ear branch number (EBN) was scored for every individual and adjusted means were calculated for each treatment subclass and the difference between subclasses, using the GLIMMIX procedure of SAS (SAS Institute, 2012). In addition, unadjusted subclass means and mean differences were calculated across all replicates. Eight KASP markers were assayed on pools of 6 individuals representing each subclass of the 37 recombinant treatments. In cases where multiple seed sources were represented within a single subclass, genotyping was performed separately on each source. Consequently, we identified three lines that were segregating for novel recombination events. These were treated as a third subclass within the recombinant treatment and all combinations of comparisons were performed between the three subclasses.

Single marker analysis was performed on adjusted and unadjusted subclass means using genotype data across all eight markers. Genotypes of parental and recombinant subclasses were concatenated in order to regress the difference of the means on genotype (Figure 4). This was accomplished using the indicator variables (0,1), whereby a zero indicates that the parental and recombinant subclasses are identical in genotype at the given locus and a one signifies that the two subclasses differ in genotype at that position. Using these genotypes, linear regression was performed on the adjusted and unadjusted mean difference between subclasses.

A web-based tool was created to aid in the identification of potential candidate genes within the QTL region. The Gene Expression Search Tool (www.vollbrechtlab.org) reports integrated data about a genome interval from several existing genome-wide datasets. For each gene within the specified interval, users can view gene-specific information from a number of available public databases (CoGE, maizesequence.org, NCBI), explore results from inflorescence-specific expression and ChIP-seq experiments (Maize Inflorescence Project) and identify potential mutant lines from community transposon resources (Ac/Ds, HeritableMu, UniformMu). Using this tool, candidate genes within the chromosome 1 QTL interval were identified based on their expression in developing ears and tassels and differential expression in *ramosa* mutants (Eveland et al., 2010). Genes with B73 by Mo17 variation within their expressed sequences were identified using the HapMap2 genotype

search tool at Panzea (www.panzea.org). Within the QTL interval, UniformMu and HeritableMu lines that contained elements inside genes were ordered indiscriminate of the gene's expression pattern or promise as a candidate gene. Once the insertion was confirmed, double mutants were made using a W22 introgression of *ra1-63.3359*.

RESULTS

When introgressed into B73, ears of *ra1-63.3359* mutants displayed increased branching compared to the ears of the Mo17 introgression, which were almost always unbranched (Figure 5, Table 2). The ear branch number of the F1 was roughly half of what was observed in the B73 introgression, however, the tassel branch number of the F1 was greater than either parent, suggesting that tassel branch number displays some degree of heterosis, or that it is under the control of loci that are distinct from those influencing the ear. The B73 RIL treatments displayed a wide range of phenotypes and transgressive segregation was observed for one treatment (Figure 6). Heritability for ear branch number in the B73 backcross treatments was estimated at 57 percent. The ear branch numbers of the Mo17 treatments were lower overall than the B73 treatments and all of the lines had fewer branches on average than the B73 introgression (Figure 6). Heritability for the Mo17 treatments was estimated at 42 percent. Comparison of the B73 and Mo17 treatments indicated that there was no significant correlation between the means or rank of treatments between experiments.

In QTL analysis, four genome regions were found to exhibit significant effects on branch number. (Figure 7, Figure 8, Table 3). In the B73 backcross, two Mo17 suppressors were found, on chromosomes 1 and 5, with effects of 1.07 and 0.82 branches, respectively, and a B73 suppressor was found on chromosome 7 with an effect of 0.98 branches. A simultaneous fit of all three QTL accounted for 34.1% of the phenotypic variance and 59.8% of the genotypic variance. No epistatic interactions were detected. In the Mo17 backcross, an enhancer and suppressor were found in close linkage on chromosome 6, accounting for 31.8% of the phenotypic and 75.7% of the phenotypic variance. The proximal B73 suppressor has a net effect of subtracting 0.85 branches from the F1-BC1 average while the linked B73 enhancer adds approximately 1.09 branches. It is important to note that the marker genotypes used in the analysis represent the genotypes of the parental RIL and not

necessarily the genotype of the F1-BC1 as a whole. With respect to a single locus, only one quarter of the F1-BC1 possess both a RIL chromosome and a homozygous *ra1-63.3359* genotype. Therefore, the genetic effects estimated by these analyses will be significantly diluted by individuals within the F1-BC1 that are not representative of the parental RIL and/or not able to condition the ear branching phenotype. Furthermore, because all marker genotypes used for the analyses are homozygous, a dominance effect cannot be estimated, even though one may be present in the F1-BC1, which is at most heterozygous for the RIL chromosome at any given locus.

To confirm the chromosome 1 QTL and estimate its effect, we isolated the region by generating near isogenic lines (NILs) that carried the 1.5LOD interval for the QTL (see Methods). A heterozygote from the fourth backcross of the NIL was self pollinated to generate progeny that segregated for the QTL region (Figure 3). Non-recombinant individuals that were homozygous B73 across the modifier region averaged 9.32 branches per ear, compared to 7.51 branches for heterozygotes and 5.75 branches for Mo17 homozygotes (Figure 9). The observed difference among classes was significant ($p<0.0001$) and followed a linear trend ($R^2=0.9999$), suggesting that the majority of the chromosome 1 QTL effect can be explained by additive genetic variance.

We next analyzed the segregation of six markers spanning the QTL region and compared mean ear branch numbers of the genotypic classes at each marker. The marker RA1MOD-5 had both the most significant effect and the largest difference between the B73 and Mo17 homozygous class means (Table 4). Both markers flanking RA1MOD-5 had higher means for the Mo17 homozygous genotype possibly indicating recombination between the flanking markers and the QTL. Based on this data we decided to focus on the left half of the QTL interval. Fine-mapping was conducted on 37 individuals that were recombinant within the RA1MOD-1 RA1MOD-8 interval. Each recombinant individual was twice backcrossed to the B73 introgression of *ra1-63.3359* generating two subsets for each recombinant treatment, one that segregated for the recombinant chromosome (REC_n-R) and another that segregated for the parental chromosome from the NIL (REC_n-P) (Figure 4). Comparison of the parental and recombinant subclasses for each treatment allowed us to identify which treatments had experienced a recombination event that resulted in a gain or

loss of the QTL. We mapped these effects on six left side markers and identified two significant markers, RA1MOD-2 and RA1MOD-3, (Figure 10) however they were concordant except for one missing data point in the RA1MOD-3 dataset. Nevertheless, this allowed us to further narrow the QTL region to a 3.7cM interval flanked by the markers RA1MOD1 and RA1MOD3.5. The intervening sequence is 750 kilobases in length and contains 21 genes. Using a web-based tool developed to integrate data from multiple genome-wide datasets, we determined that seven of these genes are not expressed in developing inflorescences. Furthermore, five genes are expressed in inflorescences but encode genes involved in basic cellular processes such as photosynthetic enzymes, or components of the ribosomal nucleoprotein complex. The remaining nine genes encode a wide variety of proteins (Table 5). Using the maize HapMap2 genotype search (www.panzea.org) we identified B73-Mo17 variation within the expressed sequence of a subset of six genes. Putative insertion events from the AcDs (Vollbrecht et al., 2010) and UniformMu (Settles et al., 2007) transposon collections were found for three of the candidates and have been crossed to *ra1-63.3359* for future double mutant analysis.

DISCUSSION

The cloning of mutants that alter inflorescence branching has uncovered a number of genes that are involved in regulating inflorescence architecture. Among these, the *ramosa* genes have been shown to control inflorescence branch number by imposing short branch identity on lateral meristems of the inflorescence. Additionally, a number of QTL have been discovered which alter the branching of the male inflorescence, however little overlap exists between these QTL and known inflorescence branching mutants, indicating that some components of this pathway have yet to be discovered (Brown et al., 2011). We undertook a quantitative genetics approach to map QTL that are able to modify the *ra1-63.3359* phenotype, which varies according to genetic background. This approach builds on the concept of a suppressor/enhancer screen by using natural variation in place of induced mutations (Guo et al., 2012). While the effects of naturally variant loci are likely to be more subtle than some induced mutations, they can be detected through quantitative scoring and mapping approaches. Furthermore, the natural variation present at these loci takes many

forms—differential expression, missense substitutions, splice site variation, to name a few—and therefore one is not limited to identifying genes that give strong loss-of-function phenotypes. Finally, crossing *ra1-63.3359* into these naturally variant backgrounds may release cryptic variation for ear branch number that would not normally be observed in the parent lines. For these reasons, mapping of natural phenotypic modifiers using quantitative methods is a useful supplement to traditional mutagenesis and suppressor/enhancer screens.

In the present study, we mapped QTL that alter the branching of *ra1-63.3359* ears. Through this approach we identified QTL on chromosomes 1, 5, 6, and 7 that are associated with changes in ear branch number. Previously identified inflorescence or branching mutants were not found within the QTL intervals, except for the chromosome 5 QTL region, within which resides the *narrow leaf2* (*nl2*) mutant of maize. *nl2* plants are characterized by increased branching and tillering of the stalk (Neuffer et al., 1997), but branching of the inflorescence has not been examined. Nevertheless, tillering mutants of both rice and maize often display pleiotropic effects on inflorescence branch number (Doebley et al., 1995; Li et al., 2003; Miura et al., 2010; Whipple et al., 2011) so it is possible that natural variation at the *nl2* locus, which has yet to be cloned, could alter inflorescence branching phenotypes. More work is needed to fine-map this region and examine the phenotypic interactions between *nl2* and *ra1-63.3359*.

In the B73 experiment, a particularly significant effect was observed on chromosome 1S. The peak co-localizes with a QTL for ear branch number in *ra2-R* mutants (Chapter 4) and with QTL for tassel branch number in the IBM and NAM populations. While an effect on tassel branching was not observed for our QTL region (data not shown), it is possible that our sample sizes were too small (N=11 per genotype) to detect small but significant changes in tassel branch number. Using NILs, we generated additional recombinants and narrowed the chromosome 1 QTL region to a 750 kilobase interval containing 21 genes. After elimination of genes not expressed in inflorescences and genes involved in basic cellular processes, nine genes remained. Variation between B73 and Mo17 sequences was prevalent within the candidate genes and four candidates contained variation that putatively alters the amino acid sequence of the protein. We have obtained insertion lines for three of the nine

candidate genes and have initiated crosses to *ra1-63.3359* in order to generate double mutant lines for observation.

We employed a quantitative genetics approach in order to identify modifiers of the *ra1-63.3359* phenotype. Through this technique we discovered five putative loci that suppress or enhance the branching of *ramosa1* inflorescences. The small degree of overlap of these QTL with cloned inflorescence mutants and previously identified QTL suggests that the underlying genes may represent novel components of the inflorescence branching pathway. By fine-mapping these loci and using additional approaches to identify their causal variants we hope to gain useful information about the complex genetic network involved in regulating inflorescence architecture.

LITERATURE CITED

Bortiri, E., Chuck, G., Vollbrecht, E., Rocheford, T., Martienssen, R. and Hake, S. (2006). ramosa2 encodes a LATERAL ORGAN BOUNDARY domain protein that determines the fate of stem cells in branch meristems of maize. *Plant Cell* **18**, 574-85.

Brown, P. J., Upadyayula, N., Mahone, G. S., Tian, F., Bradbury, P. J., Myles, S., Holland, J. B., Flint-Garcia, S., McMullen, M. D., Buckler, E. S. et al. (2011). Distinct genetic architectures for male and female inflorescence traits of maize. *PLoS Genet* **7**, e1002383.

Doebley, J., Stec, A. and Gustus, C. (1995). teosinte branched1 and the origin of maize: evidence for epistasis and the evolution of dominance. *Genetics* **141**, 333-46.

Eveland, A. L., Satoh-Nagasawa, N., Goldshmidt, A., Meyer, S., Beatty, M., Sakai, H., Ware, D. and Jackson, D. (2010). Digital gene expression signatures for maize development. *Plant Physiol* **154**, 1024-39.

Gallavotti, A., Long, J. A., Stanfield, S., Yang, X., Jackson, D., Vollbrecht, E. and Schmidt, R. J. (2010). The control of axillary meristem fate in the maize ramosa pathway. *Development* **137**, 2849-56.

Guo, Y. L., Todesco, M., Hagmann, J., Das, S. and Weigel, D. (2012). Independent FLC mutations as causes of flowering-time variation in Arabidopsis thaliana and Capsella rubella. *Genetics* **192**, 729-39.

Jansen, R. C. and Stam, P. (1994). High resolution of quantitative traits into multiple loci via interval mapping. *Genetics* **136**, 1447-55.

Lee, M., Sharopova, N., Beavis, W. D., Grant, D., Katt, M., Blair, D. and Hallauer, A. (2002). Expanding the genetic map of maize with the intermated B73 x Mo17 (IBM) population. *Plant Mol Biol* **48**, 453-61.

Li, X., Qian, Q., Fu, Z., Wang, Y., Xiong, G., Zeng, D., Wang, X., Liu, X., Teng, S., Hiroshi, F. et al. (2003). Control of tillering in rice. *Nature* **422**, 618-21.

Miura, K., Ikeda, M., Matsubara, A., Song, X. J., Ito, M., Asano, K., Matsuoka, M., Kitano, H. and Ashikari, M. (2010). OsSPL14 promotes panicle branching and higher grain productivity in rice. *Nat Genet* **42**, 545-9.

Neuffer, M. G., Coe, E. H. and Wessler, S. R. (1997). Mutants of Maize: Cold Spring Harbor Laboratory Press.

SAS Institute. (2012). SAS 9.3, (ed. Cary, NC.

Satoh-Nagasawa, N., Nagasawa, N., Malcomber, S., Sakai, H. and Jackson, D. (2006). A trehalose metabolic enzyme controls inflorescence architecture in maize. *Nature* **441**, 227-30.

Schön, C. C., Melchinger, A. E., Boppenmaier, J., Brunklaus-Jung, E., Herrmann, R. G. and Seitzer, J. F. (1994). RFLP Mapping in Maize: Quantitative Trait Loci Affecting Testcross Performance of Elite European Flint Lines. *Crop Sci.*, 378-389.

Settles, A. M., Holding, D. R., Tan, B. C., Latshaw, S. P., Liu, J., Suzuki, M., Li, L., O'Brien, B. A., Fajardo, D. S., Wroclawska, E. et al. (2007). Sequence-indexed mutations in maize using the UniformMu transposon-tagging population. *BMC Genomics* **8**, 116.

Sigmon, B. and Vollbrecht, E. (2010). Evidence of selection at the ramosa1 locus during maize domestication. *Mol Ecol* **19**, 1296-311.

Van Ooijen, J. W. (1999). LOD significance thresholds for QTL analysis in experimental populations of diploid species. *Heredity (Edinb)* **83 (Pt 5)**, 613-24.

Vollbrecht, E., Duvick, J., Schares, J. P., Ahern, K. R., Deewatthanawong, P., Xu, L., Conrad, L. J., Kikuchi, K., Kubinec, T. A., Hall, B. D. et al. (2010). Genome-wide distribution of transposed Dissociation elements in maize. *Plant Cell* **22**, 1667-85.

Vollbrecht, E., Springer, P. S., Goh, L., Buckler, E. S. t. and Martienssen, R. (2005). Architecture of floral branch systems in maize and related grasses. *Nature* **436**, 1119-26.

Wang, S., Basten, C. J. and Seng, S.-B. (2012). Windows QTL Cartographer 2.5., (ed. N. C. S. U. Department of Statistics). Raleigh, NC.

Whipple, C. J., Kebrom, T. H., Weber, A. L., Yang, F., Hall, D., Meeley, R., Schmidt, R., Doebley, J., Brutnell, T. P. and Jackson, D. P. (2011). grassy tillers1 promotes apical

dominance in maize and responds to shade signals in the grasses. *Proc Natl Acad Sci U S A* **108**, E506-12.

Zeng, Z. B. (1994). Precision mapping of quantitative trait loci. *Genetics* **136**, 1457-68.

TABLE 1

KASPar markers

Marker	Locus	Position (Mb)	B73	Mo17
RA1MOD-1	MAGI4_3406	14.11	C	A
RA1MOD-2	MAGI4_50699	14.39	G	A
RA1MOD-3	csu1171.2	14.58	A	G
RA1MOD-3.5	GRMZM2G162764	14.86	T	C
RA1MOD-4	PZA01652.1	14.90	G	A
RA1MOD-5	GRMZM2G034302	15.07	T	G
RA1MOD-6	GRMZM2G022363	15.47	G	A
RA1MOD-7	PZA02094.9	15.73	T	A
RA1MOD-8	GRMZM2G000686	15.81	C	A
RA1MOD-9	GRMZM5G855347	16.33	G	T
RA1MOD-10	GRMZM2G175164	16.47	C	T
RA1MOD-11	GRMZM5G838098	16.78	A	G
RA1MOD-12	GRMZM2G000427	17.02	G	A
RA1MOD-13	PZB00648.5	17.60	A	G
RA1MOD-14	GRMZM2G109480	17.70	A	G
RA1MOD-15	GRMZM2G093197	17.88	T	C

TABLE 2

Ear Branch Number (EBN) among RILs

Genotype	Ear branch number (EBN)
B73	7.13±0.69
Mo17	0.02±0.01
F1	2.67±0.66
B73 RIL BC1s	2.33±0.20
Range	0-18.4
Heritability (%)	52.5
Mo17 RIL BC1s	1.22±0.14
Range	0-15.75
Heritability (%)	44.3

TABLE 3

QTL positions and effects

Recurrent parent	Chromosome number	Nearest marker	Position (IBM)	Support interval	LOD	"Additive" effect[a]	Model R^2 (%)[a]
ra1-63>B73	1	bnlg1429	144	134-147	6.40	1.07	18.0
	5	umc1447	248	246-249	3.81	0.82	10.4
	7	asg34a	132	117-137	4.15	-0.98	14.6
						Total	34.1
ra1-63>Mo17	6	umc2323	484	483-492	3.79	-0.85	45.3
	6	bnlg1759a	503	502-506	7.01	1.09	76.0
						Total	31.8

[a] Estimated from a simultaneous fit of all QTL

TABLE 4

NIL-F2 mapping results

	non-	RA1MOD-1		RA1MOD-5		RA1MOD-6		RA1MOD-8		RA1MOD-10		RA1MOD-15	
Genotype	recom	mean	N	mean	N	mean	N	mean	N	mean	N	mean	N
B	9.32	9.31	228	9.40	251	9.29	250	9.44	257	9.73	247	9.51	241
H	7.51	7.62	371	7.67	510	7.66	375	7.75	473	7.80	492	7.45	483
M	5.75	6.04	173	5.65	205	6.04	167	6.15	201	6.19	200	6.25	184
pr>F	-	5.85E-06		1.48E-09		9.44E-07		5.04E-07		6.85E-08		5.48E-07	
pr>χ^2	-	1.10E-02		2.47E-02		2.00E-04		3.05E-02		3.24E-02		4.40E-03	

TABLE 5

QTL candidate genes

Gene model	Annotation	B73 x Mo17 variation[a]	Differential Expression[b]	Expression pattern[c]	T.F. Targeted[d]	Available insertions
GRMZM2G424020	Calmodulin binding	None	-	Ubiquitous	-	Ds: in gene
GRMZM2G115131	Expressed protein	5'UTR 3'UTR	ra1: 1mm, 2mm ra2: 2mm ra3: 2mm	Ubiquitous	kn1: +377	-
GRMZM2G417835	G-protein receptor	CDS-C (2) Intron-SS	ra2: 2mm	Inflorescences	kn1: -1369	-
GRMZM2G112793	Phosphatase	None	-	Ubiquitous	-	-
GRMZM2G412674	F-box protein	None	-	Ubiquitous	-	-
GRMZM2G362942	PPR-containing protein	CDS-NC	ra1: 1mm	Ubiquitous	-	-
GRMZM2G091916	SET domain-containing protein	CDS-NC (2)	-	Ubiquitous	-	UfMu: Exon
GRMZM2G136113	Growth regulator-related protein	3'UTR (3)	-	Ubiquitous	-	UfMu: 5'UTR
GRMZM2G464818	PPR protein	5'UTR (2) CDS-C CDS-NC	-	Ubiquitous	-	-

[a] B73-Mo17 HapMap2 variants. CDS-C, conservative substitution; CDS-NC, non-conservative substitution; Intron-SS, intron splice site.

[b] Differential expression in immature ears of *ra1-R*, *ra2-R*, and *ra3-R* mutants (Eveland et al, 2010)

[c] Expression pattern from qTeller expression tool (www.qteller.com)

[d] ChIP-seq targets for *knotted1* (Bolduc et al, 2012) and *ramosa1* (Vollbrecht, Jackson, unpublished)

TABLE 6

IBM RILs used in this study

Intermated B73 × Mo17 (IBM) RILs			
M0001	M0034	M0262	M0322
M0005	M0035	M0264	M0323
M0007	M0039	M0265	M0325
M0008	M0040	M0266	M0326
M0010	M0043	M0267	M0328
M0012	M0045	M0269	M0337
M0014	M0046	M0272	M0341
M0015	M0048	M0275	M0344
M0016	M0051	M0276	M0345
M0017	M0052	M0281	M0352
M0021	M0054	M0284	M0354
M0022	M0055	M0287	M0355
M0023	M0057	M0288	M0357
M0024	M0058	M0296	M0360
M0025	M0060	M0297	M0364
M0027	M0061	M0298	M0365
M0028	M0066	M0309	M0368
M0029	M0067	M0310	M0369
M0030	M0075	M0311	M0378
M0031	M0076	M0315	M0379
M0032	M0077	M0317	M0382
M0033	M0079	M0321	M0384

FIGURE LEGENDS

Figure 1. Phenotypes of *ramosa1* mutants in the B73 and Mo17 backgrounds. A) *ra1-63.3359* phenotype in B73 tassel (A) and ear (C). *ra1-63.3359* phenotype in Mo17 tassel (B) and ear (D). E) Comparison of ear branch numbers in B73 and Mo17 introgressions of *ra1-63.3359*, *ra1-RS*, and *ra1-RSd.*

Figure 2. Genetic approach used to map modifiers of the *ra1-63.3359* phenotype in the IBM population. Genotypes shown are for *ra1-63.3359* and a potential modifier locus (QTL). Photographs show segregation of phenotypes in the Mo17 (left) and B73 (right) backcrosses.

Figure 3. Strategy used to identify recombinants for the chromosome 1 QTL using near isogenic lines (NILs). NIL-F2 individuals were genotyped at six markers spanning the QTL region. Recombinant individuals were tagged and later crossed by B73-introgressed *ra1-63.3359.*

Figure 4. Generation and comparison of recombinant subclasses. Example is of recombinant line REC-38. Recombinant individuals within the NIL-F2 were crossed by *ra1-63.3359* generating a family that segregated for the recombinant chromosome. Individuals from this family were once again crossed by *ra1-63.3359* resulting in two subclasses, one that segregated for the recombinant chromosome and one that segregated for the parental chromosome of the NIL-F2 individual. Each subclass was genotyped and scored for ear branch number. Subclass genotypes were concatenated using indicator variables (0,1) whereby a zero indicates they share a genotype at a given locus and a one indicates they differ in genotype at that position.

Figure 5. Tassel and ear branch number for B73 and Mo17 introgressions of *ra1-63.3359* and an F1. Ear phenotypes of *ra1-63.3359* appear additive, while tassel phenotypes display over-dominance.

Figure 6. Treatment means for the B73 and Mo17 RIL treatments. The Mo17 treatment means are lower overall and all means fall within the range of the parent introgressions. B73 treaments display a wide distribution of means that extend beyond the means of the high parent indicating transgressive segregation among treatments.

Figure 7. Composite interval mapping results for chromosomes containing significant QTL for ear branch number in the B73 treatments. LOD scores and additive effects for B73 treatments are shown in black. For comparison, LOD scores and effects in the Mo17 treatments are shown in red. X-axis coordinates are shown in IBM recombination units.

Figure 8. Composite interval mapping results for chromosomes containing significant QTL for ear branch number in the B73 treatments. LOD scores and additive effects for Mo17 treatments are shown in red. For comparison, LOD scores and effects in the B73 treatments are shown in black. X-axis coordinates are shown in IBM recombination units.

Figure 9. Mean ear branch number for each genotypic class of the NIL-F2 calculated from non-recombinant individuals. The QTL effect is significant ($p<0.0001$) and follows a linear trend ($R^2=0.9999$) indicating that the allelic interaction is additive.

Figure 10. Fine-mapping results for the chromosome 1 QTL. Single marker analysis results for the subclass means (black) and subclass comparisons (blue dashed). X-axis indicates physical coordinates of markers in million base pair (Mb) increments. Y-axis is the ratio of likelihoods for the alternative hypothesis (QTL present) and null hypothesis (no QTL).

Figure 1 Weeks *et al.*

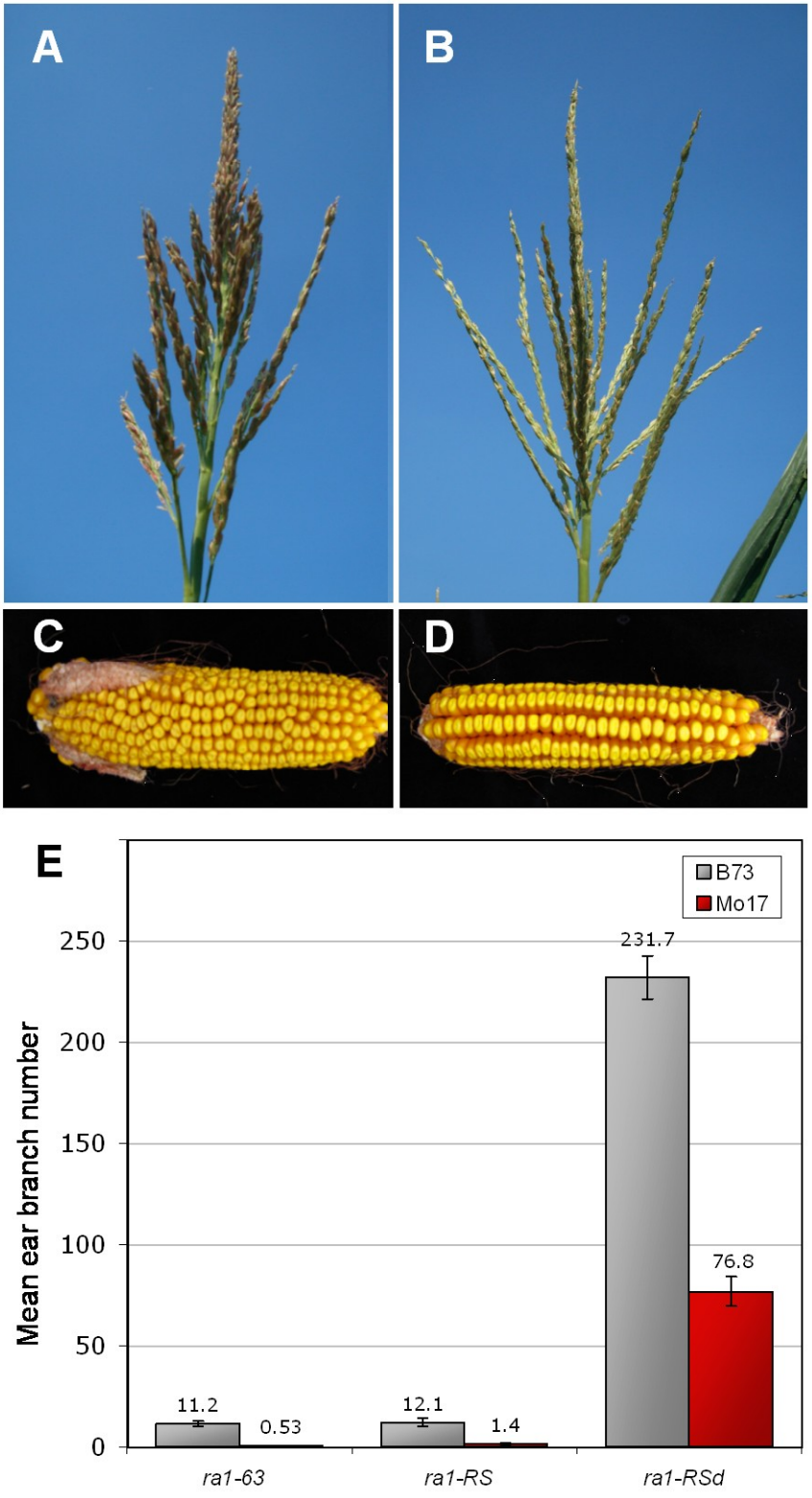

Figure 2 Weeks *et al.*

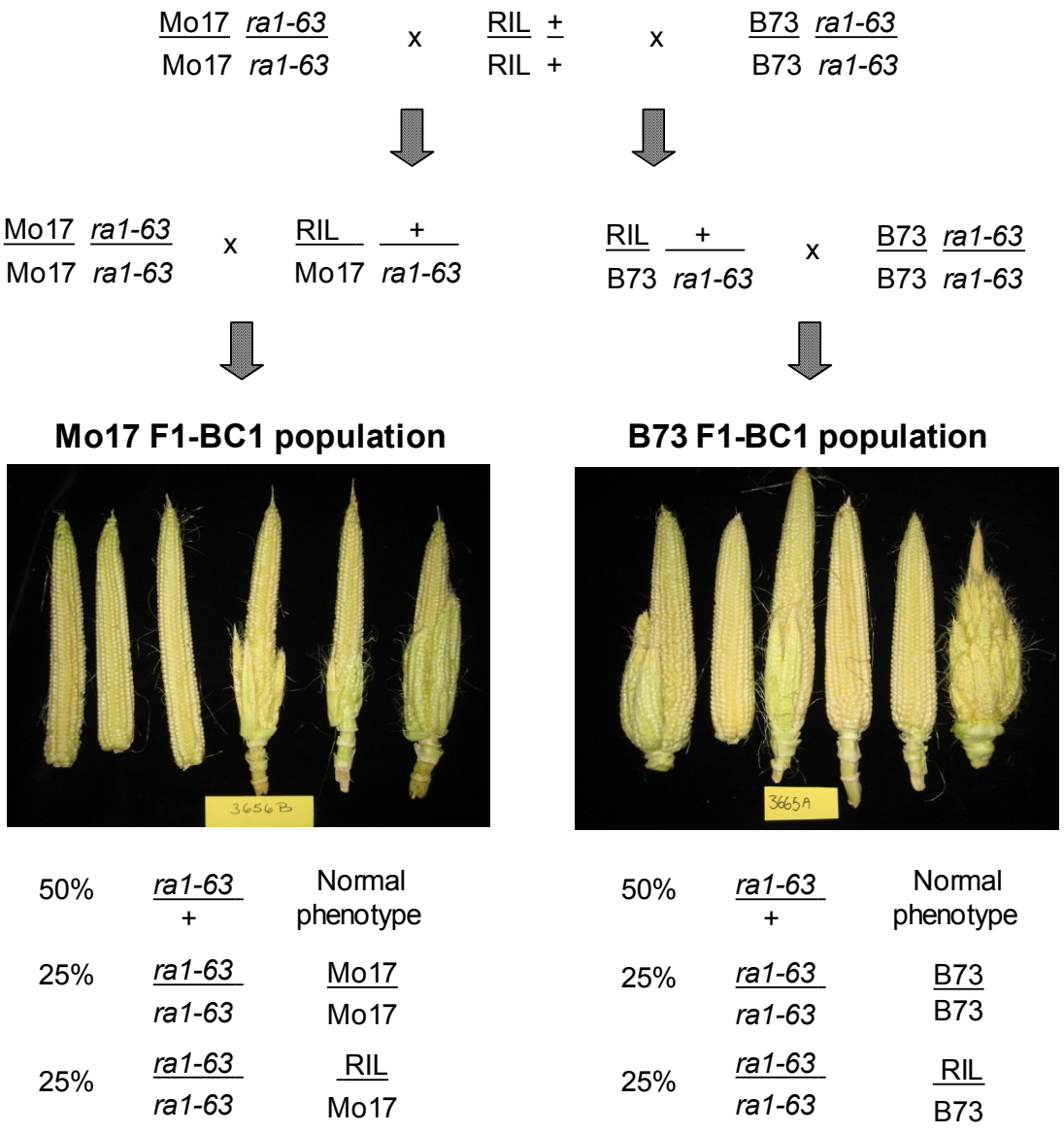

Figure 3 Weeks *et al.*

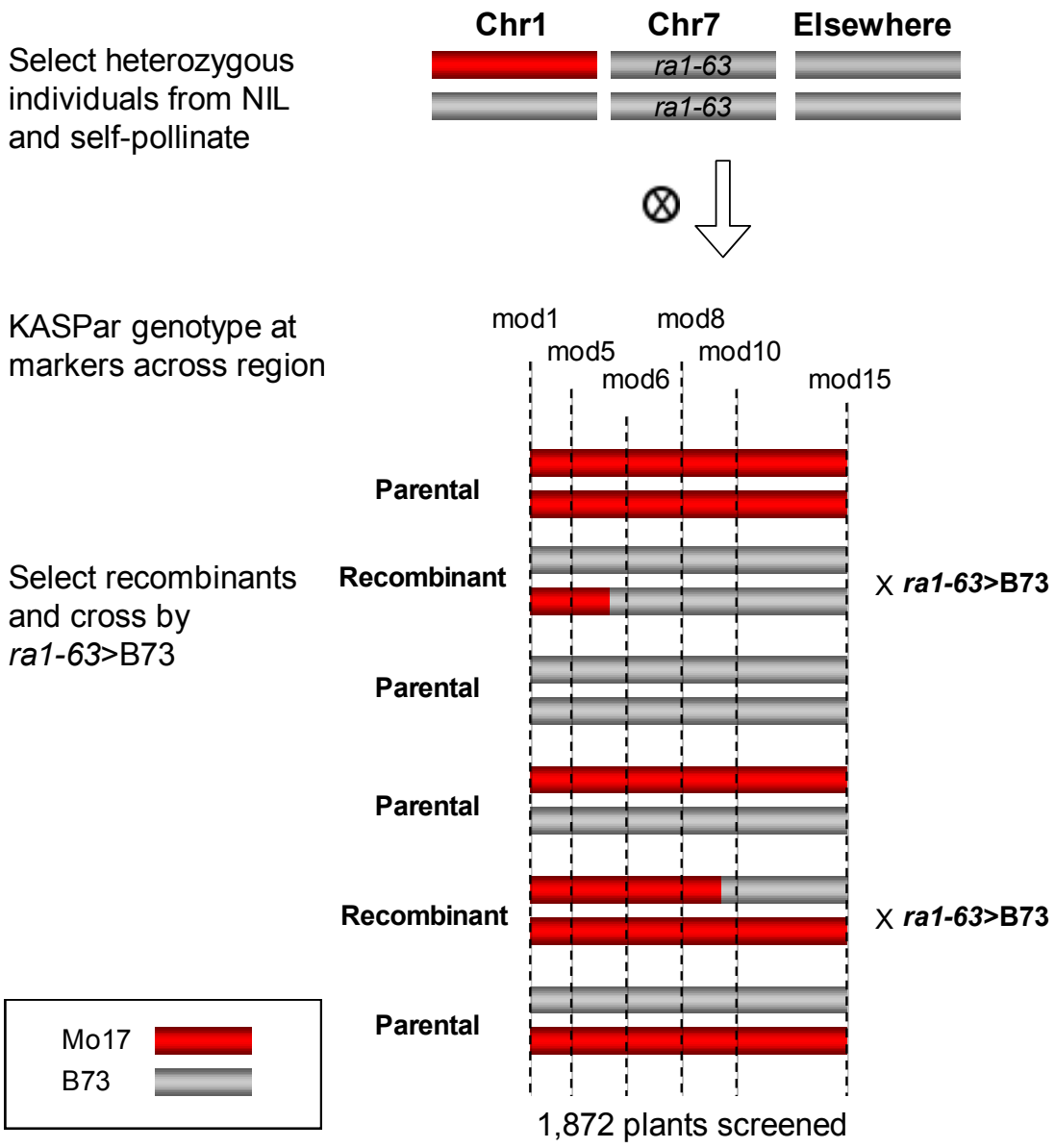

Figure 4 Weeks *et al.*

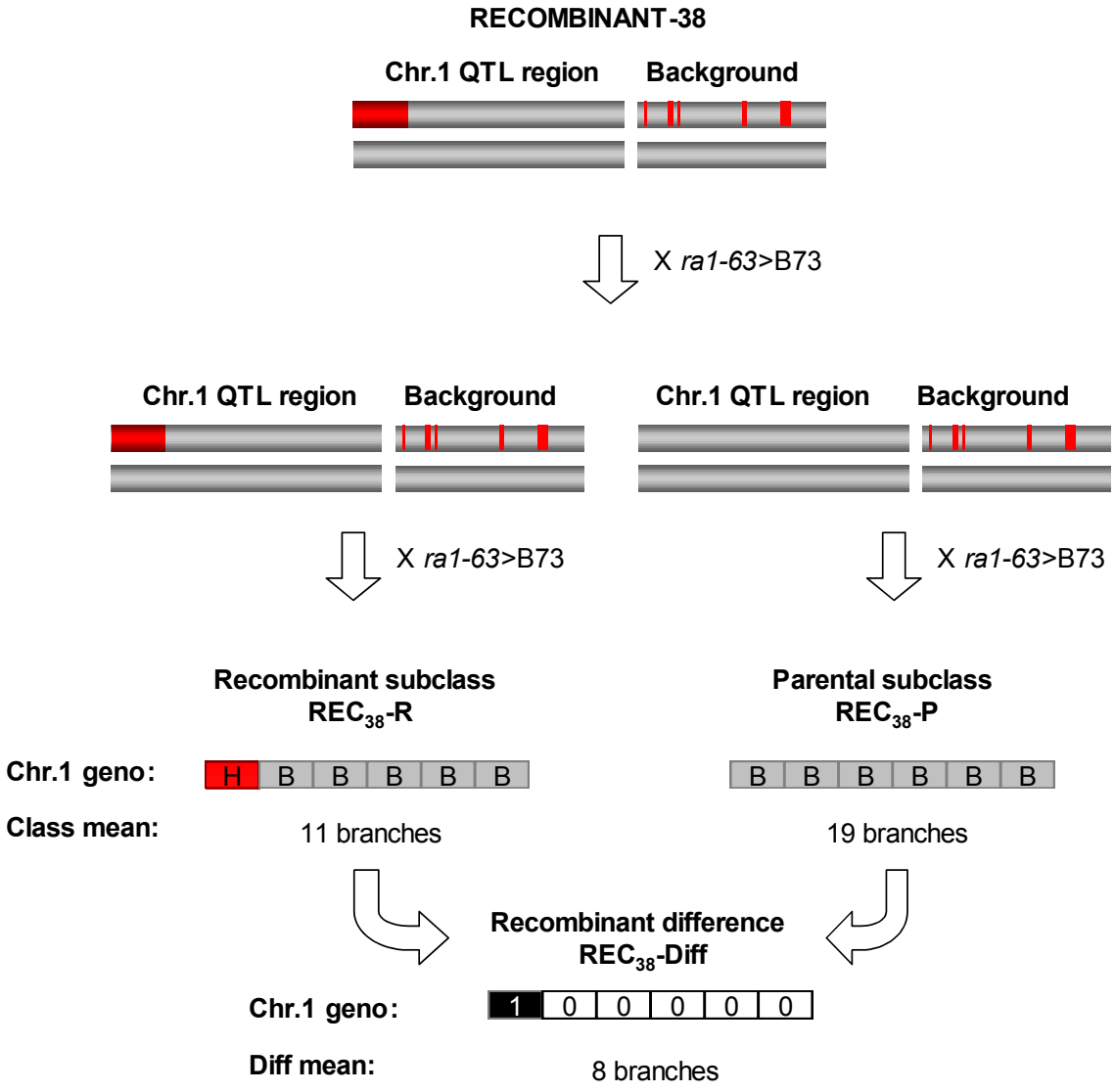

Figure 5 Weeks *et al.*

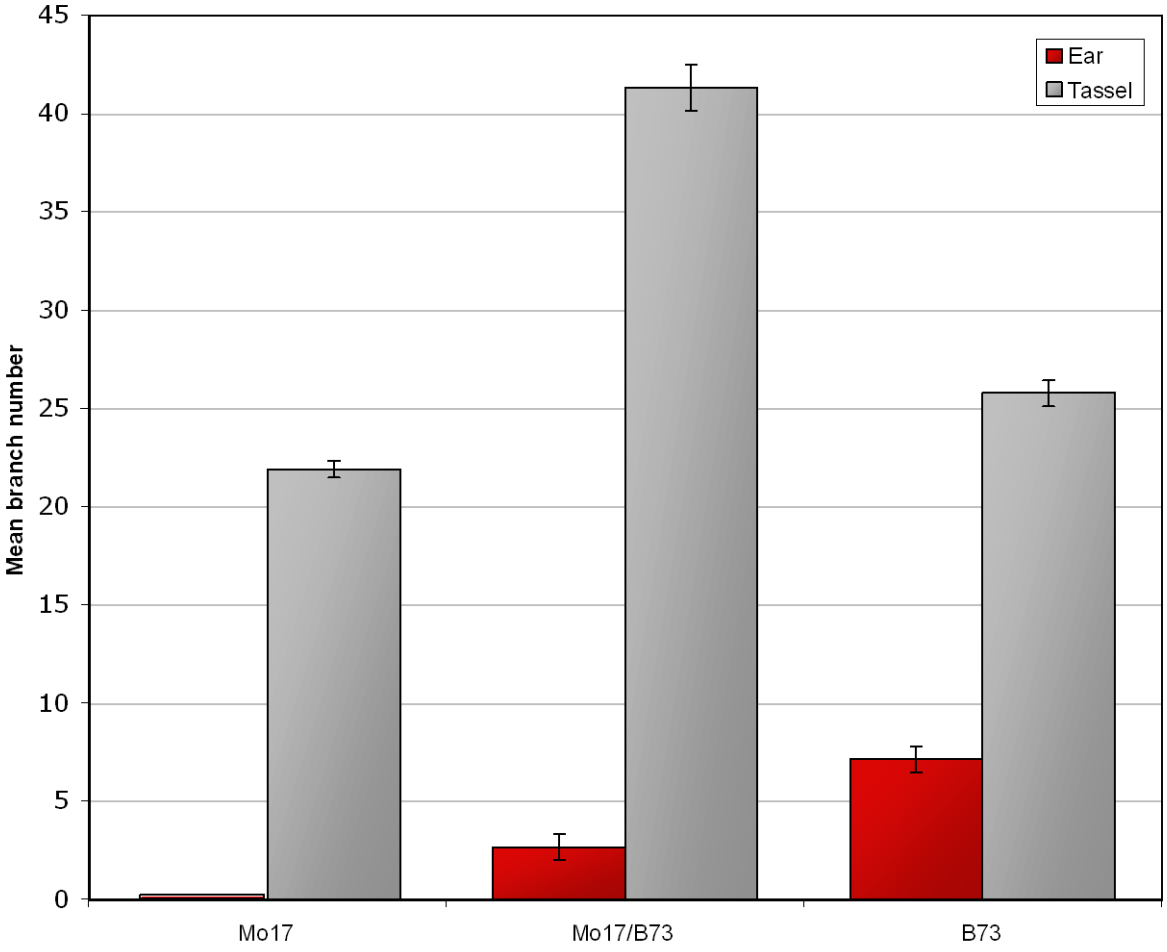

Figure 6 Weeks *et al.*

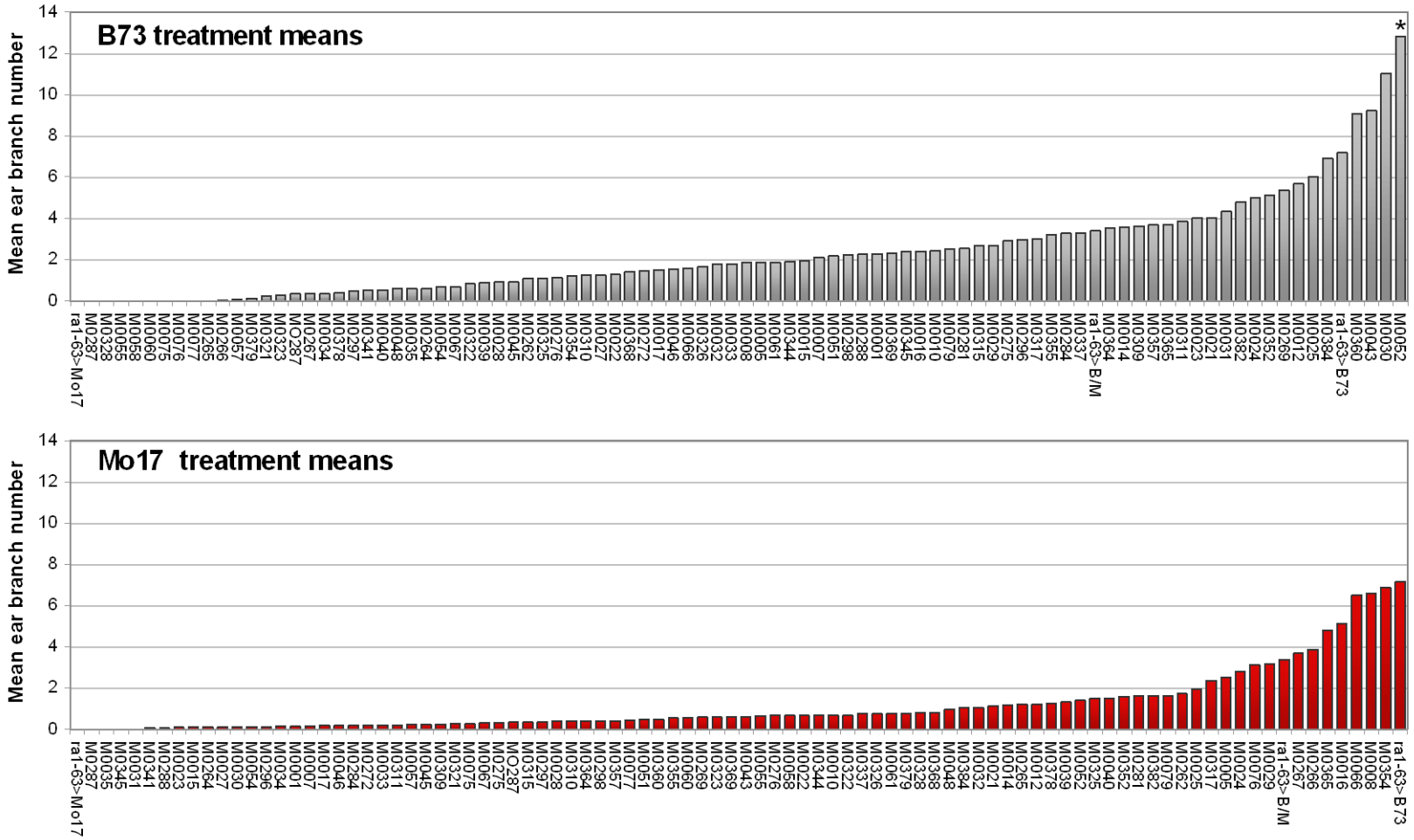

* Significantly different from *ra1-63.3359*>B73 at LSD0.05

Figure 7 Weeks *et al.*

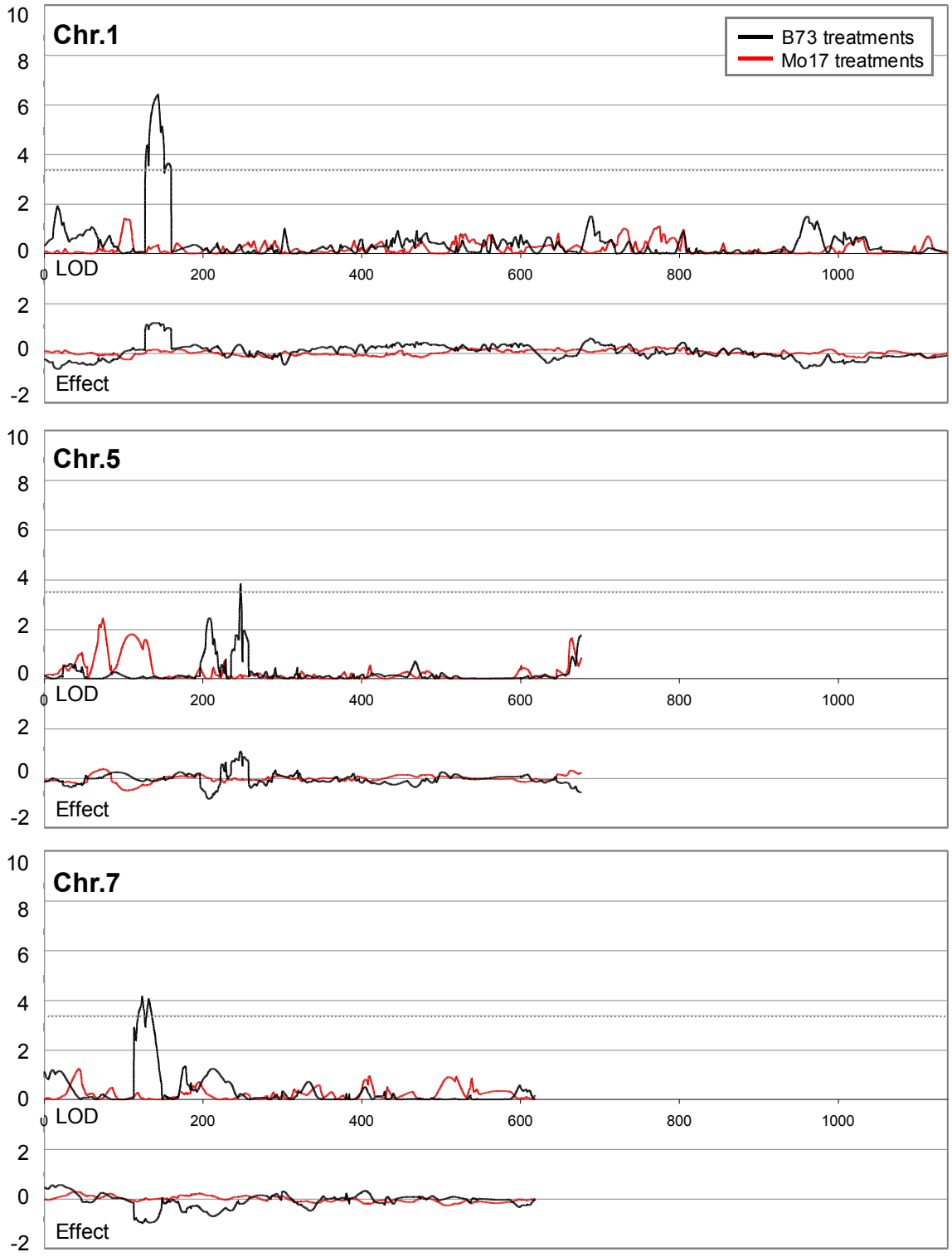

Figure 8 Weeks *et al.*

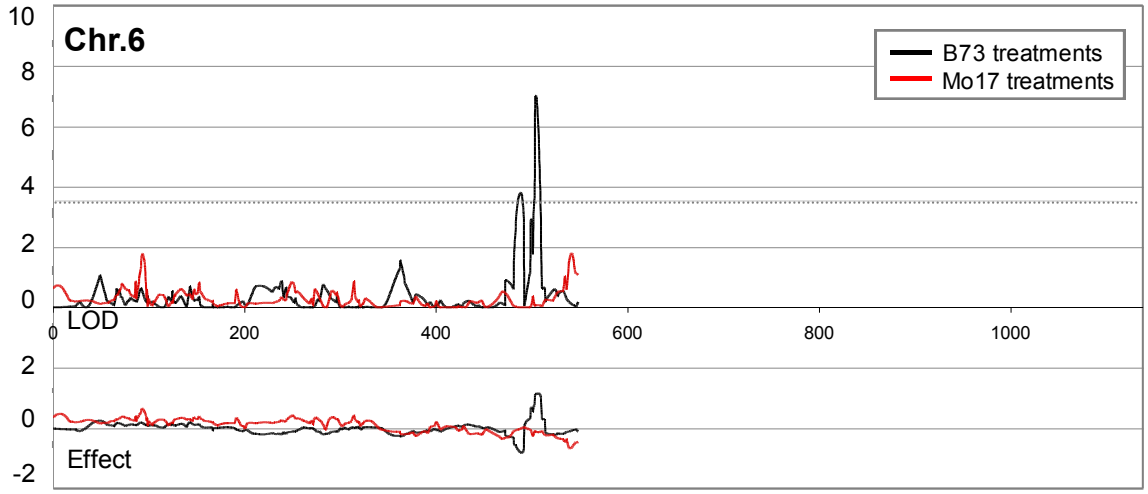

Figure 9 Weeks *et al.*

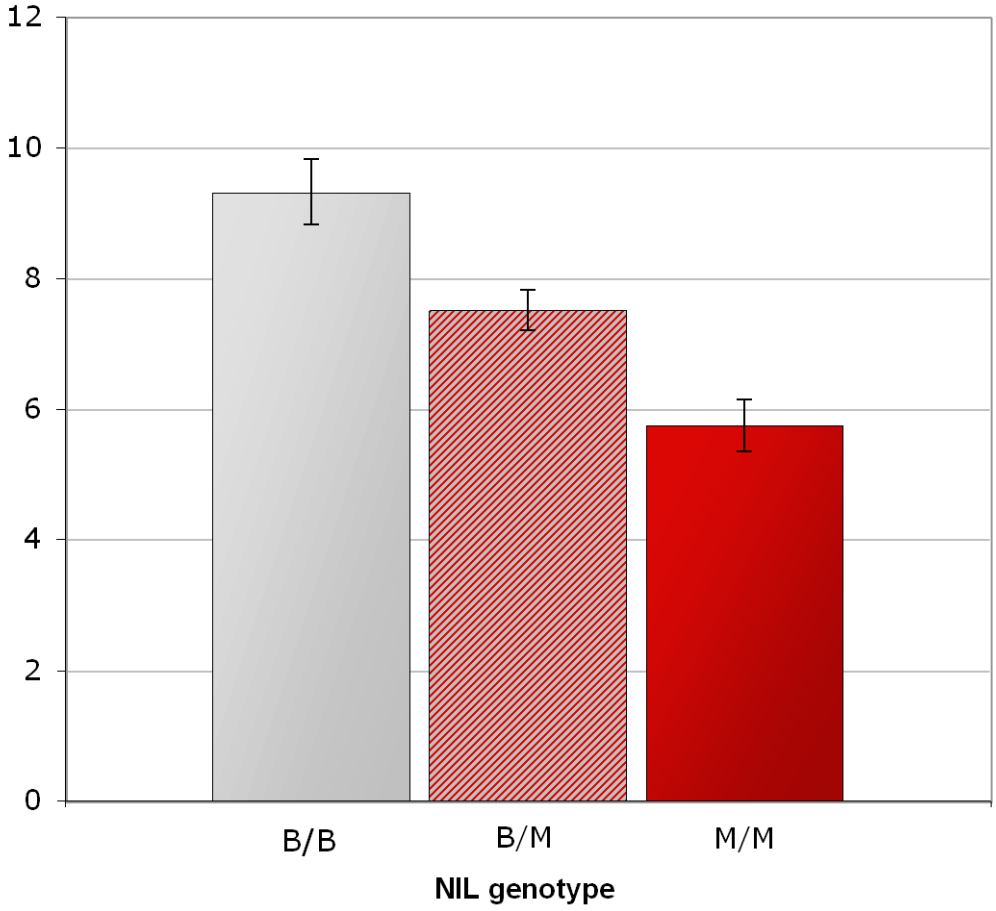

Figure 10 Weeks *et al.*

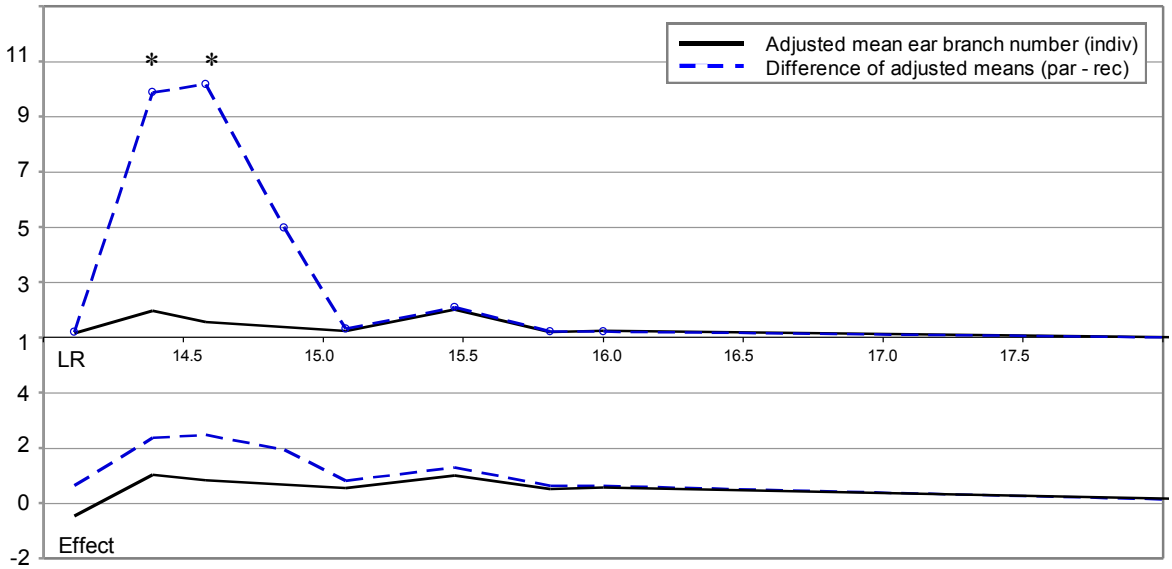

* Significant effect ($p<0.05$)

CHAPTER 4. QUANTITATIVE TRAIT LOCI FOR EAR BRANCH NUMBER IN *RAMOSA2* MUTANTS

A manuscript to be submitted to *BMC Plant Biology*

Rebecca Weeks and Erik Vollbrecht

ABSTRACT

The maize gene *ramosa*2 (*ra2*) plays an important role in regulating inflorescence architecture by imposing determinacy upon the lateral meristems of the tassel and ear. The tassels of *ra2-R* mutants are characterized by increased branching and more acute branch angles and ears exhibit unorganized rows and/or lateral branching. The severity of these phenotypes, however, varies according to genetic background. In B73, for example, ears display disordered rows and occasional branching, while in Mo17 branching is very rare. To identify genes underlying these phenotypic disparities, we performed a QTL mapping experiment using the intermated B73 × Mo17 (IBM) population of maize. Loci that alter the ear branching phenotype of *ra2-R* mutants were identified on chromosomes 1S, 1L and 7L. The chromosome 1S peak co-localizes with a QTL previously identified for its effect on ear branching in *ramosa1* mutants, possibly indicating the presence of a modifier functioning within a common branch of the *ramosa* pathway. A marker within the inflorescence gene *anther ear1* (*an1*) was associated with branch number in the Mo17 experiment and might implicate natural variation at or near *an1* as a source of phenotypic variation for ear branch number in *ra2-R* mutants. The remaining loci likely represent novel QTL for inflorescence branch number. In order to identify candidate genes for these regions, we integrated data from several existing transcript profiling experiments and identified genes within each region that are differentially expressed in *ramosa* mutants and/or co-expressed with *ra2* across several datasets.

INTRODUCTION

Maize, which is a monoecious plant, bears its male and female inflorescences on physically distinct locations of the plant. The male inflorescence, borne apically, is commonly referred to as the tassel and is responsible for producing pollen. The female inflorescence, which arises laterally in the axils of leaves, is commonly referred to as the ear and bears the female flowers of maize. Upon fertilization, each female flower will go on to produce a single starch-filled fruit, also known as a kernel. While the male and female inflorescences are physically separated and are visually distinct, they are derived through remarkably similar developmental programs. In either case, development begins from a group of pluripotent stem cells known as the inflorescence meristem. Shortly after their inception, inflorescence meristems initiate a second order of meristems acropetally along their flanks. In the male inflorescence, a few of these meristems are indeterminate, and will go on to produce the long branches normally present at the base of the tassel. The remaining meristems of the tassel and all meristems of the ear, however, are determinate and will terminate in the production of a defined quantity of derivatives. These determinate meristems, known as spikelet pair meristems (SPMs), each give rise to a pair of spikelet meristems (SMs), from each of which a pair of floral meristems (FMs) arises. At this point, the developmental programs of the male and female inflorescences begin to diverge. In the flowers of the ear, lower floral meristems abort and the remaining FM produces a flower bearing only female-specific organs. In the male inflorescence, both FMs go on to produce flowers, however, pistils within these flowers abort, leaving only stamen.

Meristem determinacy is an important architectural variable, especially as it relates to the formation of branches in the tassel and ear. In theory, increased tassel branching creates the potential for greater pollen production, which is critical for efficient seed production, especially during the commercial production of hybrid seed where male plants are present in limited quantities in order to maximize the seed output of the plot. In the female inflorescence, however, increased branching is undesirable, as it leads to inefficient packing of kernels on the ear (Sigmon and Vollbrecht). Numerous studies have documented an inverse relationship between tassel branching and yield (Geraldi, 1978; Geraldi, 1985; Hunter, 1969; Sharma, 1968). However, while several hypotheses have been proposed

(Hunter, 1969), the biological mechanisms underlying this relationship are still poorly understood.

A number of genes have been discovered which, when mutated, alter the branching of maize inflorescences. Among these, the *ramosa* mutants display striking branching effects culminating from the loss of determinacy in the SPMs of their inflorescences. All three of these genes have been cloned; *ra1* encodes a cys2-his2 zinc finger transcription factor (Vollbrecht et al., 2005), *ra2* encodes a LATERAL ORGAN BOUNDARY (LOB) domain transcription factor (Bortiri et al., 2006), and *ra3* encodes a trehalose-6-phosphate phosphatase metabolic enzyme (Satoh-Nagasawa et al., 2006). Double mutant and expression analyses suggest that *ra2* and *ra3* function in parallel upstream of *ra1*, and regulate inflorescence development by imposing determinacy on SPMs of the male and female inflorescences.

The branching phenotypes of all three *ramosa* mutants vary according to genetic background. In the previous chapter, we described efforts to identify and map QTL that alter branch number in the *ra1-63.3359* mutant. Here we describe a similar experiment aimed at identifying QTL that alter the branching phenotype of *ra2-R* mutants. In the present study, the IBM-94 population was used to map naturally occurring modifiers in B73 and Mo17 that either suppress or enhance the ear branching phenotype of *ra2-R*. Four QTL were identified, two of which enhance and two of which suppress branching of *ra2-R* in the B73 relative to Mo17. One of these QTL closely aligns with a modifier identified in the *ra1-63.3359* experiment. Efforts to validate allelism of these two modifiers are currently underway. Another QTL interval includes the *an1* gene of maize, which causes reduced tassel branching when mutated. The remaining two QTL represent novel loci involved in determining inflorescence branch number in the perturbed *ra2-R* background. Efforts to fine-map these QTL and pinpoint the genes or sequences underlying the phenotypic effects are currently underway.

METHODS

The *ra2-R* allele was originally characterized in the B73 and A188 backgrounds (Bortiri et al., 2006). We additionally introgressed *ra2-R* into Mo17 by backcrossing six

times into the inbred line. At this stage, comparisons of inflorescence branching phenotypes were performed on the B73 and Mo17 introgressions and an F1 hybrid. Statistical evaluation of these differences was performed using the SAS software package.

A subset of 88 lines originating from the IBM-94 population (Lee et al., 2002) was used to identify and map modifiers of the *ra2-R* ear branching phenotype. B73 and Mo17 introgressions of *ra2-R* were used as recurrent backcross parents to generate two F1-BC1 populations for each recombinant inbred line RIL; each population is henceforth referred to as a treatment (Figure 2). The resulting collections of treatments were planted in the summer of 2012 in a completely randomized design (CRD) replicated three times with each experimental unit consisting of a single row of 20 kernels (Table 1). Because two doses of the recessive allele *ra2-R*, are required to observe branching in the ear, only half of the F1-BC1 individuals within each treatment could be scored for ear branch number. These individuals were identified based on their upright tassel phenotypes and selected for scoring, which was performed by harvesting mature top ears, husking, and counting branches as they were removed from the ear.

Mean ear branch number was computed for each plot in the three replicates as the mean of the *ra2-R* homozygous plants scored in each plot. The distribution of phenotypes based on means of treatments across replicates was not normal as tested for normality by the Shapiro-Wilk test statistic in the SAS univariate procedure (SAS Institute, 2012). Transformations using natural log, log 10, square root, and Box-Cox failed to confer normality to the distribution of phenotypes, so analyses were performed using untransformed data. Heritability, defined as the proportion of the phenotypic variance explained by the treatments, was estimated by performing a one-way ANOVA of treatments on mean ear branch number between replicates. The standard error of heritability was calculated according to the formula $(MS_g/n)^{1/2}$ where MS_g is the genotype mean square and n=treatments x replications (Berke and Rocheford, 1999). Transgressive segregation was investigated by making pairwise comparisons of treatments with parent lines and testing for significance using LSD0.05. Comparison of *ra1*-63.3359 and *ra2-R* backcross means was performed using the Spearman rank-order and Pearson correlation tests in SAS (SAS Institute, 2012).

The IBM-94 population (Lee et al., 2002) has been genotyped for approximately 4000 markers spanning the maize genome, of which we used 2,025 framework markers to perform the QTL analysis. Genotypes for the IBM-94 population can be obtained from www.maizegdb.org (Schaeffer et al.). Composite Interval mapping (CIM) was performed on ear branch number averaged across replicates using WinQTLCartographer version 2.5 (Wang et al., 2012). Cofactors were selected by stepwise regression using the forward selection, backward elimination method with a cutoff of 0.05 for cofactor selection and elimination. A LOD threshold of 3.55 was applied on a per chromosome basis (Van Ooijen, 1999), which corresponds to a chromosome-wise error rate of 0.005 and a genome-wise error rate of 0.05. It is important to note that this method uses an average chromosome length, 250cM for maize, to determine LOD thresholds. Therefore, smaller chromosomes will experience a slightly more stringent threshold relative to larger chromosomes. QTL support intervals were calculated as the position along the significance peak at which the LOD score is 1.0 unit less than the peak LOD score. Estimates of additive effects and phenotypic variance explained by each QTL were calculated by fitting the final model including all putative QTL using the Multiple Interval Mapping function of WinQTLCartographer. The additive effect of a given marker was calculated as one half of the difference between the homozygous B73 and Mo17 class means, whereby a positive effect corresponds to an increase in the B73 class mean relative to Mo17. The proportion of phenotypic variance explained by each QTL and covariance estimates between QTL were used to calculate the total phenotypic variance explained by the model. Genotypic variance explained by the model was calculated by dividing the model R^2 by the trait heritability (Schön et al., 1994).

RESULTS

When introgressed into B73, ears of *ra2-R* mutants displayed increased branching compared to the Mo17 introgression, which exhibited only unbranched ears. Branching was never observed in the F1 indicating the presence of at least one Mo17 suppressor capable of masking the branched phenotype of the B73 background (Table 2). The B73 treatments displayed a wide range of phenotypes and transgressive segregation was observed among treatments (Figure 3). Heritability for ear branch number in the B73 backcross treatments

was estimated at 57%. A comparison of treatment means in the *ra1*-63.3359 and *ra2-R* B73 backcross experiments revealed significant correlation of mean ear branch numbers (Pearson r=0.23, p=.033) and overall rank of treatments (Spearman r=0.36, p=0.0006) (Figure 4).

A subset of 35 plots representing 28 RIL treatments from the Mo17 population was scored for ear branch number (Table 2). Of the 248 ears that were scored, only two were branched. Both of these were from the backcross of the RIL M0024. Scoring was suspended at this point and mapping was performed using data from the 28 RIL lines. Heritability for this population could not be estimated, as it would be inflated by the presence of mostly unbranched families and a single replicate of the M0024 treatment producing branched ears.

Two QTL located on chromosome 1 and one QTL on chromosome 7 were significantly associated with ear branch number in the B73 treatments (Table 3, Figure 5). A simultaneous fit of all three QTL accounted for 34.3% of the phenotypic variance and 60.1% of the genotypic variance. No epistatic interactions were detected for these QTL as tested by multiple regression analysis. The LOD scores for the 1S, 1L, and 7L QTL were 4.39, 5.69, and 3.84 respectively. For both of the chromosome 1 QTLs, the B73 allele exhibited a positive, or enhancing effect on branch number while a negative or suppressive effect was observed for the B73 allele of the chromosome 7 QTL. Because mapping was conducted using RIL genotypes, which are homozygous for either parent allele at a given locus, dominance effects could not be estimated.

Two linked QTL located on chromosome arm 1L were significantly associated with ear branch number in the Mo17 backcross treatments (Table 1, Figure 5). These QTL collectively explained 15.5% of the phenotypic variance. Their share of the genotypic variance could not be calculated since a heritability estimate was not available. For each QTL, the B73 allele exhibited an equal but opposite effect of 0.21 branches with the proximal QTL effect being negative and the distal effect positive. Comparison of the distal 1L QTL with the similarly placed QTL identified in the B73 backcross treatments revealed significant overlap (Figure 5).

DISCUSSION

Inflorescence branch number in maize is quantitatively inherited, with the phenotype of the individual ultimately being determined by the collective actions of a large number of genes (Berke and Rocheford, 1999; Mickelson et al., 2002; Romay et al., 2013). Presumably due to redundancy within the maize genome, many of these genes display subtle phenotypic effects when mutated and are therefore difficult to identify through traditional mutagenesis techniques. The vast interspecific diversity observed in maize (Romay et al., 2013) presents a unique opportunity to quantitatively map regions of the genome underlying the phenotypic differences observed between inbred backgrounds. We exploited this diversity using the IBM-94 population and were able to identify four loci, each of which imparts a significant effect on mean ear branch number of *ra2-R* mutant families.

In the B73 experiment, a significant effect was observed on chromosome 1S. The significance peak co-localized with a QTL previously identified in a similar experiment aimed at mapping modifiers of *ra1-63.3359*. The identification of a QTL that is able to influence both *ra1* and *ra2* phenotypes is not surprising, given that the genes function in the same pathway and mutation of *ra2* results in reduced expression of *ra1* (Bortiri et al., 2006; Vollbrecht et al., 2005). Ongoing experiments to analyze the effect of the 1S QTL in *ra2* mutants using a near isogenic line (NIL) generated for the *ra1-63.3359* modifier fine-mapping experiment will help determine whether these QTL are allelic. While tassel traits were not evaluated in this experiment, overlap of this QTL with another for tassel branch number in IBM (Mickelson et al., 2002), warrants further investigation of the region's effect on tassel branch number in *ra2-R* mutants.

In both the B73 and Mo17 backcross experiments, we identified a QTL in bin 1.08. Interestingly, the direction of the QTL effect was backcross-dependent suggesting that the heterozygote suppressed branching relative to either homozygous parent. This result was unexpected and more work is needed to confirm the significance and magnitude of the effects for each population. However, one possible hypothesis for this phenomenon could be the presence a modifier that functions as protein dimer. In such a case, a B73/Mo17 heterozygote might produce a heterodimer that functions poorly relative to the homodimer of either parent. In any case, the presence of overlapping significance peaks in both

experiments is promising and indicates that the heterozygote displays a phenotype that is non-parental (ie dominance is either not present or is incomplete.) A combined analysis of the significance peaks from both populations produced a 8Mb region containing 183 genes. We filtered the candidate gene list to include only those genes that showed differential expression in one or more of the *ra1-R*, *ra2-R*, or *ra3-R* mutants at the 1mm stage, the approximate developmental time point at which long branches are being initiated. A total of 39 genes were identified (Table 4). We further assessed these candidates based on their co-expression with *ramosa2* across several transcription profiling experiments performed on immature tassels and ears (Eveland et al. 2010) and identified a subset of five genes whose expression is significantly correlated with that of *ra2* (Table 4).

In the Mo17 backcross, we identified an additional QTL in tight linkage with the 1.08 QTL described above. For this interval, the most significant marker was *anther ear1* (*an1*) a gene that, when mutated, is characterized by a reduction in tassel branch number (Bensen et al., 1995). The *an1* locus is closely linked to the kernel color marker *bronze2* (*bz2*) and consequently, this region has been characterized extensively. Brunner et al. sequenced allelic regions containing the *bz2* and *an1* loci from B73 and Mo17 and observed tremendous diversity between the inbred lines (Brunner et al., 2005). Based on comparison of fingerprint patterns, the *bz1-an1* containing BACs of B73 and Mo17 were classified as highly divergent and over the 295kb of compared contiguous sequence, 60% non-homology was observed. Most of the non-shared sequences consisted of LTR-transposons and other retroelements, however numerous instances of non-collinear gene arrangements were observed and the majority of genes (15/21) were not shared between inbreds. Eleven of these non-shared genes are present in the current filtered gene set. Because this QTL was detected from a small subset of lines (N=28) it will be interesting to see whether the scoring of additional lines is able to further resolve the QTL peak.

The final QTL is located in bin 7.05. After filtering for differential expression in *ramosa* mutants, 13 candidate genes were identified (Table 5). None of these genes clustered with *ramosa2*. It is possible, however, that a modifier gene will display a distinct expression pattern relative to the modified locus as is the case with *ramosa1 enhancer locus2* (*rel2*), which enhances the inflorescence phenotypes of *ramosa1* and *ramosa2* mutants despite being

more ubiquitously expressed (Gallavotti et al., 2010). Also, as previously discussed, the genomes and gene complements of B73 and Mo17 are unique and therefore it is possible that the modifier gene is not present in the B73 gene set.

We undertook a quantitative genetics approach in order to identify regions of the maize genome, which through natural variation, are able to alter the inflorescence branching phenotype of *ra2-R* mutants. Using this technique, we were able to identify four loci significantly associated with changes in the ear branch number of *ra2-R* mutants. These loci likely represent novel components of the inflorescence development pathway and therefore efforts to identify the causative genes or sequences may be helpful in understanding the mechanisms involved in regulating meristem determinacy. Ongoing efforts to confirm and fine-map these QTL using near isogenic lines (NILs) are underway. By mapping these small-effect genes and investigating their interactions with known inflorescence genes, we hope to gain valuable insight into the inner workings of the inflorescence development pathway.

LITERATURE CITED

Bensen, R. J., Johal, G. S., Crane, V. C., Tossberg, J. T., Schnable, P. S., Meeley, R. B. and Briggs, S. P. (1995). Cloning and characterization of the maize An1 gene. *Plant Cell* **7**, 75-84.

Berke, T. G. and Rocheford, T. R. (1999). Quantitative Trait Loci for Tassel Traits in Maize. *Crop Sci.* **1999**, 1439-1443.

Bortiri, E., Chuck, G., Vollbrecht, E., Rocheford, T., Martienssen, R. and Hake, S. (2006). ramosa2 encodes a LATERAL ORGAN BOUNDARY domain protein that determines the fate of stem cells in branch meristems of maize. *Plant Cell* **18**, 574-85.

Brunner, S., Fengler, K., Morgante, M., Tingey, S. and Rafalski, A. (2005). Evolution of DNA sequence nonhomologies among maize inbreds. *Plant Cell* **17**, 343-60.

Eveland, A. L., Satoh-Nagasawa, N., Goldshmidt, A., Meyer, S., Beatty, M., Sakai, H., Ware, D. and Jackson, D. (2010). Digital gene expression signatures for maize development. *Plant Physiol* **154**, 1024-39.

Gallavotti, A., Long, J. A., Stanfield, S., Yang, X., Jackson, D., Vollbrecht, E. and Schmidt, R. J. (2010). The control of axillary meristem fate in the maize ramosa pathway. *Development* **137**, 2849-56.

Geraldi, I. O., Miranda Filho, J.B. Vencovski, R. (1978). Prospects of breeding maize (Zea mays L.) with reference to tassel characters. In *Brazilian Sociey for Scientific Progress*, vol. 30 (ed., pp. 533-534.

Geraldi, I. O., Miranda Filho, J.B. Vencovski, R. (1985). Estimates of ggenetic parameters for tassel characters in maize (Zea mays L.) and breeding perspectives. *Maydica*, 1-14.

Hunter, R. B., T.B. Daynard, D.J. Hume, J.W.Tanner, J.D. Curtis, and L.W. Kannenberg. (1969). Effect of tassel removal on grain yield of corn (Zea mays L.). *Crop Sci.* **9**, 405-406.

Institute, S. (2012). SAS 9.3, (ed. Cary, NC).

Lee, M., Sharopova, N., Beavis, W. D., Grant, D., Katt, M., Blair, D. and Hallauer, A. (2002). Expanding the genetic map of maize with the intermated B73 x Mo17 (IBM) population. *Plant Mol Biol* **48**, 453-61.

Mickelson, S. M., Stuber, C. S., Senior, L. and Kaeppler, S. M. (2002). Quantitative Trait Loci Controlling Leaf and Tassel Traits in a M73 x Mo17 Population of Maize. *Crop Sci.*, 1902-1909.

Romay, M. C., Millard, M. J., Glaubitz, J. C., Peiffer, J. A., Swarts, K. L., Casstevens, T. M., Elshire, R. J., Acharya, C. B., Mitchell, S. E., Flint-Garcia, S. A. et al. (2013). Comprehensive genotyping of the USA national maize inbred seed bank. *Genome Biol* **14**, R55.

Satoh-Nagasawa, N., Nagasawa, N., Malcomber, S., Sakai, H. and Jackson, D. (2006). A trehalose metabolic enzyme controls inflorescence architecture in maize. *Nature* **441**, 227-30.

Schaeffer, M. L., Harper, L. C., Gardiner, J. M., Andorf, C. M., Campbell, D. A., Cannon, E. K., Sen, T. Z. and Lawrence, C. J. (2011). MaizeGDB: curation and outreach go hand-in-hand. *Database (Oxford)* **2011**, bar022.

Schön, C. C., Melchinger, A. E., Boppenmaier, J., Brunklaus-Jung, E., Herrmann, R. G. and Seitzer, J. F. (1994). RFLP Mapping in Maize: Quantitative Trait Loci Affecting Testcross Performance of Elite European Flint Lines. *Crop Sci.*, 378-389.

Sharma, P. P. a. N. L. D. (1968). Correlation between tassel and ear characters and yield in maize. *Indian J. Genet. Plant Breed.* **28**, 196-204.

Sigmon, B. and Vollbrecht, E. (2010). Evidence of selection at the ramosa1 locus during maize domestication. *Mol Ecol* **19**, 1296-311.

Van Ooijen, J. W. (1999). LOD significance thresholds for QTL analysis in experimental populations of diploid species. *Heredity (Edinb)* **83 (Pt 5)**, 613-24.

Vollbrecht, E., Springer, P. S., Goh, L., Buckler, E. S. t. and Martienssen, R. (2005). Architecture of floral branch systems in maize and related grasses. *Nature* **436**, 1119-26.

Wang, S., Basten, C. J. and Seng, S.-B. (2012). Windows QTL Cartographer 2.5., (ed. N. C. S. U. Department of Statistics). Raleigh, NC.

TABLE 1

Experimental layout

	Recurrent backcross parent							
	ra2-R>B73				*ra2-R*>Mo17			
RIL:	M0001	M0005	M0007	…M0384	M0001	M0005	M0007	…M0384
Plot:	1	4	7	262	1	4	7	262
	2	5	8	263	2	5	8	263
	3	6	9	264	3	6	9	264

TABLE 2

Ear Branch Number (EBN) among lines used in this study

Genotype	Ear branch number (EBN)
B73	0.58±0.09
Mo17	0
F1	0
B73 RIL BC1s	0.74±0.07
Range	0-4.6
Heritability (%)	57.6±1.2
Mo17 RIL BC1s	0.0625±0.012
Range	0-1.75
Heritability (%)	-

TABLE 3

QTL positions and effects

Recurrent parent	Chromosome number	Nearest marker	Position (IBM)	Support interval	LOD	"Additive" effect[a]	Model R^2(%)
ra2-R>B73	1	umc2225	125	117-127	4.39	0.21	7.6
	1	umc2240	803	797-810	5.69	0.34	19.7
	7	mmp25	544	541-551	3.84	-0.22	8.9
							34.3
ra2-R>Mo17	1	*an1*	785	785-791	5.30	0.16	24.4
	1	ufg53	800	796-800	6.19	-0.16	23.4
							15.5

[a] Estimated from a simultaneous fit of all QTL using multiple regression

TABLE 4

Candidate genes in chromosome 1L QTL support interval

Gene model	*ramosa2* co-expression[b]	Differential expression in *ramosa* mutants[a]		
		ra1-R	*ra2-R*	*ra3-R*
GRMZM2G167986 (cyp8)	Y	X	X	X
GRMZM2G044550	N	-	-	X
GRMZM2G173732	N	-	X	-
GRMZM2G150169	N	-	X	-
GRMZM2G120085	-	X	-	-
GRMZM2G070825	N	-	-	X
GRMZM2G146994	N	X	X	X
GRMZM2G145412	Y	-	-	X
GRMZM2G145458	Y	-	-	X
GRMZM2G083156	N	-	-	X
GRMZM2G083091	N	-	-	X
GRMZM5G800723	N	X	-	-
GRMZM5G879127	-	X	-	-
GRMZM2G152419	-	X	-	-
GRMZM2G105971	N	-	-	X
GRMZM2G010831	-	-	-	X
GRMZM2G011269	-	X	-	-
GRMZM2G011559	-	-	-	X
GRMZM2G011912	-	-	X	-
GRMZM2G012119	N	X	-	-
GRMZM2G146818	-	-	-	X
GRMZM2G034417	N	X	X	X
GRMZM2G034217	N	-	-	X
GRMZM2G110298	Y	-	-	X
GRMZM2G153928	Y	-	-	X
AC196066.3_FG003	N	X	-	-
GRMZM5G830403	N	X	X	-
GRMZM2G129540	N	X	-	-
GRMZM2G058057	N	-	X	X
GRMZM2G172584	N	-	X	X
GRMZM2G165005	N	X	-	-
GRMZM2G466394	-	-	X	-
GRMZM2G157456	N	X	-	-
GRMZM2G364069 (cdj2)	N	-	X	X
GRMZM2G318671	Y	X	-	-
GRMZM2G070323	N	-	X	-
GRMZM2G020142	N	-	X	X
GRMZM2G027991	-	X	-	-
GRMZM2G081099	N	X	-	-

[a] Eveland *et al.*, unpublished
[b] Eveland *et al*., 2011

TABLE 5

Candidate genes in chromosome 7L QTL support interval

Gene model	*ramosa2* co-expression[b]	Differential expression in *ramosa* mutants[a]		
		ra1-R	*ra2-R*	*ra3-R*
GRMZM2G013652	N	-	-	X
GRMZM2G018771	-	X	-	-
GRMZM2G032759	-	-	-	X
GRMZM2G037177	-	-	-	X
GRMZM2G039954	-	-	-	X
GRMZM2G040600	N	-	-	X
GRMZM2G055527	N	-	X	X
GRMZM2G083555	-	X	X	-
GRMZM2G083580	N	-	X	X
GRMZM2G111672	-	X	-	-
GRMZM2G161544	-	X	-	-
GRMZM2G301934	N	-	-	X
GRMZM2G412296	N	-	X	X

[a] Eveland *et al.*, unpublished
[b] Eveland *et al*., 2011

TABLE 6

IBM RILs used in this study

Intermated B73 × Mo17 RILs			
M0001	M0034	M0262	M0322
M0005	M0035	M0264	M0323
M0007	M0039	M0265	M0325
M0008	M0040	M0266	M0326
M0010	M0043	M0267	M0328
M0012	M0045	M0269	M0337
M0014	M0046	M0272	M0341
M0015	M0048	M0275	M0344
M0016	M0051	M0276	M0345
M0017	M0052	M0281	M0352
M0021	M0054	M0284	M0354
M0022	M0055	M0287	M0355
M0023	M0057	M0288	M0357
M0024	M0058	M0296	M0360
M0025	M0060	M0297	M0364
M0027	M0061	M0298	M0365
M0028	M0066	M0309	M0368
M0029	M0067	M0310	M0369
M0030	M0075	M0311	M0378
M0031	M0076	M0315	M0379
M0032	M0077	M0317	M0382
M0033	M0079	M0321	M0384

FIGURE LEGENDS

Figure 1. Comparison of tassel (top) and ear (bottom) branch numbers in B73 and Mo17 introgressions of *ra2-R*. Figure shows the disparity in ear branch number that exists between B73 and Mo17 introgressions of *ra2-R*.

Figure 2. Genetic approach used to map modifiers of the *ra1-63.3359* phenotype in the IBM population. Genotypes shown are for *ra2-R* and a potential modifier locus (QTL). Backcrosses were performed using both B73 and Mo17 introgressions of *ra2-R*, generating two sets of RIL F1-BC1s.

Figure 3. Treatment means for the B73 and Mo17 RIL treatments. The B73 treatments display a wide distribution of phenotypes that extend beyond the mean of the high parent indicating transgressive segregation among treatments. The Mo17 treatment means are not shown as all but one treatment were unbranched.

Figure 4. Correlation between *ra1* and *ra2* treatment means. Correlation was significant as tested by the Pearson correlation test in SAS. Significant correlation of treatment rank order was also observed.

Figure 5. Composite interval mapping results for chromosomes containing significant QTL for ear branch number in the B73 or Mo17 treatments. LOD scores and additive effects for B73 treatments are shown in black and Mo17 treatments in red. X-axis coordinates are shown in IBM recombination units.

Figure 6. Chromosome 1 composite interval mapping results for *ra2-R* overlaid with results from *ra1-63.3359* modifier mapping experiment. Co-localization of the chromosome 1 QTL in the two experiments may indicate presence of a modifier that alters both B73 and Mo17 phenotypes.

Figure 1 Weeks & Vollbrecht

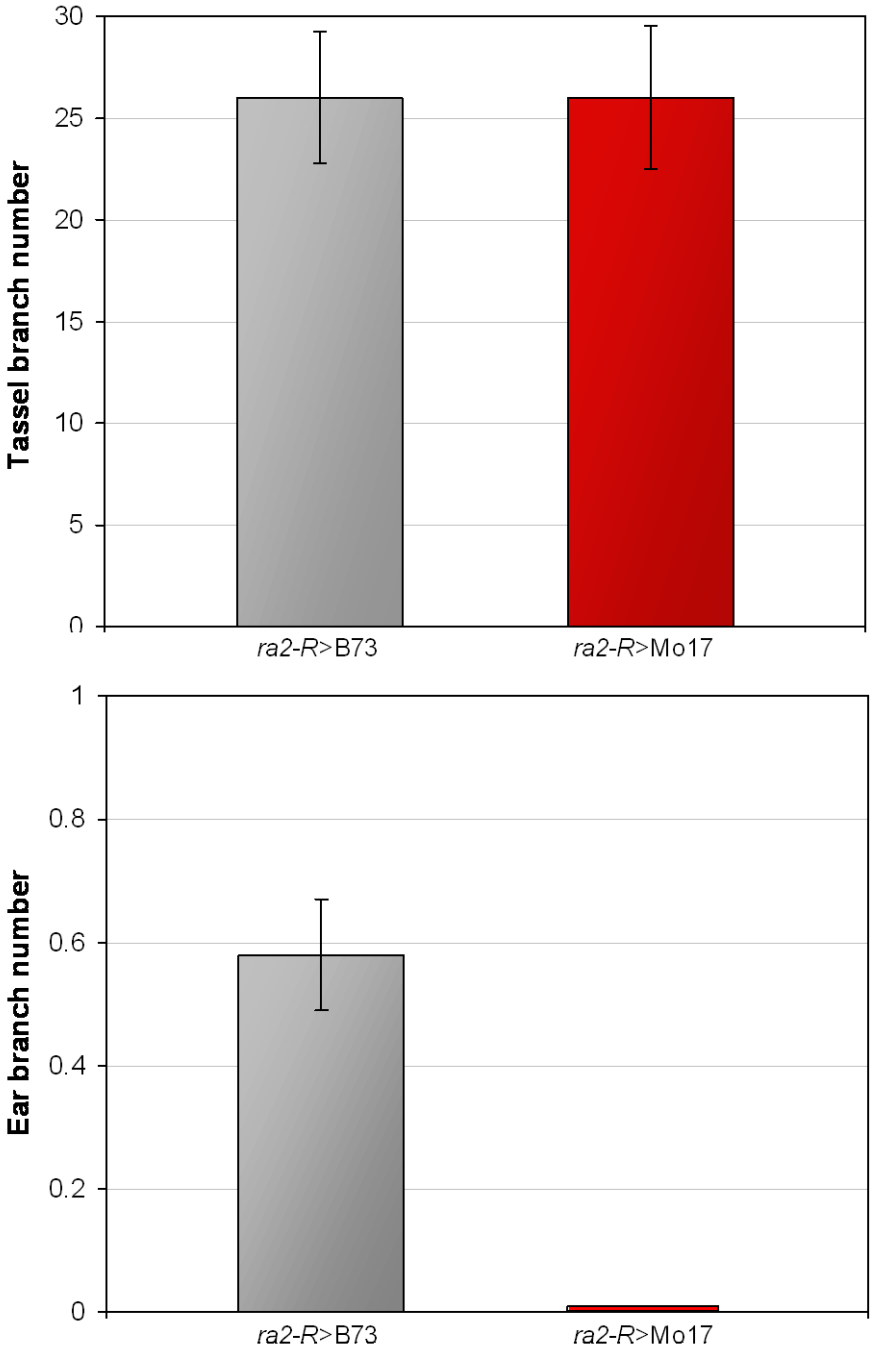

Figure 2 Weeks & Vollbrecht

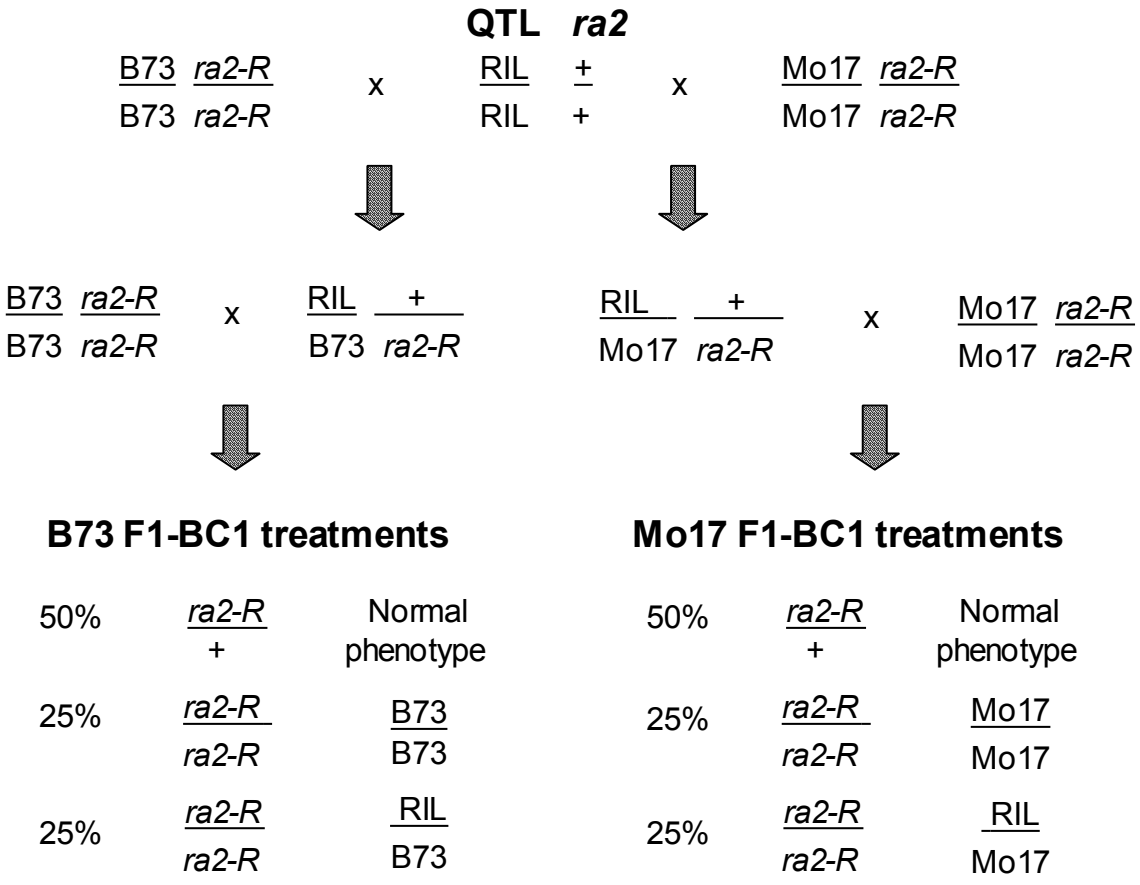

Figure 3 Weeks & Vollbrecht

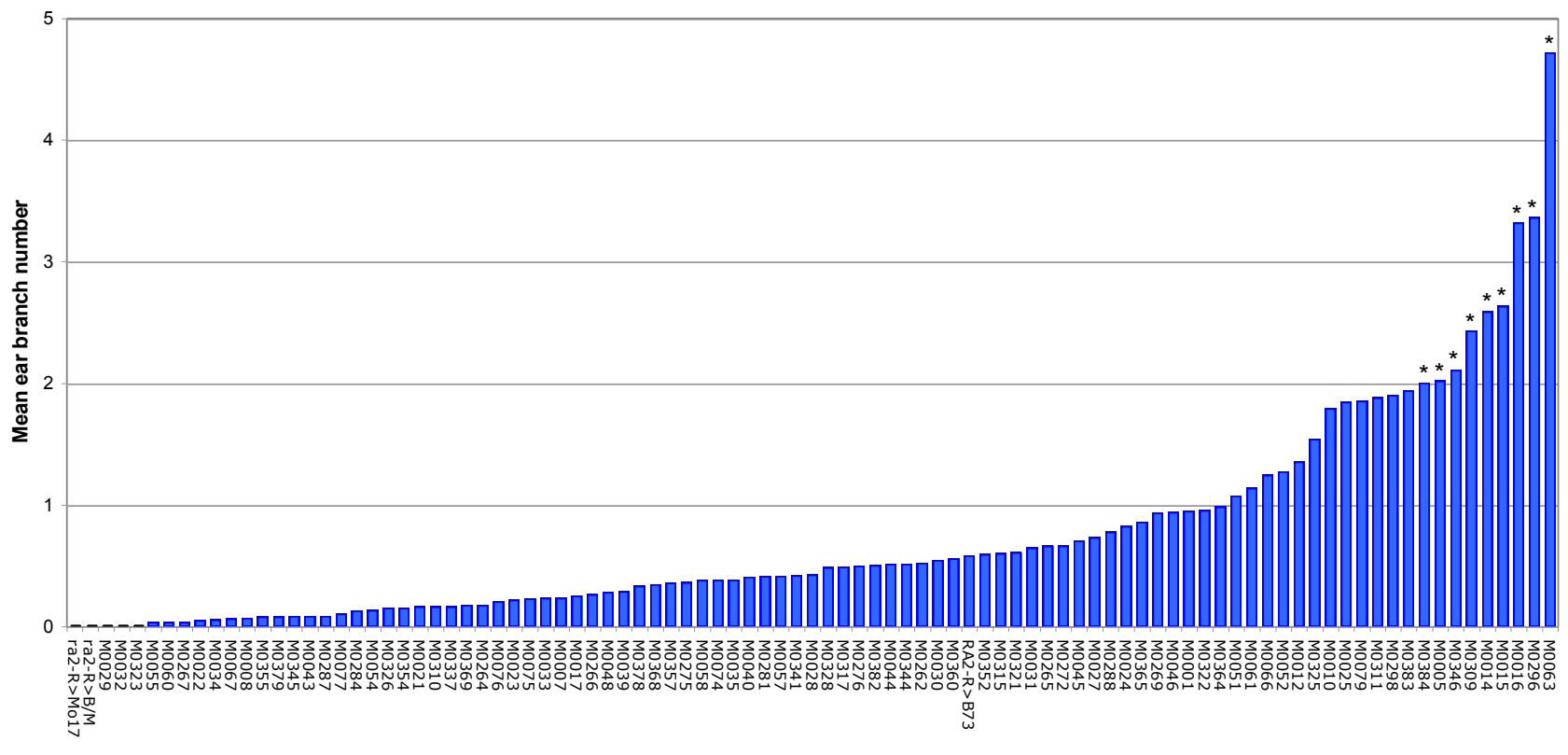

* Significantly different from *ra2-R>B73* as tested by LSD0.05

Figure 4 Weeks & Vollbrecht

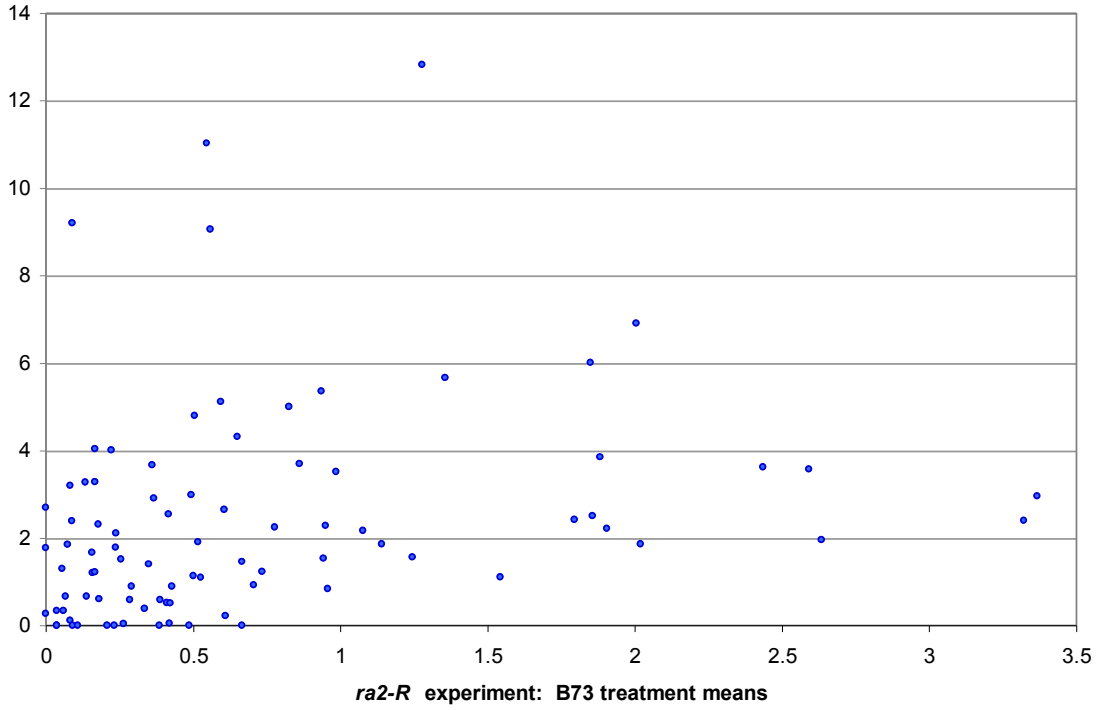

Figure 5 Weeks & Vollbrecht

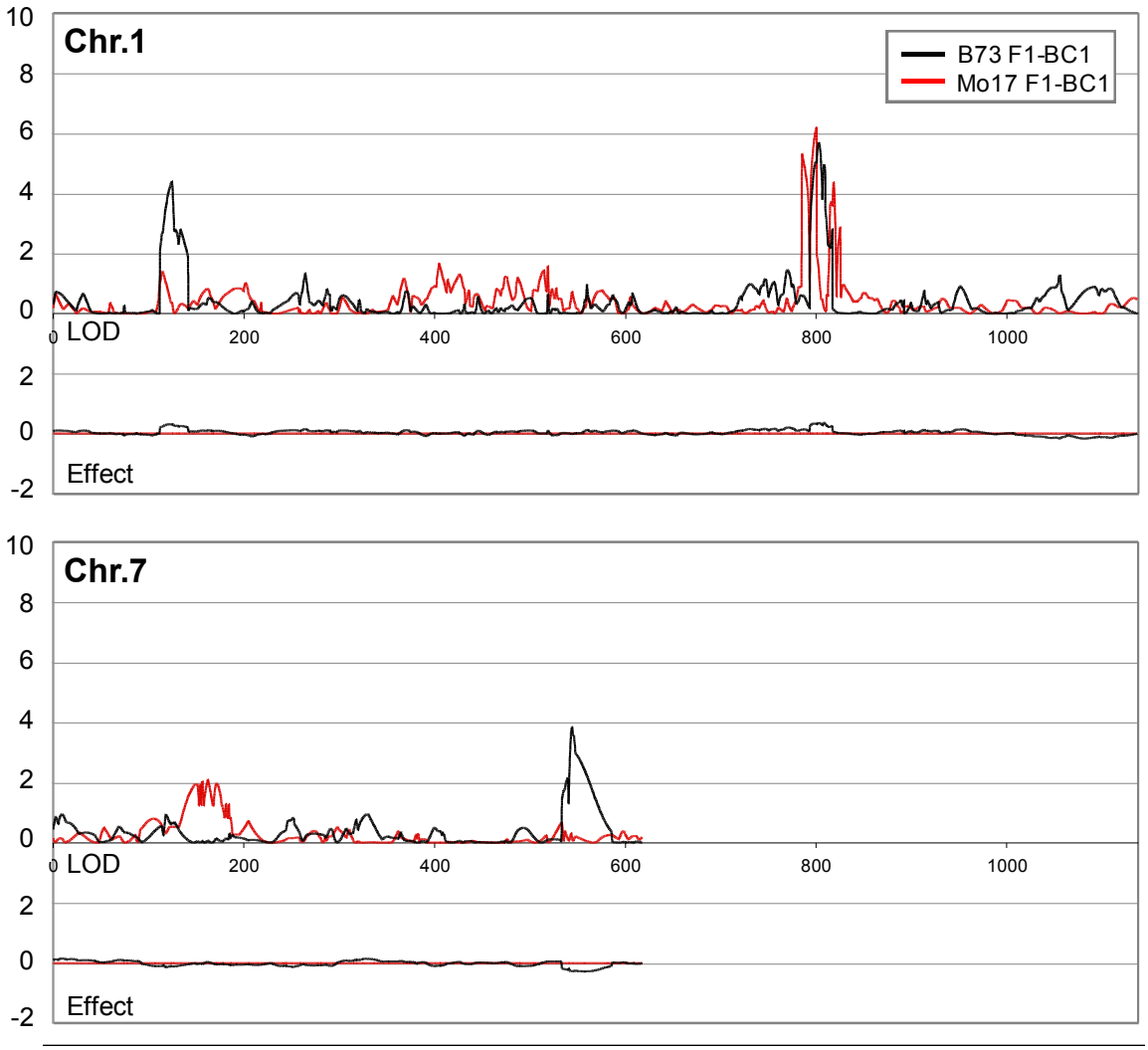

Figure 6 Weeks & Vollbrecht

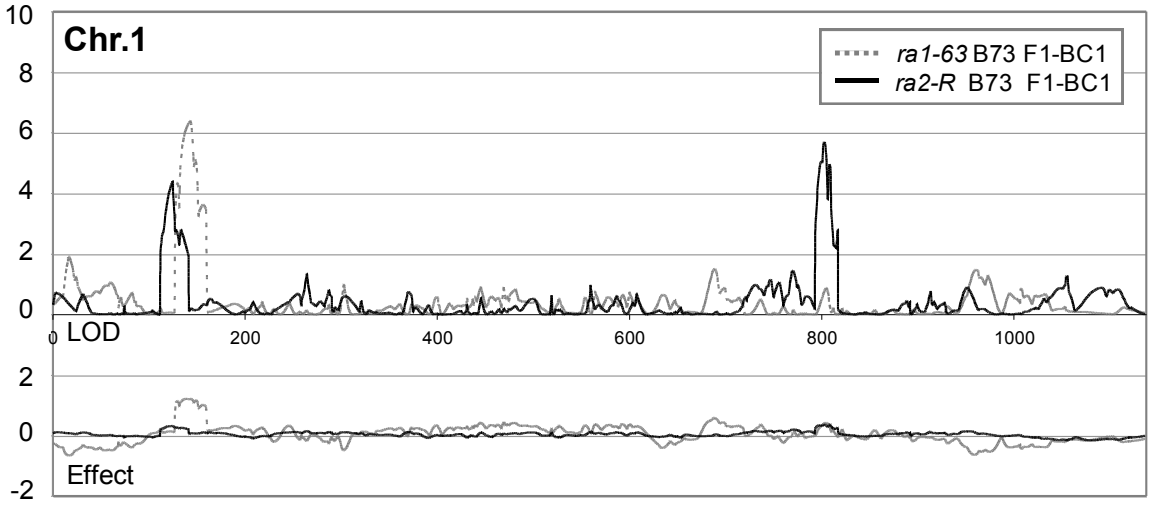

CHAPTER 5. GENERAL CONCLUSIONS

SUMMARY AND DISCUSSION

To identify novel components of the inflorescence branching pathway, we performed a suppressor/enhancer screen using the *ramosa* mutants of maize. Our approach exploited sensitized *ramosa* backgrounds in order to uncover novel mutations whose subtle phenotypes might have otherwise gone unnoticed. Through this approach, twenty-two mutants were identified, ten of which were subsequently mapped using bulked segregant analysis. Four of these mutants map to regions of the genome not known to harbor inflorescence genes. These mutants likely represent novel inflorescence genes and therefore additional work to more carefully characterize the mutant phenotypes and to identify the underlying mutations is warranted. The map positions of the remaining mutants co-localized with the previously cloned genes *ramosa3* (*ra3*), *branched silkess1* (*bd1*), *ramosa1 enhancer locus2* (*rel2*), and *fasciated ear4* (*fea4*) of which we identified two alleles that were subsequently utilized as part of the cloning effort (Pautler et al., unpublished). While the identification of previously cloned mutants does not further our understanding of the genetic pathway regulating inflorescence branch number, the discovery of mutants such as *ra3* and *rel2*, which are known to enhance *ramosa1* but alone produce subtle inflorescence phenotypes, demonstrates the utility of suppressor/enhancer screens for uncovering alleles with weak phenotypes. Ongoing efforts to characterize the remaining mutants will help to expand our knowledge of the genetic network regulating inflorescence branching.

As an extension of the suppressor/enhancer approach, we also sought to identify natural modifiers that were able to alter the branching of *ramosa1* mutants. We utilized the intermated B73 × Mo17 (IBM) population and exploited the phenotypic disparity that exists between B73 and Mo17 introgressions of *ra1-63.3359*. From this experiment, we identified several putative QTL that either enhance or suppress the ear branching phenotype of *ra1-63.3359*. Consistent with what has been previously reported (Brown et al., 2011), little overlap was observed between QTL and cloned inflorescence genes. For one particularly significant QTL, we isolated the region using near isogenic lines (NILs) and generated recombinants to further delineate the QTL interval. This allowed us to narrow the region to a

small interval containing 14 candidate genes. By mining community transposon resources such as AcDs, HeritableMu, and UniformMu we were able to identify potential mutant lines for four of the candidate genes and have initiated crosses to generate double mutants with *ra1-63.3359*.

While screening the chromosome 1 NILs for recombinants, we identified a line (REC1.2.1) that, based on genetic marker data, carries the QTL segment but does not display a phenotypic effect for the interval. These observations indicate that this line has lost or altered the modifier gene or sequence. After confirming this observation in two subsequent generations and validating the genotype across the interval, we have initiated a transcript profiling experiment to test the expression of genes in this line against those of the NIL (Figure 1). Material was planted in 2013 and genotyped to identify genotypic subclasses (MB or BB) within each treatment (NIL or REC1.2.1). For each of these four subclasses, 1mm to 2mm ears were harvested and stored in TRIzol® so that RNA can later be extracted. By comparing the expression of genes between subclasses, it may be possible to detect changes in the sequence or expression level of genes within the interval, which might point to the causative gene, and/or outside the interval, which might point to a specific pathway affected by the QTL.

Because *ramosa2* mutants display similar phenotypic disparity between B73 and Mo17 backgrounds, it was of interest to determine if the background effects could be explained by the same QTL that affect *ra1-63.3359* introgressions. We therefore repeated an iteration of the IBM mapping experiment, but with B73 and Mo17 introgressions of *ra2-R* as recurrent parents. In total, four QTL were identified, only one of which co-localizes with QTL from the *ra1-63.3359* experiment. The remaining QTL are unique to the *ra2-R* background and with one exception map to regions not known to carry inflorescence mutants. Efforts to confirm and fine-map these QTL using publicly available NILs (Eichten et al., 2011) are currently underway. We are additionally performing crosses of NILs for *ra1-63.3359* QTL to *ra2-R* mutants to determine if the effects can be seen in both *ramosa* backgrounds.

Forward genetic screens have identified a number of genes involved in regulating inflorescence architecture. To further expand our knowledge of the genetic network

determining inflorescence branch number, we performed suppressor/enhancer screens for induced and natural mutations that alter the inflorescence branching phenotype of *ramosa* mutants.

In combination, these phenotype-driven methods provide a broad-based approach to identify genes with a diversity of functions and genomic contexts. For example, suppressor/enhancer screens are able to detect mutations whose subtle phenotypes might go undetected in traditional forward genetic screens. However, this method has difficulty detecting genes for which there is genetic redundancy. Furthermore, mutagenesis screens are biased towards the identification of genes that give strong loss-of-function phenotypes. Natural modifier screens on the other hand are able to detect phenotypes that arise from different types of mutations such as those that alter the expression level of a gene or slightly alter the amino acid sequence of its protein. The detection of these phenotypes is facilitated by a quantitative scoring approach and a mapping strategy that allows for the detection of small, but stable effects. We see only a small degree of overlap between loci discovered in each of our experiments indicating that these methods have indeed diversified the collection of relevant mutants and natural variant loci. Ongoing work to positionally clone suppressor/enhancer mutants and fine-map modifier QTL will be helpful in elucidating the genetic mechanisms regulating inflorescence architecture.

LITERATURE CITED

Bortiri, E., Chuck, G., Vollbrecht, E., Rocheford, T., Martienssen, R. and Hake, S. (2006). ramosa2 encodes a LATERAL ORGAN BOUNDARY domain protein that determines the fate of stem cells in branch meristems of maize. *Plant Cell* **18**, 574-85.

Brown, P. J., Upadyayula, N., Mahone, G. S., Tian, F., Bradbury, P. J., Myles, S., Holland, J. B., Flint-Garcia, S., McMullen, M. D., Buckler, E. S. et al. (2011). Distinct genetic architectures for male and female inflorescence traits of maize. *PLoS Genet* **7**, e1002383.

Chuck, G., Muszynski, M., Kellogg, E., Hake, S. and Schmidt, R. J. (2002). The control of spikelet meristem identity by the branched silkless1 gene in maize. *Science* **298**, 1238-41.

Eichten, S. R., Foerster, J. M., de Leon, N., Kai, Y., Yeh, C. T., Liu, S., Jeddeloh, J. A., Schnable, P. S., Kaeppler, S. M. and Springer, N. M. (2011). B73-Mo17 near-isogenic lines demonstrate dispersed structural variation in maize. *Plant Physiol* **156**, 1679-90.

Gallavotti, A., Long, J. A., Stanfield, S., Yang, X., Jackson, D., Vollbrecht, E. and Schmidt, R. J. (2010). The control of axillary meristem fate in the maize ramosa pathway. *Development* **137**, 2849-56.

Satoh-Nagasawa, N., Nagasawa, N., Malcomber, S., Sakai, H. and Jackson, D. (2006). A trehalose metabolic enzyme controls inflorescence architecture in maize. *Nature* **441**, 227-30.

Vollbrecht, E., Springer, P. S., Goh, L., Buckler, E. S. t. and Martienssen, R. (2005). Architecture of floral branch systems in maize and related grasses. *Nature* **436**, 1119-26.

FIGURE LEGEND

Figure 1. Design of experiment to profile transcript differences between the chromosome 1 near-isogenic line (NIL) and REC1.2.1 which carries the Mo17 QTL region but has lost the modifier. Comparisons between subclasses of the NIL reveal differentially expressed genes within the region. Comparison of these differentially expressed genes with those from REC1.2.1 subclasses, might allow us to determine which gene is responsible for the QTL eff

Figure 1 Weeks